A STUDY ON THE COMMON AMPLIFICATION OF PM PULSES BY A DOUBLE LADDER TYPE MILLIMETER WAVE TRAVELING WAVE TUBE

Shoji Tsuchiya and Hideki Ishio

(NASA-TT-F-16176) A STUDY ON THE COMMON AMPLIFICATION OF PM PULSES BY A DOUBLE LADDER TYPE MILLIMETER WAVE TRAVELING WAVE TUBE (Scientific Translation Service) 100 p HC $4.75 CSCL 09C G3/33

N75-20606

Unclas 14728

Translation of: "Millimeter-Hado 2-Ju Hasigoke Singkohakan Niyoru PM-Pulse Kyoto Zhotokusei-No Kendyu" Elec. Commun. Lab. Tech Journal, Vol. 18, No. 4, 1969. pp. 101-154, Nippon Telegraph and Telephone Public Corporation, Tokyo (Japan).

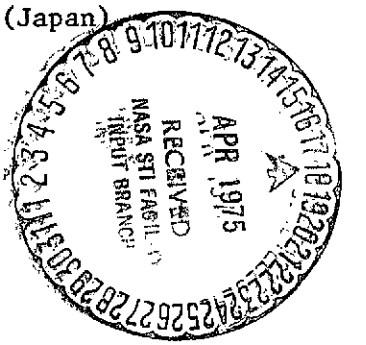

NATIONAL AERONAUTICS AND SPACE ADMINISTRATION
WASHINGTON, D. C. 20546 MARCH 1975

STANDARD TITLE PAGE

1. Report No. NASA TT F-16,176	2. Government Accession No.	3. Recipient's Catalog No.
4. Title and Subtitle: A STUDY ON THE COMMON AMPLIFICATION OF PM PULSES BY A DOUBLE LADDER TYPE MILLIMETER WAVE TRAVELING WAVE TUBE		5. Report Date: April, 1975 6. Performing Organization Code
7. Author(s): Shoji Tsuchiya & Hideki Ishio		8. Performing Organization Report No. 10. Work Unit No.
9. Performing Organization Name and Address: SCITRAN, Box 5456, Santa Barbara, CA 93108		11. Contract or Grant No. NASw-2483 13. Type of Report and Period Covered: Translation
12. Sponsoring Agency Name and Address: National Aeronautics and Space Administration, Washington, D.C. 20546		14. Sponsoring Agency Code

15. Supplementary Notes

Translation of: "Millimeter-Hado 2-Ju Hasigoke Singkohakan Niyoru PM-Pulse Kyoto Zhotokusei-No Kendyu", Elec. Commun. Lab. Tech J., Vol 18, No. 4, 1969, pp. 101-154, Nippon Telegraph and Telephone Public Corp., Tokyo, Japan.

16. Abstract

An experimental and theoretical study of traveling waves is presented for broad-band application. The pulse is assumed to be either a square or a Gaussian PM pulse with Gaussian band distribution. Common amplification characteristics for a 1- and 2- cycle wave is studied theoretically and results of experiments are verified for the square PM pulse. It is found the TW tubes are most promising for high-speed PCM millimeter band communications. The double-ladder traveling wave tube is assumed in this study.

17. Key Words (Selected by Author(s))	18. Distribution Statement
	Unclassified - Unlimited

19. Security Classif. (of this report)	20. Security Classif. (of this page)	21. No. of Pages	22. Price
Unclassified	Unclassified	100	

A STUDY ON THE COMMON AMPLIFICATION OF PM PULSES BY A DOUBLE LADDER TYPE MILLIMETER WAVE TRAVELING WAVE TUBE

Shoji Tsuchiya and Hideki Ishio*

When traveling wave tubes are used in a millimeter wave communication process, it is natural that the multi-frequency common amplification with a PCM pulse should be considered in recognizing the broad band structure of traveling wave tubes, in order to economically utilize this advantage. However, a double ladder traveling wave tube, as is well known, is nonlinear, and it has a very wide frequency characteristic. On the other hand, in a millimeter wave communication process, the high speed PCM many phase PM method seems to be most promising. Consequently, it is an important problem in circuit design to know what effects it will cause when a high speed PM pulse passes through the previously mentioned circuit. /101**

This paper is concerned with a theoretical and experimental study on this point. In other words, theoretically the pulse is assumed to be either a square or a Gaussian PM pulse with a Gaussian band distribution. With this assumption, a theoretical study is made on the common amplification characteristics for a 1-cycle and a 2-cycle wave, and finally, the results are experimentally confirmed (but only for the case of a square PM pulse). From this study, it has become clear that such a traveling wave tube is indeed very practical.

---

*Special Research Investigators at the Millimeter Wave Laboratory, Department of Wave Propagation Research.

**Numbers in the margin indicate the pagination of the original foreign text.

1. Introduction

A theoretical and experimental study is made on the amplification characteristics of AM pulses by use of double ladder type traveling wave tubes for millimeter waves, especially to clarify [1] the characteristics of the traveling wave tubes with respect to the common amplification. In short, AM pulses of a millimeter wave of about 1 ns half-amplitude, used for the purpose of communication amplification, have been satisfactorily utilized in the common amplification of 1-cycle or 2-cycle waves.

The PCM communication method of millimeter waves is one of the important research projects, because it can increase the number of channels for a system and, therefore, raise the beat rate and produce phase multiplication. Any method that can do these jobs has advantages, namely in fulfilling the important task of "practical multi-phase phase modulation — the multi-phase PM delay rectification method" [2 — 6].

In fact, the 2-phase and 4-phase phase modulation method with a pulse repeating cycle number of 300 — 500 MHz seems to be most promising. Consequently, it is necessary to study the PM pulse amplification characteristics along with the AM pulse amplification characteristics in traveling wave tube communication amplification. The millimeter wave double ladder type tube has often been mentioned for performing these functions. It is nonlinear (saturation characteristics and phase shift characteristics), and at the same time, it has quite a large frequency number characteristic. If one passes the aforementioned high speed PCM-PM pulse through a circuit with such characteristics, the important problem is to know what kind of an output pulse will be obtained; that is, a lot of important problems occur in the circuit design, such as the problem of the AM-PM transformation which will compress the output power, the appearance of some echo pulses which are really the interference waves which distort the principal wave, the maximum output, and the cross docking phenomena, etc.

When one makes a theoretical study on the amplification characteristics of a PM pulse in a traveling wave tube, the problem is what kind of an input should be used; in other words, a theoretical PM pulse maintains a constant amplitude, but changes only its phase, while an experimental PM pulse is always accompanied by some AM components, due to the limitation of the range it can command, and for this reason, in some PM pulses the phase shift can be neglected; while in other cases, it cannot be ignored. Hence, in this work, we will deal with some representative input pulses that can be easily handled /102 mathematically, but at the same time have the realistical wave forms. They are the following two types of PM pulses:

i) a theoretical square wave PM pulse with a Gaussian band distribution;
ii) a theoretical Gaussian PM pulse with a Gaussian band distribution (see figure 3).

The pulse of type i) can be called an "AM-like PM pulse," and it is similar to the much discussed conventional PM pulse [2 — 5]. In this case, the AM component does not cause great problems in regard to the phase. Also, when the sum of the AM wave and the continuous wave is considered, a change of frequencies does not appear. The pulse of the type ii) can be called an "FM-like PM pulse." Recently, it has been increasingly reported. It contains only a small AM component, but the component cannot be ignored for the phase problem [5 — 8, 15]. This means that both the phase and the frequency vary with respect to the time, and for this reason, it is called a FM pulse.

Thus, these two contrasting types are assumed for the PM pulse, and the discussion will be treated in a quasi-static manner, as in the previous report [1], and as in the case of a 2-phase PM wave. First, in the case of 1-cycle pulse amplification, we will consider the region of small signals in terms of their gains and the influence of frequency characteristics of the phase. Then in the region of large signals, we will analyze the saturation and phase shift characteristics. From these results, we shall estimate the realistic actual characterisitcs of the large signal region, and finally, we shall discuss the case of the 2-cycle pulse common amplification. As a result, an output

decline will appear due to the frequency characteristics and nonlinearity, and the perpendicular component will also appear due to some phase shifts, and the shape of the envelope wave will also change, etc. All these points are also discussed in terms of the interference between the plus and minus sign or between different channels, but this influence turns out to be very insignificant.

Finally, we will present the experimental results to confirm the above theory. We obtained the result as predicted, and all the activities were confirmed. All the results indicate that the millimeter wave double ladder traveling wave tube can be practically used in the communication amplification for 2-cycle PM pulses up to the 2 ns range.

The computation on the Gaussian PM pulses was carried out in the numerical computation research laboratory by electronic computers.

2. The Problem of the PM Pulse Amplification By a Traveling Wave Tube

Our research on a traveling wave tube amplifier has led us to believe that if a two-terminal circuit is used, the following theoretical characteristics of the circuitry are present:

i) Nonlinearity — A nonlinear relationship exists between the input and the output (input-output saturation characteristics); the input dependency of the output phase (the output phase shift characteristics).

ii) Frequency number characteristics — the gain and the frequency number characteristics of the phase; the saturation input and the frequency number characteristics of the saturation output.

Consequently, when a PM pulse is sent through a circuit in which nonlinearity and some frequency number characteristics exist, it is a major problem to determine what effect these characteristics may give to the shape of the output pulse.

2.1 Distortion Evaluation and the Model For Analysis

We are generally interested in the PM pulse which has non-negligible AM components. We begin with some simple cases and gradually progress to complex situations.

i) In the activity of a 1-cycle pulse amplitude in the small signal region, the effect of the frequency number characteristics can be a problem, because it is expected to cause some perpendicular component. Consequently, due to the gain frequency number characteristics (it is 3 dB/GHz for a double ladder tube), a PM-AM transformation will occur, and from this transformation, a fairly large change will appear in the shape of the envelope wave. Also, owing to the higher order components (Fourier components) of the gain and phase frequency number characteristics, some internal echo pulse will naturally be present.

ii) For operation with a 1-cycle pulse amplitude in the large signal region, owing to the nonlinearity caused by the distortion, as mentioned in i), a very complex distortion appears, such as an output reduction due to the /103
saturation characteristics and the combination of two kinds of distortions caused by the AM-PM transformation due to the phase shift characteristics. As a result, a change in the shape of the envelope wave, accompanied by a phase modulation due to the presence of the AM component, can cause a large distortion to the PM pulse.

iii) In the common amplification of a 2-cycle pulse by operation in a large signal region, distortions will also occur, as mentioned in ii); nonlinearity will cause a complex modulation, and create a phase shift characteristic, and thus, some interference waves will also appear as a result. This phenomenon will become a problem, and a very complex distortion should be expected.

Thus, in amplifying a PM pulse, a very complex distortion will occur, but it is impossible to study separately the effect, due to the frequency

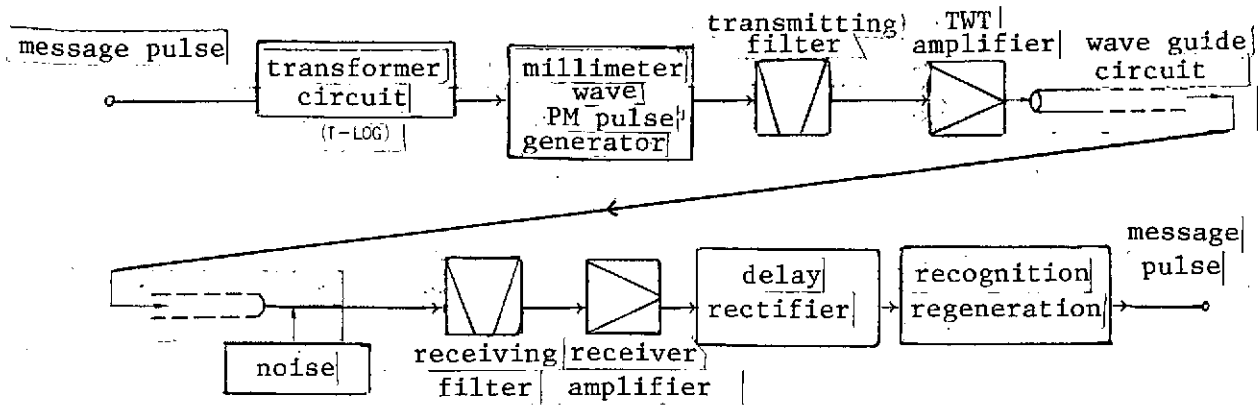

Figure 1. Millimeter wave PCM-PM communication method (a 2-phase, phase modulation — a traveling wave tube transmission amplification method).

number characteristics and the effect due to the nonlinearity. On the other hand, when both these effects are dealt with together, an exact solution is hard to come by. Nevertheless, for the convenience of analysis, we managed to consider these two effects separately, and then put the results together for the final analysis of real operation. In other words, we will first investigate the 1-cycle amplification in the small signal region to confirm that the effect due to the frequency number characteristics in this case is very small. Then, by neglecting this effect also in the large signal region, we will investigate the effect of nonlinearity. Finally, for the common amplification of a 2-cycle pulse, the frequency number characteristics are neglected for each pulse, and then the distortion of the wave, the complex modulation, and the interference waves are evaluated.

Our problem is to evaluate distortions, but in this case, our purpose is to clarify distortions appearing in a traveling wave tube. The model for analysis, as shown in Figure 2, is to compare the wave forms of the input and output wave, so that the distortion can be evaluated. In general, the millimeter wave PCM-PM communication method using a traveling wave tube has a transmitter and receiver set, as shown in Figure 1. In the figure, the transmitting filter and the receiving filter imply, respectively, a set consisting of the pulse generator and the transmitting frequency analyzer, and a set consisting of the receiving frequency analyzer and receiver amplifier.

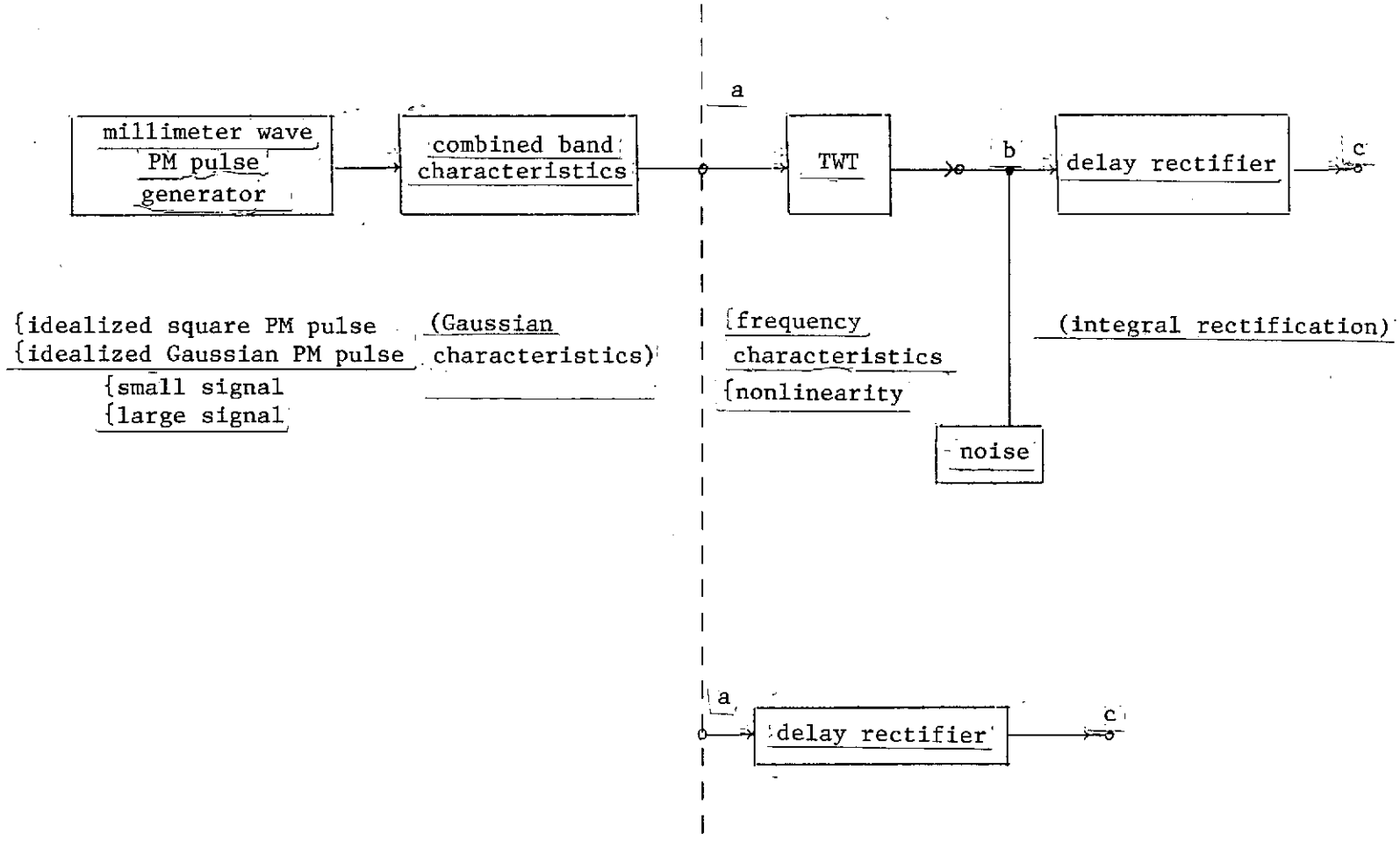

Figure 2. A model for analyzing the wave distortion in a traveling wave tube.

The receiver amplifier consists of a frequency transformer and an intermediate frequency amplifier; they are all linearly related, and therefore, they can be ideally compensated for by a retardator or by a second order distortion /104 from a wave guide circuitry. In other words, the combination of a wave guide circuitry and a receiver amplifier can quench the distortion and transmit the original envelope and phase faithfully. The behavior of a traveling wave amplifier in a small signal region can also stay very nearly linear by placing the transmitting filter and the receiving filter at the transmitting side, as well as at the receiving side, such that the combined band characteristics are taken into account. However, since in our case, the problem lies between the millimeter wave generator and the retardation rectifier, the combined band characteristics may be able to be taken care of at the receiver side. For this purpose, the equivalent model for Figure 1 would be Figure 2. This equivalent model is suitable for a theoretical study of the wave distortion and the interference between signs. However, to study the interference between the different channels, we have to refer back to Figure 1 by separating the transmitting and receiving filter.

Next, when a traveling wave amplifier is working in the large signal region, it is a nonlinear amplifier, and consequently, Figure 2 cannot be the equivalent model of Figure 1. However, for the sake of simplicity, and due to the nature of the wave distortion in a traveling wave tube as it will be described in a later section (Section 3.3.2), instead of considering the transmitting and receiving filter separately, as in Figure 1, the combined band characteristics are taken care of at the transmitting side, and then the circuit of Figure 2 can be studied. Thus, the case of a large signal region is also analyzed with the model of Figure 2, because of two reasons which show that the distortion will be evaluated to be quite large.

Any model must resemble the actual wave form, and at the same time, must be easily handled mathematically. Such a pulse form can be found in an idealized square or Gaussian PM pulse, and the combined band characteristics are also assumed to be in a Gaussian form.

One can obtain the wave distortion in Figure 2 by comparing the wave form at point a and the one at point b. Thus, as a PM method, the delay rectification method is most promising; that is, the input and output power can be found by a delay rectification process at point c and point c', respectively, and from the input and output potential wave forms at these two points, one can evaluate the interference between signs by measuring the power increase and decrease at these sample points. As for the interference among different channels, one distributes the combined band characteristics equally to the transmitting and receiving filter, and estimates the amount of interference by considering appropriate channel gaps. However, for the sake of simplicity, in the present study, we treat the interference among different channels only by comparing the maximum value of the spectrum of a filtered wave in the neighboring channel and the maximum value of the principal signal spectrum. The value for the filtered wave is equal to the value from the exact solutions [9], obtained by integrating the electric power spectrum of the filtered wave. The justification in this evaluation method by such a simplification is due to the fact that our main purpose is to know the increase and decrease of the amount of interference in a traveling wave tube.

When we study the case of the common amplication by a 2-cycle PM pulse, we assume a square wave form or a Gaussian PM pulse at point a which is restricted by an input Gaussian band distribution equivalent to a 2-cycle wave. The procedure thereafter is the same as in the above case. However, as for the cross docking, we will also have the problem of the phase shift characteristics and the cross docking of the interference wave, beside the above two problems. This is due to the fact that some complicated changes do occur, caused by the relationship of the time slots of a 2-cycle wave pulse. A theoretical study can always be made with some simplified cases.

As for the retardation rectifier, we use the conventional 1-beat delay rectification method [3, 4] to make a computation on the output electric potential.

2.2 Modulated Wave Forms

In this study, the modulated signal is (...00100...), and it is limited to the case of a single pulse (namely, 1 pulse of RZ signal). This type of pulse is called the worst possible case [8] with respect to the sign interference. However, (...011...), the 100% duty general case (namely, NRZ signal), is also considered, and the distortion of this wave form and the amount of interference can thoroughly be evaluated as a result of the present study.

The PM pulse described in this article is somewhat different from the FM-DCPSK pulse described in references [6] and [7], in terms of the modulated wave form and the degree of modulation (in the latter case, it was a $\pm\pi/2$ modulation). The distortion in the $0-\pi$ modulation is a little smaller than the $0-\pi/2$ modulated wave, because of the previously mentioned reason and other reasons to be described later. Consequently, the distortion and the amount of interference in the wave form, described in reference [7], can also be adequately evaluated as a result of the present study.

We would like to refer to reference [15] for the method of generating a Gaussian PM pulse and the actual examples which resemble the model very closely. This is accomplished by use of a barracuda diode to generate an 11 GHz band PM pulse, and then one can obtain a millimeter PM pulse by transforming the wave to 4 times its original frequency. However, when one uses a barracuda as a modulator to generate pulses, in most cases one cannot neglect the cases which have extremely small widths, and, therefore, extremely high beat rates, caused by the time duration in the phase. In short, as an actual problem, the case of an extremely high beat rate is similar to the case /105 of the "FM-like PM pulse", and the case of low beat rate is similar to the case of the "AM-like PM pulse" as in the microwave PCM communication method [2 — 4].

3. Analysis on the PM Pulse Amplification Characteristics in a Millimeter Wave Double Ladder Traveling Wave Tube

3.1 Two Kinds of the PM Pulse Characteristics

If an idealized square or Gaussian type PM pulse (Figure 3) is considered, as described in the previous chapter, and an idealized Gaussian band distribution is imposed on the pulse, two kinds of the PM pulse characteristics exist to generate wave distortions. There have been a number of reports concerned with the square type of the PM pulse [4, 5]. However, in Section 3.2, we will present some of the mathematical formulas for this problem.

3.1.1 Square PM pulse

i) Wave form and its spectrum:

The wave form $G_1(t)$ and the frequency spectrum $F_1(\omega)$ of an idealized square PM pulse can be found in Figure 3.

$$G_1(t) = Ee^{j(\omega_0 t+\varphi(t))},$$
$$\varphi(t) = \begin{cases} 0 : t < -T_1/2 \\ k : -T_1/2 < t < T_1/2 \\ 0 : t > T_1/2 \end{cases} \tag{1}$$

$$\begin{aligned} F_1(\omega) &= \int_{-\infty}^{\infty} G_1(t) e^{-j\omega t} dt \\ &= E\left[\int_{-\infty}^{\infty} e^{-j(\omega-\omega_0)t} dt - (1-e^{jk}) \right. \\ &\quad \left. \cdot \int_{-T_1/2}^{T_1/2} e^{-j(\omega-\omega_0)t} dt \right] \\ &= E\left[S_0(f-f_0) - (1-e^{jk}) \right. \\ &\quad \left. \cdot \frac{2\sin(\omega-\omega_0)T_1/2}{\omega-\omega_0} \right] \end{aligned} \tag{2}$$

where $S_0(f-f_0) = \lim_{a\to 0} \frac{1}{a} e^{-\frac{\pi(f-f_0)^2}{a^2}}$

unit impulse at $f = f_0$ (see reference [11], No. 982).

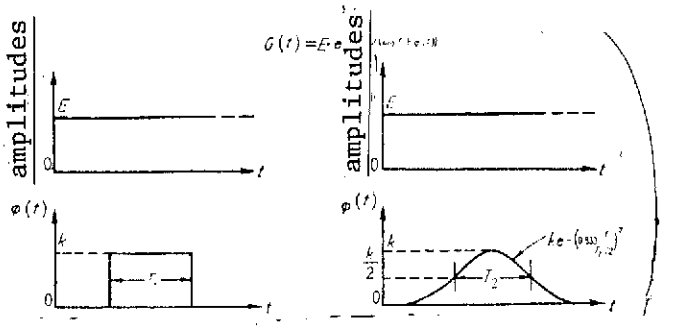

(a) square PM pulse (b) Gaussian PM pulse

Figure 3. Two kinds of idealized PM pulses.

Consequently, at $k = \pi$, $F_1(\omega) = E\left[S_0(f-f_0) - 2\frac{2\sin(\omega-\omega_0)T_1/2}{\omega-\omega_0}\right]$

and at $k = \pi/2$, $F_1(\omega) = E\left[S_0(f-f_0) - (1-j)\frac{2\sin(\omega-\omega_0)T_1/2}{\omega-\omega_0}\right]$ (2')

The [ ] part in the second term of Equation (2') can be shown as in Figure 4. From it, one sees that at $k = \pi$, the wave contains two in-phase spectra, while at $k = \pi/2$, it contains two in-phase, but mutually perpendicular spectra.

ii) When the pulse passes through an idealized filter:

The idealized filter $F_2(\omega)$ is characterized by

$$F_2(\omega) = \begin{cases} 0 : \omega < (\omega_0 - \omega_B) \\ 1 : (\omega_0 - \omega_B) < \omega < (\omega_0 + \omega_B) \\ 0 : \omega > (\omega_0 + \omega_B) \end{cases} \quad (3)$$

where the phase shift is neglected and the passing band width is $2\omega_B$.

Consequently, the output wave form $G_2(t)$ can be found from the following formula:

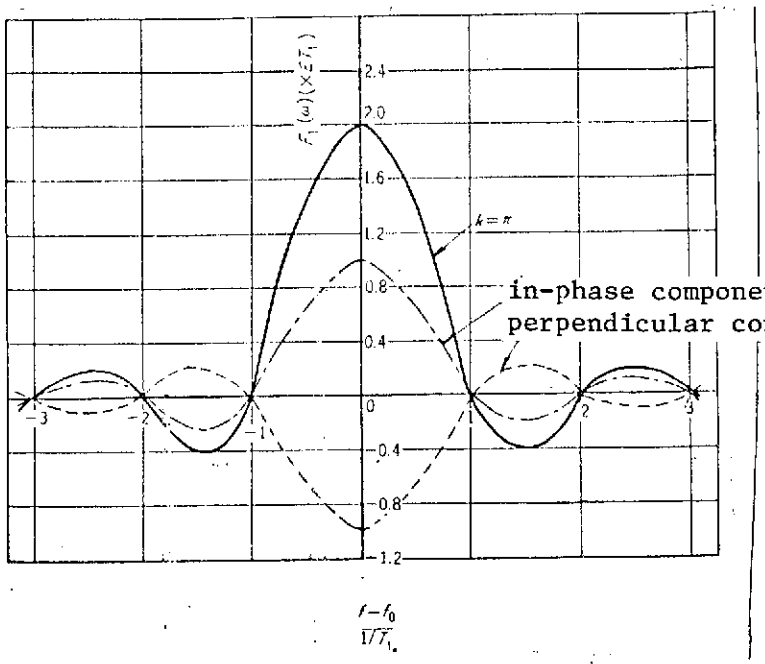

Figure 4. The spectrum of a square PM pulse.

$$
\begin{aligned}
G_2(t) &= \frac{1}{2\pi}\int_{-\infty}^{\infty} F_1(\omega)F_2(\omega)e^{j\omega t}d\omega \\
&= \frac{Ee^{j\omega_0 t}}{2\pi}\int_{\omega_0-\omega_B}^{\omega_0+\omega_B}\left[S_0(f-f_0)\right. \\
&\quad \left.-(1-e^{jk})\frac{2\sin(\omega-\omega_0)T_1/2}{\omega-\omega_0}\right]\cdot e^{j(\omega-\omega_0)t}d\omega \\
&= E\left[1-(1-e^{jk})\cdot\frac{1}{\pi}\left\{S_i\left(\frac{1+x_1}{d_1}\right)\right.\right. \\
&\quad \left.\left.+S_i\left(\frac{1-x_1}{d_1}\right)\right\}\right]e^{j\omega_0 t} \\
&= E\left[e^{j\omega_0 t}-\frac{\sqrt{2}(1-\cos k)}{\pi}\left\{S_i\left(\frac{1+x_1}{d_1}\right)\right.\right. \\
&\quad \left.\left.+S_i\left(\frac{1-x_1}{d_1}\right)\right\}e^{j\left(\omega_0 t-\tan^{-1}\frac{\sin k}{1-\cos k}\right)}\right]
\end{aligned}
\tag{4}
$$

where

$$x_1=\frac{t}{T_1/2},\quad d_1=\frac{2}{\omega_B T_1}$$

$$S_i(z)=\int_0^z \frac{\sin z}{z}\,dz$$

Now since

$$g_2(t)\equiv\frac{\sqrt{2}(1-\cos k)}{\pi}\left\{S_i\left(\frac{1+x_1}{d_1}\right)+S_i\left(\frac{1-x_1}{d_1}\right)\right\},\quad \xi\equiv\tan^{-1}\frac{\sin k}{1-\cos k}$$

Formula (4) becomes

$$G_2(t)=E\{1+g_2(t)^2-2g_2(t)\cos\xi\}^{1/2}\cdot e^{j\left(\omega_0 t-\tan^{-1}\frac{g_2(t)\sin\xi}{1-g_2(t)\cos\xi}\right)} \tag{5}$$

Consequently, at $k=n\pi$,

$$G_2(t)=E\left\{1-\frac{2}{\pi}\left\{S_i\left(\frac{1+x_1}{d_1}\right)+S_i\left(\frac{1-x_2}{d_2}\right)\right\}\right\}e^{j\omega_0 t} \tag{5'}$$

and at $k=\pi/2$

$$G_2(t)=E\left\{1+g_2(t)^2-\sqrt{2}\,g_2(t)\right\}^{\frac{1}{2}}\cdot e^{j\left(\omega_0 t-\tan^{-1}\frac{g_2(t)}{\sqrt{2}-g_2(t)}\right)}$$

where

$$g_2(t)=\frac{\sqrt{2}}{\pi}\left\{S_i\left(\frac{1+x_1}{d_1}\right)+S_i\left(\frac{1-x_1}{d_1}\right)\right\}$$

Therefore, $\alpha_1\equiv\frac{2f_B}{1/T_1}$, $d_1=\frac{2}{\pi}\cdot\frac{1}{\alpha_1}$ and $d_1 = 0.2$ or 0.1. Consequently, for $\alpha_1 = 3.18$ and 6.37, Equation (5') can be computed as shown in Figures 5a and b. From Figure 5 and Equation (5'), one sees that, at $k = \pi$, there is a distortion in the amplitude but not in the phase, while at $k = \pi/2$, a distortion appears in the amplitude as well as in the phase around $t=\pm T_1/2$.

/107

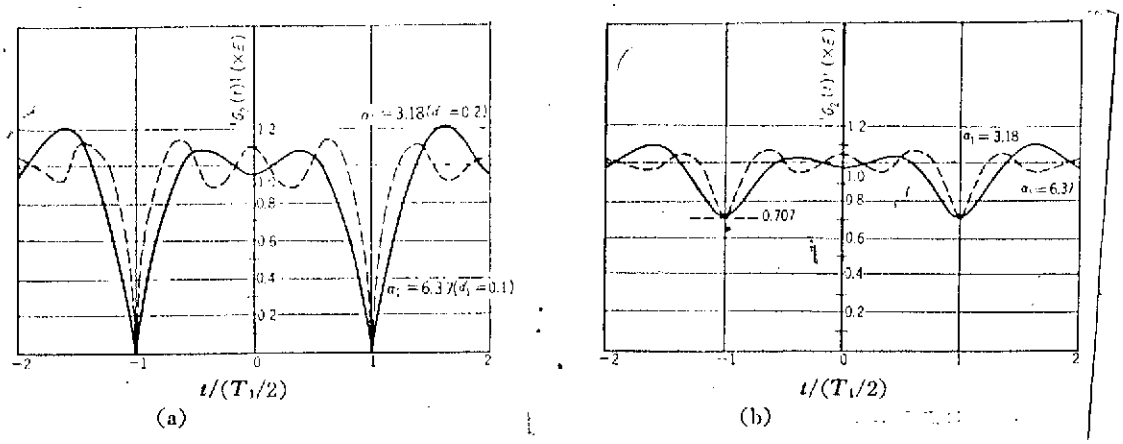

Figure 5. The amplitude distortion of a square PM pulse by an idealized filter.

a- at k = π; b- at k = π/2. Here $\alpha_1 = 2f_B/(1/T_1)$ where T_1 is the pulse amplitude and $2f_B$ is the pass bandwidth of the filter.

iii) When a wave passes through a Gaussian filter:

The characteristic of a Gaussian filter $f_{3_1}(\omega)$ is:

$$F_3(\omega) = e^{-\alpha(\omega-\omega_0)^2}$$
$$\alpha = \left(0.589 - \frac{1}{\Delta\omega_B/2}\right)^2, \quad \Delta\omega_B = 2\pi \cdot \Delta F_B \tag{6}$$

where the phase shift is neglected and ΔF_B is the 3 dB bandwidth. Consequently, the output spectrum is $F_1(\omega) \cdot F_3(\omega)$ and the output wave form $G_3(t)$ can be given as follows:

$$G_3(t) = \frac{1}{2\pi}\int_{-\infty}^{\infty} F_1(\omega)\cdot F_3(\omega)e^{j\omega t}d\omega$$
$$= \frac{E\cdot e^{j\omega_0 t}}{2\pi}\int_{-\infty}^{\infty}\left[S_a(f-f_0) - (1-e^{jk})\right.$$
$$\left.\cdot\frac{2\sin(\omega-\omega_0)T_1/2}{\omega-\omega_0}\right]e^{-\alpha(\omega-\omega_0)^2}\cdot e^{j(\omega-\omega_0)t}d\omega \tag{7}$$
$$= E\left[1-(1-e^{jk})\frac{1}{2}\left\{\varepsilon_{rf}\left(\frac{1+x_1}{d_2}\right)\right.\right.$$
$$\left.\left.+\varepsilon_{rf}\left(\frac{1-x_2}{d_2}\right)\right\}\right]e^{j\omega_0 t}$$

/108

where

$$d_2=\frac{4\sqrt{2}}{T_1},\quad \varepsilon_{rf}(z)=\frac{2}{\sqrt{\pi}}\int_0^z e^{-u^2}du$$

Therefore, for

$$g_3(t)\equiv\frac{\sqrt{2(1-\cos k)}}{2}\left\{\varepsilon_{rf}\left(\frac{1+x_1}{d_2}\right)+\varepsilon_{rf}\left(\frac{1-x_1}{d_2}\right)\right\}-$$

$$G_3(t)=E\{1+g_3(t)^2-2g_3(t)\cos\xi\}^{1/2}\cdot e^{j\left(\omega_0 t-\tan^{-1}\frac{g_3(t)\sin\xi}{1-g_3(t)\cos\xi}\right)} \qquad (8)$$

Consequently, at k = π,

$$G_3(t)=E\left\{1-\left\{\varepsilon_{rf}\left(\frac{1+x_1}{d_2}\right)+\varepsilon_{rf}\left(\frac{1-x_1}{d_2}\right)\right\}\right\}e^{j\omega_0 t} \qquad (8')$$

and at k = π/2,

$$G_3(t)=E\left\{1+g_3(t)^2-\sqrt{2}\,g_3(t)\right\}^{\frac{1}{2}}\cdot e^{j\left(\omega_0 t-\tan^{-1}\frac{g_3(t)}{\sqrt{2}-g_3(t)}\right)}$$

where

$$g_3(t)=\frac{1}{\sqrt{2}}\left\{\varepsilon_{rf}\left(\frac{1+x_1}{d_2}\right)+\varepsilon_{rf}\left(\frac{1-x_1}{d_2}\right)\right\}$$

/109

and, therefore, for $\alpha_2\equiv\frac{\Delta F_n}{1/T_1}$, $d_2=\frac{2.356}{\pi}\cdot\frac{1}{\alpha_2}$, and for the cases of α_2 = 1, 1.5, and 3, $F_1(\omega)\cdot F_3(\omega)$ and Equation (8') can be given as in Figures 6, 7a, and b.

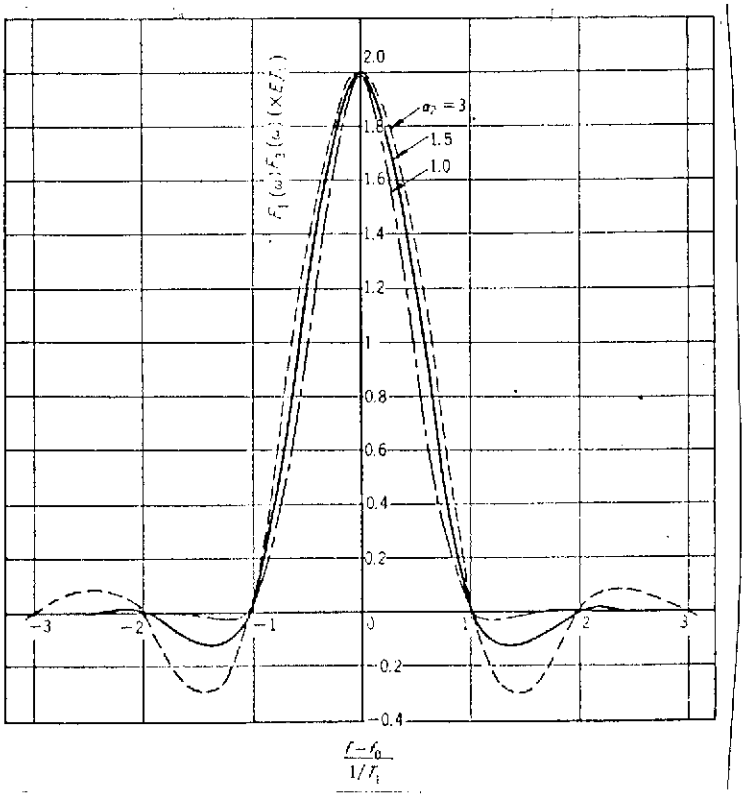

Figure 6. The spectrum of a square PM pulse under the Gaussian distribution (at h = π).

3.1.2. The Gaussian PM pulse

i) The wave form and the spectrum:

An idealized Gaussian PM pulse, as shown in Figure 3, is

$$G_1(t) = E \cdot e^{j(\omega_0 t + \varphi(t))}, \quad \varphi(t) = k e^{-at^2} \tag{9}$$

where $a = \left(\frac{1.665}{T_2}\right)^2$, T_2 shows the half-width of the phase modulation. The above formulas can be written as

$$\left.\begin{aligned} G_1(t) &= E \cdot e^{j\omega_0 t} \cdot e^{j\varphi(t)} = E \cdot e^{j\omega_0 t} \sum_{n=0}^{\infty} j^n \frac{\varphi(t)^n}{n!} \\ &= E\left(1 + \sum_{n=1}^{\infty} j^n \frac{k^n}{n!} e^{-nat^2}\right) e^{j\omega_0 t} \end{aligned}\right\} \tag{9'}$$

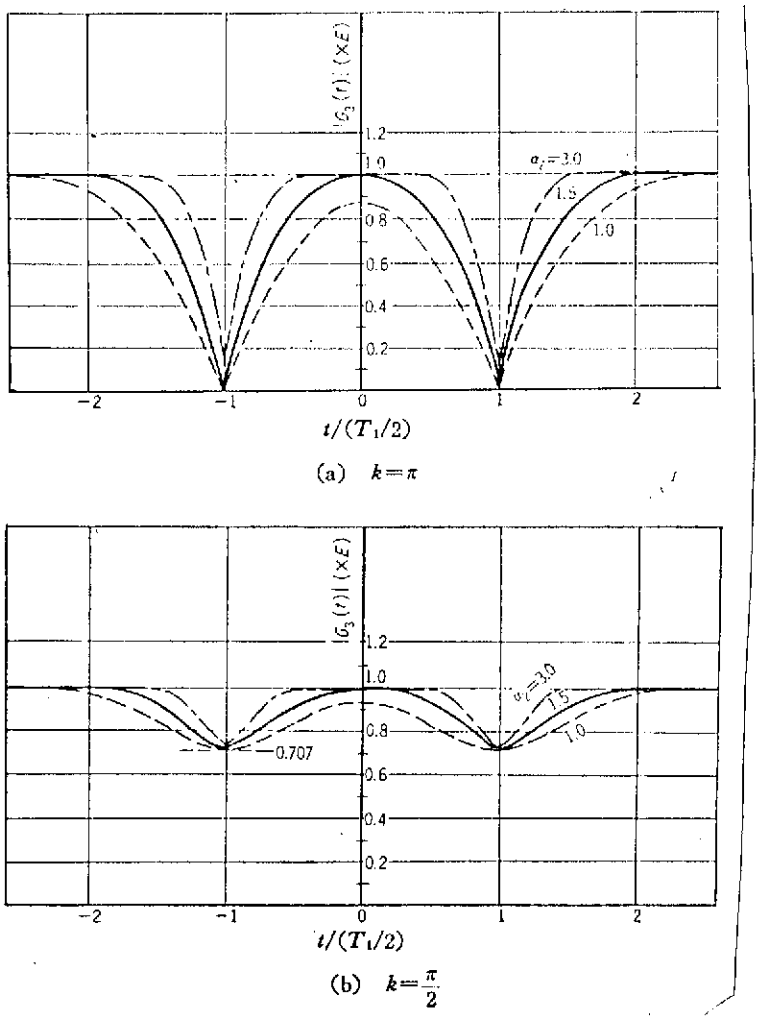

Figure 7. The amplitude distortion of a square PM pulse by a Gaussian filter. Here $\alpha_2=\Delta F_B/(1/T_1)$, where T_1 is the pulse amplitude and ΔF_B is the 3 dB width of the Gaussian filter.

and, therefore, $F_4(\omega)$ can be written as /110

$$\begin{aligned} F_4(\omega) &= \int_{-\infty}^{\infty} G_4(t) e^{-j\omega t} dt \\ &= E\left[\int_{-\infty}^{\infty} e^{-j(\omega-\omega_0)t} dt \right. \\ &\left. + \int_{-\infty}^{\infty} \sum_{n=1}^{\infty} j^n \frac{k^n}{n!} e^{-n\alpha t^2} \cdot e^{-j(\omega-\omega_0)t} dt \right] \end{aligned} \tag{10}$$

$$
\begin{aligned}
&= E\left[S_0(f-f_0) + \sum_{n=1}^{\infty} j^n \frac{k^n}{n!} \cdot \sqrt{\frac{\pi}{na}} \cdot e^{-\frac{(\omega-\omega_0)^2}{4na}}\right] \\
&= E \cdot S_0(f-f_0) \\
&+ E \cdot \sqrt{\frac{\pi}{a}}\left[\left\{-\frac{k^2}{2!\sqrt{2}} e^{-\frac{(\omega-\omega_0)^2}{2\cdot 4a}} + \frac{k^4}{4!\sqrt{4}} e^{-\frac{(\omega-\omega_0)^2}{4\cdot 4a}} - \cdots\right\}\right. \\
&\left. + j\left\{k e^{-\frac{(\omega-\omega_0)^2}{4a}} - \frac{k^3}{3!\sqrt{3}} e^{-\frac{(\omega-\omega_0)^2}{3\cdot 4a}} + \frac{k^5}{5!\sqrt{5}} \cdot e^{-\frac{(\omega-\omega_0)^2}{5\cdot 4a}} - \cdots\right\}\right]
\end{aligned}
\qquad (10)
$$

From (9') and (10), one sees that a Gaussian PM pulse consists of a carrier wave and the perpendicular Gaussian AM pulse group. Hence, if ΔF is the 3 dB width of the Gaussian AM pulse spectrum with a half-width T_2,

$$
\Delta F = \frac{0.624}{T_2}, \quad \frac{(\omega-\omega_0)^2}{4a} = \left(1.178 \frac{f-f_0}{\Delta F}\right)^2
$$

With these values, for the cases of $k = \pi$ and $\pi/2$, Equation (10) can be shown as in Figures 8a and b. One can compare the envelope with the Gaussian AM pulse as in Figure 9a.

From the figure, one sees that, in the region of $|f-f_0/\Delta F|<1$, these two cases almost coincide and, therefore, the 3 dB width of the Gaussian PM pulse is also ΔF, but in the region of $|f-f_0/\Delta F|>1$, the PM case, it is extremely great. Hence, the idealized PM pulse, as compared to the AM pulse with the same modulated wave form (in a finite time duration), is characterized by the presence of an extremely large area in the spectrum. /111

In the numerical computation of Formula (10), it is problematical how many terms should be retained in the series expansion. For this reason, in Table 1, the series convergence of Formulas (9') and (10) is shown. For $k = \pi$, the expansion should proceed up to $n = 11$, and for $k = \pi/2$, it should go to $n = 7$ in order to limit the error to 1%.

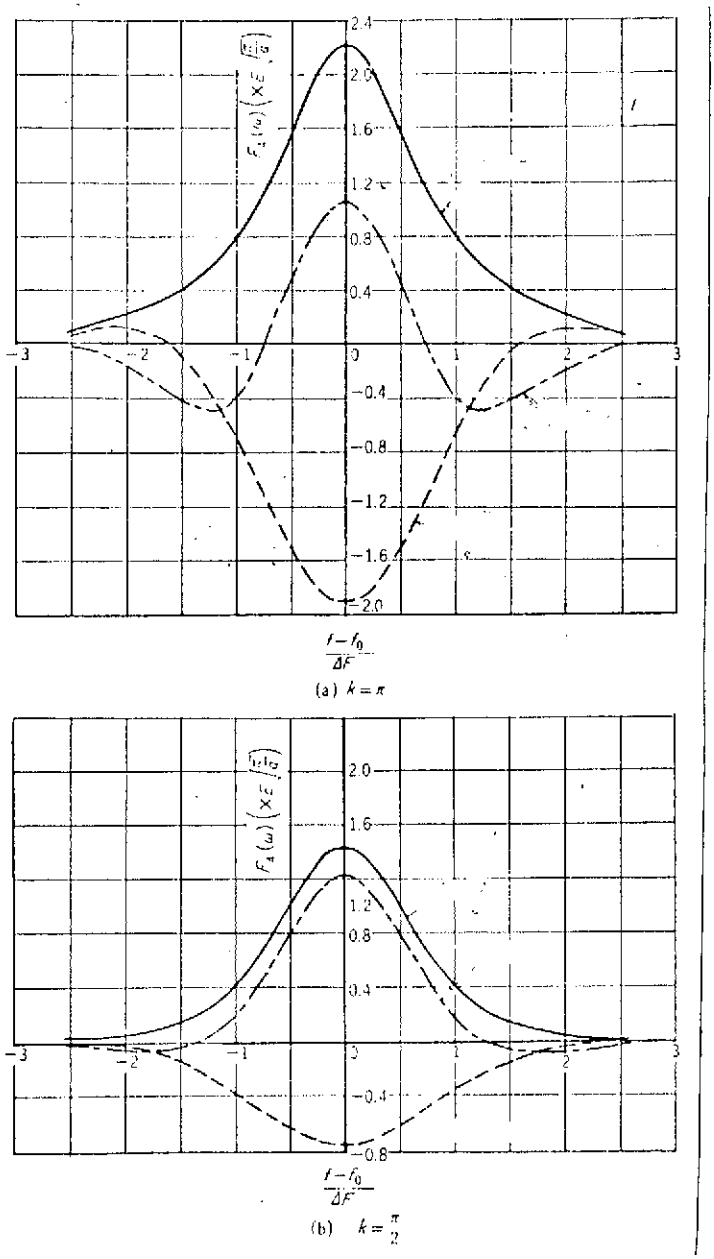

Figure 8. The spectrum of a Gaussian PM pulse.
—— envelope; — - —— perpendicular component; —-- in-phase component.

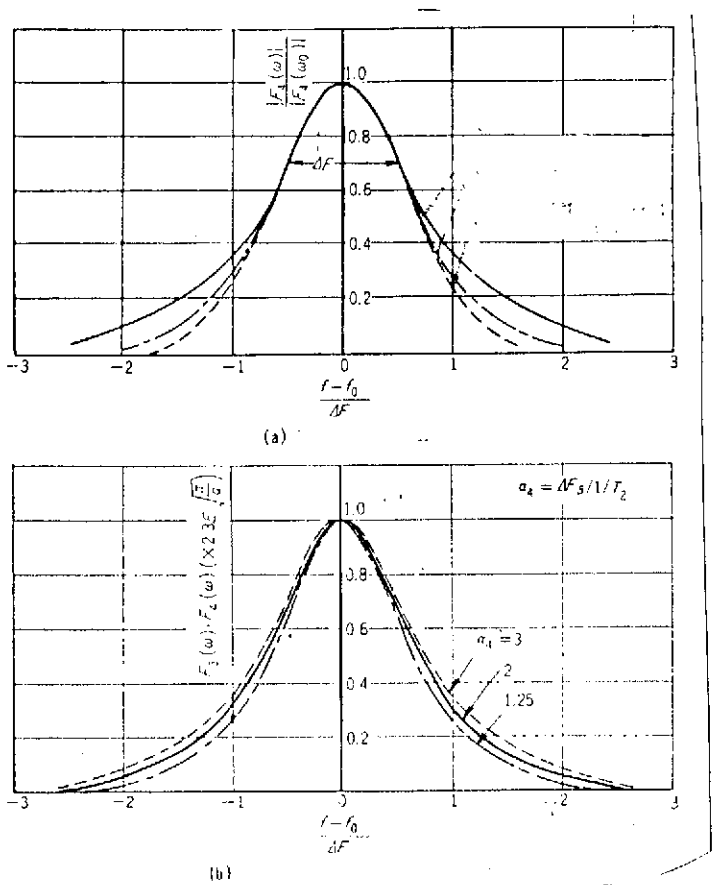

Figure 9. The spectrum of a Gaussian PM pulse.

a- comparison with the AM pulse; b- the case with a Gaussian distribution ($k = \pi$). —— Gaussian PM pulse, $k = \pi$; — - — Gaussian PM pulse, $k = \pi/2$; --- Gaussian PM pulse, $k \ll 1$, and Gaussian AM pulse.

ii) When the wave passes through an idealized filter:

The characteristics of an idealized filter are shown in Formula (3) and, therefore, the output spectrum is $F_2(\omega)\cdot F_4(\omega)$ and the output wave form $G_3(t)$ can be written as:

$$G_3(t) = \frac{1}{2\pi}\int_{-\infty}^{\infty} F_2(\omega)\cdot F_4(\omega)e^{j\omega t}d\omega$$
$$= \frac{E}{2\pi}\left[\int_{\omega_0-\omega_B}^{\omega_0+\omega_B} S_i(f-f_0)e^{j\omega t} + e^{j\omega_0 t}\right] \qquad (11)$$

TABLE 1

VALUES OF $k^n/n!$

n	$k^n/n!$			
	$k=\pi$	$k=\pi/2$	$k=\pi/4$	$k=\pi/8$
1	3.1416	1.5708	0.7854	0.3927
2	4.935	1.234	0.308	0.0771
3	5.168	0.646	0.0807	0.0101
4	4.059	0.253	0.0158	0.000988
5	2.550	0.0797	0.00249	
6	1.335	0.0209	0.000326	
7	0.599	0.00468		
8	0.235	0.00092		
9	0.0821			
10	0.0258			
11	0.00737			
12	0.00192			

$$\cdot\int_{\omega_0-\omega_B}^{\omega_0+\omega_B}\sum_{n=1}^{\infty} j^n\frac{k^n}{n!}\sqrt{\frac{\pi}{a}}\,e^{-\frac{(\omega-\omega_0)^2}{4na}}\,e^{j(\omega-\omega_0)t}d\omega\Big]$$

$$=E\cdot e^{j\omega_0 t}\Big[1+\frac{1}{2\pi}\int_{-\omega_B}^{\omega_B}\sum_{n=1}^{\infty} j^n\frac{k^n}{n!}\cdot\sqrt{\frac{\pi}{na}}\,e^{-\frac{\omega^2}{4na}}\cdot e^{j\omega t}d\omega\Big] \tag{11}$$

$$=E\cdot e^{j\omega_0 t}\Big[1+\sum_{n=1}^{\infty} j^n\frac{k^n}{n!}e^{-nat^2}\cdot\mathrm{Re}\cdot\varepsilon_{rf}\Big(\frac{\omega_B}{2\sqrt{na}}-j\sqrt{na}\,t\Big)\Big]$$

where

$$\mathrm{Re}\cdot\varepsilon_{rf}(x+jy)=\mathrm{Re}\cdot\frac{2}{\sqrt{\pi}}\int_0^{x+jy}e^{-z^2}dz$$

ORIGINAL PAGE IS
OF POOR QUALITY

One can rewrite the above formula as:

$$
\begin{aligned}
G_5(t) &= |G_5(t)| \cdot e^{j(\omega_0 t+\varphi_5(t))} = E\{\mathrm{Re}(t)^2 \\
&\quad + \mathrm{Im}(t)^2\}^{1/2} \cdot e^{j\left(\omega_0 t+\tan^{-1}\frac{\mathrm{Im}(t)}{\mathrm{Re}(t)}\right)} \\
\mathrm{Re}(t) &= 1-\frac{k^2}{2!}e^{-2at^2} \\
&\quad \cdot \mathrm{Re}\cdot\varepsilon_{rf}\left(\frac{\omega_n}{2\sqrt{2a}}-j\sqrt{2a}\,t\right)+\frac{k^4}{4!}e^{-4at^2} \\
&\quad \cdot \mathrm{Re}\cdot\varepsilon_{rf}\left(\frac{\omega_n}{2\sqrt{4a}}-j\sqrt{4a}\,t\right)-\cdots\cdots \\
\mathrm{Im}(t) &= ke^{-at^2}\mathrm{Re}\cdot\varepsilon_{rf}\left(\frac{\omega_n}{2\sqrt{a}}-j\sqrt{a}t\right) \\
&\quad -\frac{k^3}{3!}e^{-3at^2}\cdot\mathrm{Re}\cdot\varepsilon_{rf}\left(\frac{\omega_n}{2\sqrt{3a}}-j\sqrt{3a}\,t\right) \\
&\quad +\cdots\cdots \\
&\quad \mathrm{Re}\cdot\varepsilon_{rf}\left(\frac{\omega_n}{2\sqrt{na}}-j\sqrt{na}\,t\right) \\
&= \frac{2}{\sqrt{\pi}}\left[\frac{0.942}{\sqrt{n}}\alpha_3+\sum_{m=1}^{\infty}(-1)^m\frac{\left\{\left(\frac{0.942}{\sqrt{n}}\alpha_3\right)^2+(0.833\sqrt{n}x_2)^2\right\}^{\frac{2m+1}{2}}}{m!(2m+1)}\right. \\
&\quad \left.\cdot\cos\left\{(2m+1)\tan^{-1}\frac{0.833\sqrt{n}x_2}{\frac{0.942}{\sqrt{n}}\alpha_3}\right\}\right]
\end{aligned}
\tag{12}
$$

where

$$x_2=\frac{t}{T_2\sqrt{2}}\ ,\quad \alpha_3=\frac{2f_n}{1/T_2}\ \text{is assumed.}$$

Consequently, for α_3 = 1.25, 2.0, and 2.5, and for the cases of k = π and k = $\pi/2$, Equation (12) can be calculated for $|G_5(t)|$ and $\varphi_3(t)$, as in Figures 10a and b, and Figures 11a and b, respectively. In Figure 10, one sees that, for k = π, the amplitude does not reach the zero value as in Figure 5, while for k = $\pi/2$, with α_3 > 2.5 and for k = $\pi/2$ with α_3 > 2, the distortion in the amplitude and the phase is generally very small.

In the numerical computation of Equation (12), the value of n has been discussed in i). In computing $|\mathrm{Re}\cdot\varepsilon_{rf}(\ )|$, the value of m is determined by: /112

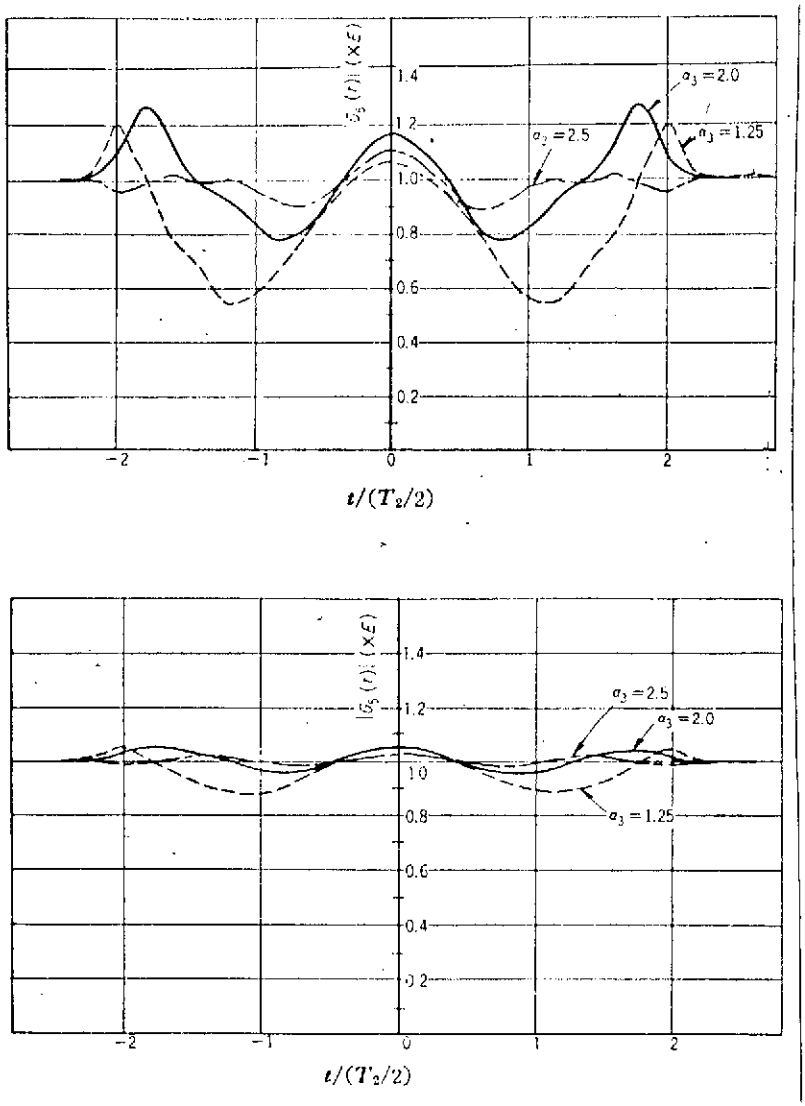

Figure 10. The amplitude distortion of the Gaussian PM pulse by an idealized filter.

a- for k = π; b- for k = π/2; $\alpha_3 = 2f_B/(1/T_2)$; T_2- half-width of the Gaussian phase modulation; $2f_B$- pass bandwidth of the filter.

$$\left\{\left(\frac{0.912}{\sqrt{n}}\alpha_3\right)^2 + (0.833\sqrt{n}\,x_2)^2\right\}^{1/2} = z,$$

and for each value of z, that of m is shown in Table 2; the error, in general, is very small. Now for $\alpha_3 < 2.5$, the smaller n, the larger the value

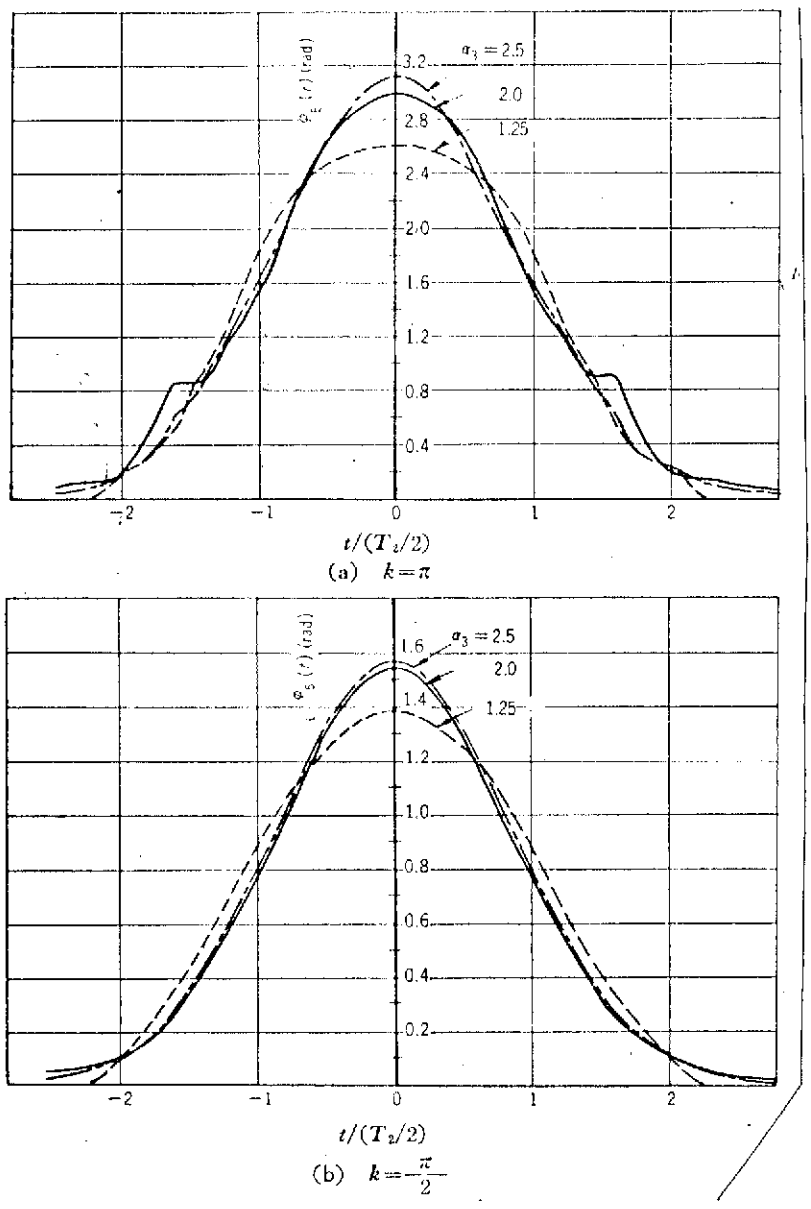

Figure 11. The phase distortion of a Gaussian PM pulse by an idealized filter.

of x_2. For the values of n, the limits of x_2 are shown in Table 3 up to m = 40.

From Equation (11) one sees that $G_*(t)$ consists of the carrier wave and the perpendicular Gaussian AM pulse group which has passed the idealized filter.

*Illegible subscript.

TABLE 2

THE RELATIONSHIP BETWEEN m AND z

z	1	2	3	4	5
m	6	12	25	50	100

TABLE 3 /113

THE RELATIONSHIP BETWEEN n AND x_2

n	1	2	3	4	5	6	7	8	9	10	11
x_2	3.0	2.0	1.8	1.6	1.4	1.4	1.2	1.2	1.0	1.0	1.0

iii) When a wave passes through a Gaussian filter:

The characteristic of a Gaussian filter is shown in (6). Consequently, the output spectrum is $F_3(\omega)\cdot F_4(\omega)$ and the output wave form $G_6(t)$ is shown as follows:

$$\begin{aligned} G_6(t) &= \frac{1}{2\pi}\int_{-\infty}^{\infty} F_3(\omega)\cdot F_4(\omega)e^{j\omega t}d\omega \\ &= \frac{E}{2\pi}\int_{-\infty}^{\infty} S_a(f-f_0)+\sum_{n=1}^{\infty} j^n\frac{k^n}{n!} \\ &\quad \cdot\sqrt{\frac{\pi}{na}}\cdot e^{-\frac{(\omega-\omega_0)^2}{4na}}\Big]\cdot e^{-n(\omega-\omega_0)^2}\cdot e^{j\omega t}d\omega \\ &= E\cdot e^{j\omega_0 t}\Big\{1+\sum_{n=1}^{\infty} j^n\frac{k^n}{n!}\cdot\frac{1}{\sqrt{1+n(\Delta F/\Delta F_B)^2}} \\ &\quad \cdot e^{-\frac{n(1.665t/T_2)^2}{1+n(\Delta F/\Delta F_B)^2}}\Big\} \end{aligned} \tag{13}$$

/114

One can rewrite it as follows:

$$\begin{aligned} G_6(t) &\equiv |G_6(t)|\cdot e^{j(\omega_0 t+\varphi_6(t))} = E\{[\mathrm{Re}(t)^2 \\ &\quad +\mathrm{Im}(t)^2]^{1/2}\cdot e^{j\left(\omega_0 t+\tan^{-1}\frac{\mathrm{Im}(t)}{\mathrm{Re}(t)}\right)} \\ &\quad \mathrm{Re}(t) = 1-\frac{k^2}{2!}\cdot\frac{1}{\sqrt{1+2\alpha_5^2}}\cdot e^{-\frac{2(0.833x_2)^2}{1+2\alpha_5^2}} \\ &\quad +\frac{k^4}{4!}\cdot\frac{1}{\sqrt{1+4\alpha_5^2}}\cdot e^{-\frac{4(0.833x_2)^2}{1+4\alpha_5^2}}-\cdots\cdots \\ &\quad \mathrm{Im}(t) = k-\frac{1}{\sqrt{1+\alpha_5^2}}\cdot e^{-\frac{(0.833x_2)^2}{1+\alpha_5^2}} \\ &\quad -\frac{k^3}{3!}\cdot\frac{1}{\sqrt{1+3\alpha_5^2}}\cdot e^{-\frac{3(0.833x_2)^2}{1+3\alpha_5^2}}+\cdots\cdots\Big] \end{aligned} \tag{14}$$

where

$$x_2 \triangleq \frac{t}{T_2/2}, \quad \alpha_3 = \frac{\Delta F}{\Delta F_B} \text{とする.}$$

If $\alpha_4 = \Delta F_B/(1/T_2)$, then $\alpha_3 = 0.624/\alpha_4$, and for α_4 = 1.25, 2.0, and 3.0, Equation (14) can be calculated for k = π and $\pi/2$. Thus, $|G_6(t)|$ and $\varphi_6(t)$ can be shown as in Figures 12a and b and Figures 13a and b, respectively. The envelope of the spectrum $F_3(\omega) \cdot F_4(\omega)$ is shown in Figure 9b. In Figures 12 and 13, one sees that, for $\alpha_4 > 2$ and k = $\pi/2$, the distortion in the amplitude and the phase is very small. In short, the PM pulse, from the comparison /115
between Figures 7 and 12, is found to be affected very insignificantly by the restriction of a band distribution. This fact agrees with the experimental results given in [8].

3.2. The Amplitude Characteristics of a 1-Cycle Pulse: the Activities in the Small Signal Region

By comparing the above disucssion with the experimental results [2 — 8] on the wave forms of PM pulses which have been reported up to the present, one sees that, in the above four kinds of PM pulses, the two kinds — namely the square and Gaussian PM pulse — which are affected by the restriction of a Gaussian band distribution are close to some realistic wave forms. Consequently, we will discuss various different cases in which these two kinds of wave forms are assumed to be the input PM pulses, being sent through the traveling wave tubes. However, we start out with a simple case, namely to discuss the activities of a 1-cycle pulse amplitude in the region of small signals to study its gain and the frequency number characteristics of its phase. When the circuit is assumed to be linear and, thus, Fourier transformation is applicable, such effects can be exactly studied theoretically.

The order of our discussion is as follows. First, we will consider the /116
experimental results of the frequency number characteristics in millimeter wave double ladder traveling wave tubes. Then we will discuss the first linear slope of

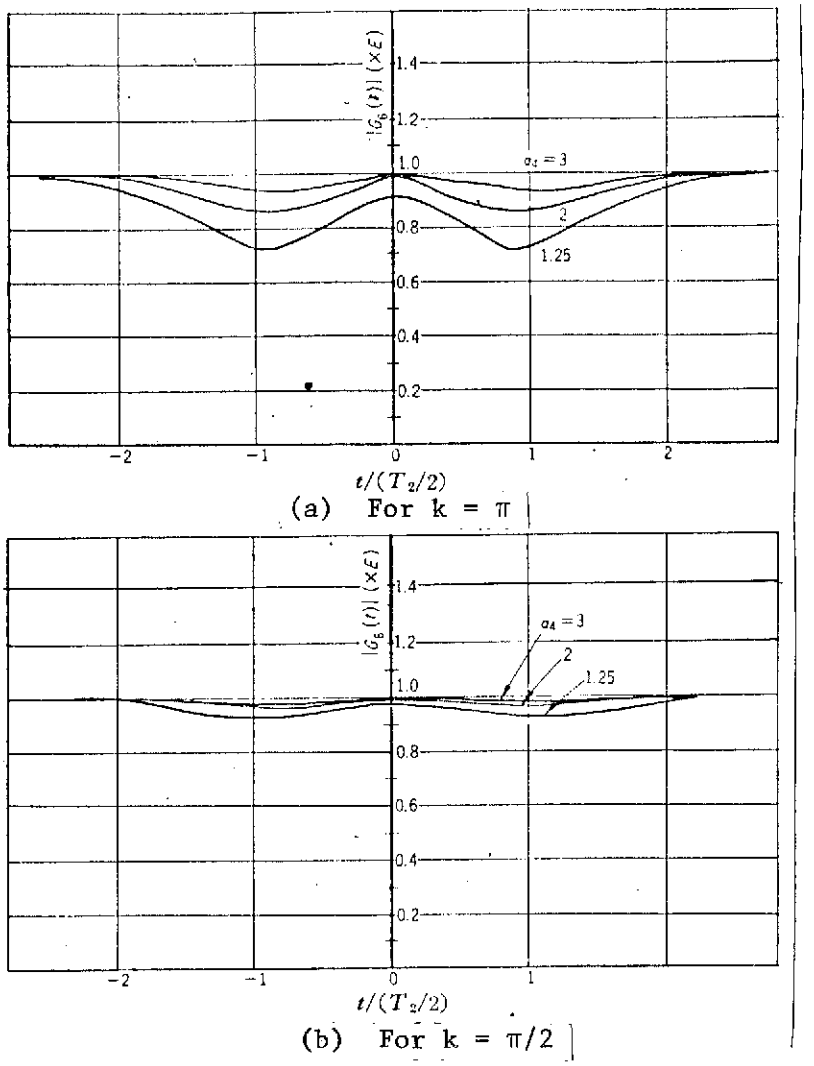

Figure 12. The amplitude distortion of a Gaussian PM pulse by a Gaussian filter.

Here $\alpha_4 = \Delta F_B/(1/T_2)$, where T_2 is the half-width of the Gaussian phase modulation and ΔF_B is the 3 dB width of a Gaussian filter.

the gain and the effect on the second order component of the phase. Finally, we will discuss the effects of higher order components of the gain and the phase (Fourier components).

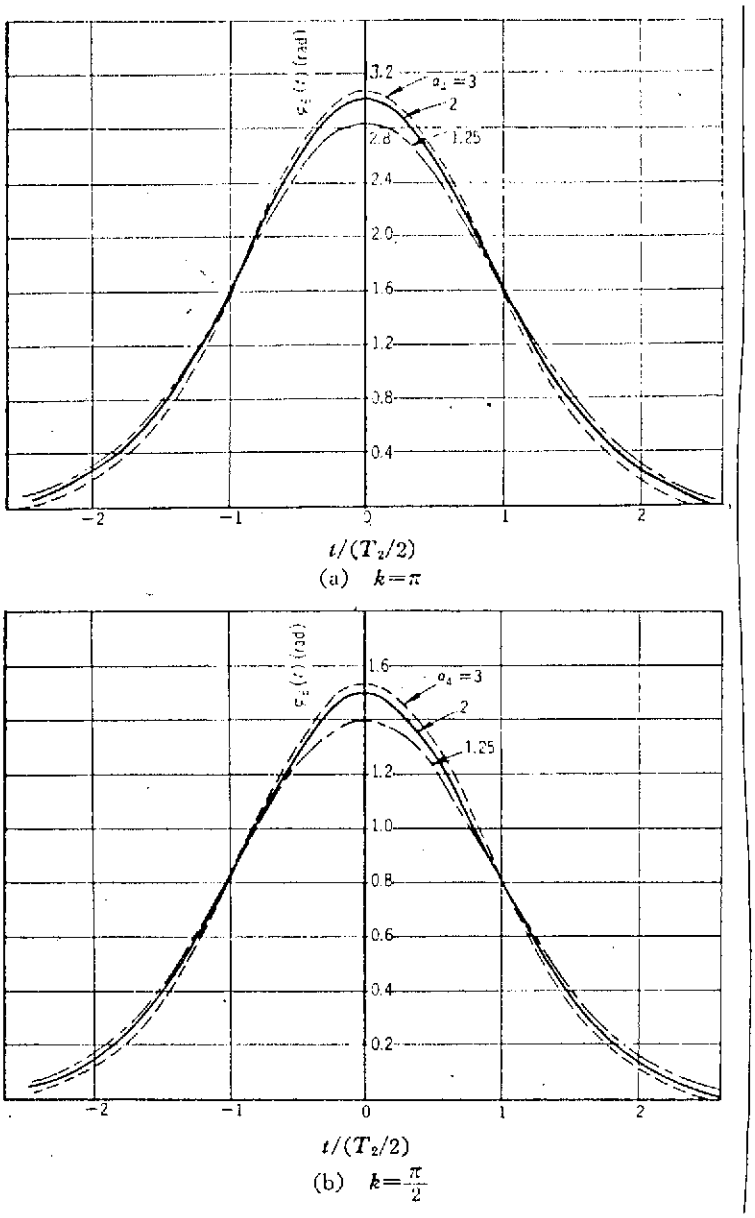

Figure 13. The phase distortion of a Gaussian PM pulse due to a Gaussian filter.

3.2.1. The distortion due to the first linear slope of the gain and the second order of the phase

The characteristics of the gain and the phase frequency number of the millimeter wave double ladder traveling wave tubes have been reported earlier [1]. In the small signal region, the gain $G_{os}(\omega)$ consists of the sum of the

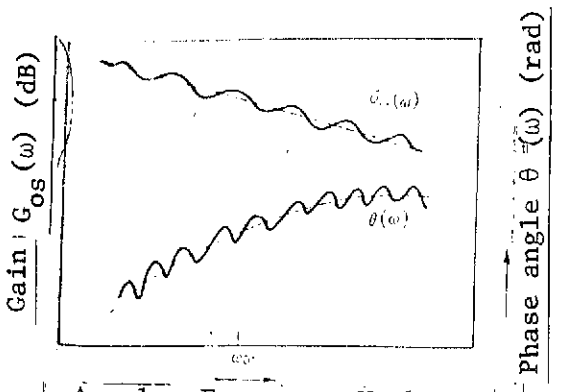

a) General characteristics

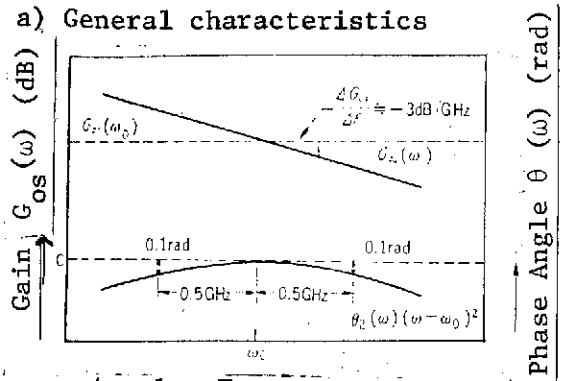

b) First order component of the gain and the second order component of the phase

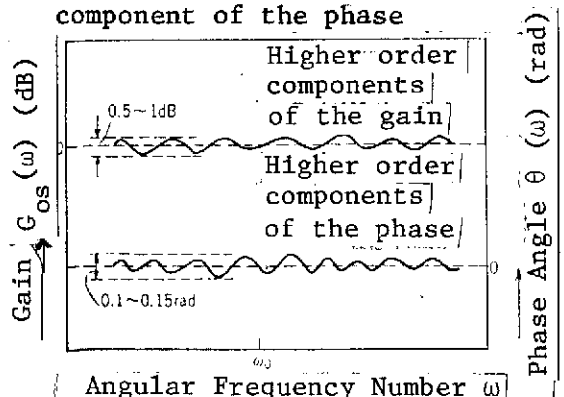

c) Ripple components.

Figure 14. Characteristics of the gain and the phase frequency number (numerical values are from the experiments in millimeter wave double ladder type traveling wave tubes).

first linear slope and higher order components and the terminal phase shift $\theta(\omega)$ of the output power can be approximated by the first order, second order component, and then higher order components (see Figure 14a). If one neglects higher orders, they can be shown as:

$$G_{os}(\omega) \fallingdotseq G_{os}(\omega_0) - \frac{\Delta G_{os}}{\Delta\omega}(\omega-\omega_0)\,(\mathrm{dB}) \qquad (15)$$

$$\theta(\omega) \fallingdotseq \theta_0(\omega_0) + \theta_1(\omega_0)(\omega-\omega_0) - \theta_2(\omega_0)(\omega-\omega_0)^2 \quad (\mathrm{rad}) \qquad (16)$$

In $G_{os}(\omega_0)$, $\theta_0(\omega_0)$ and $\theta_1(\omega_0)(\omega-\omega_0)$ no distortion appears, because the distortion begins to show up in $\frac{\Delta G_{os}}{\Delta\omega}(\omega-\omega_0)$ and $\theta_2(\omega_0)(\omega-\omega_0)^2$, and other higher order components. In Figures 14b and c, such components are especially apparent.

Although we have to discuss the effects in these terms, for the convenience of analysis, $G_{os}(\omega)$ and $\theta(\omega)$ are considered simultaneously, but in higher orders, they are studied separately. Equation (15) can be expressed in terms of the electric voltage gain $g_{os}(\omega)$.

From

$$G_{os}(\omega)=10\log_{10}g_{os}^{2}(\omega),$$

$$G_{os}(\omega_0)=10\log_{10}g_{os}^{2}(\omega_0),$$

$$-\frac{\Delta G_{os}}{\Delta\omega}=10\log_{10}e^{-\frac{1}{4.34}\cdot\frac{\Delta G_{os}}{\Delta\omega}}$$

$$g_{os}(\omega)=g_{os}(\omega_0)\cdot e^{-\frac{1}{8.68}\cdot\frac{\Delta G_{os}}{\Delta\omega}(\omega-\omega_0)} \tag{15'}$$

i) When the input power is in the form of a square PM pulse until the restriction of a Gaussian band distribution:

The wave form and the spectrum of such an input pulse are shown by $G_3(t)$ of Equations (7) and (2), and by $F_1(\omega)\cdot F_3(\omega)$ of Equation (6) (see Figures 6 and 7). Hence,

$$G_3(t)=E\left\{1-(1-e^{jk})\frac{1}{2}\left\{\varepsilon_{rf}\left(\frac{1+x_1}{d_2}\right)+\varepsilon_{rf}\left(\frac{1-x_1}{d_2}\right)\right\}\right\}e^{j\omega_0 t} \tag{7}$$

$$F_1(\omega)\cdot F_3(\omega)=E\left\{S_0(f-f_0)-(1-e^{jk})\frac{2\sin(\omega-\omega_0)T_1/2}{\omega-\omega_0}\right\}\cdot e^{-\alpha(\omega-\omega_0)x} \tag{17}$$

However, the frequency number characteristic $F(\omega)$ of a traveling wave tube can be written with Equations (15) and (16) as /117

$$F(\omega)=g_{os}(\omega_0)\cdot e^{-b(\omega-\omega_0)}\cdot e^{-j[\theta_0+\theta_1(\omega-\omega_0)-\theta_2(\omega-\omega_0)^2]} \tag{18}$$

where $b=\frac{1}{8.68}\cdot\frac{\Delta G_{os}}{\Delta\omega}(\mathrm{dB})$

and $\theta_0(\omega_0)$, $\theta_1(\omega_0)$, $\theta_2(\omega)_0$, are expressed by θ_0, θ_1, θ_2. The spectrum $F_7(\omega)$ is the wave form $G_7(t)$ of the output pulse and can be obtained from

$$F_7(\omega)=F_1(\omega)\cdot F_3(\omega)\cdot F(\omega) \tag{19}$$

$$G_7(t)=\frac{1}{2\pi}\int_{-\infty}^{\infty}F_7(\omega)e^{j\omega t}d\omega \tag{20}$$

For the convenience of the calculation, we now consider the term of $e^{-b(\omega-\omega_0)}$ where

$$b(\omega-\omega_0)=\frac{1}{8.68}\cdot\frac{dG_{os}}{d\omega}(\omega-\omega_0)$$

in which $dG_{os}/df=3\,\mathrm{dB/GHz}$ (see Figure 14b), and $|f-f_0|<0.7\,\mathrm{GHz}$ ($T_1=3\,\mathrm{ns}$ from Figure 6). Hence, $|b(\omega-\omega_0)|<0.25$, so that $e^{-b(\omega-\omega_0)}\fallingdotseq 1-b(\omega-\omega_0)$

Since

$$\frac{E\cdot g_{os}(\omega_0)}{2\pi}\int_{-\infty}^{\infty}S_0(f-f_0)\cdot e^{-\alpha(\omega-\omega_0)^2}\cdot e^{-b(\omega-\omega_0)}\cdot e^{-j[\theta_0+\theta_1\cdot(\omega-\omega_0)-\theta_2(\omega-\omega_0)^2]}\cdot e^{j\omega t}d\omega=E\cdot g_{os}(\omega_0)\cdot e^{j(\omega_0 t-\theta_0)}$$

it can be substituted into Equation (20)

$$\begin{aligned}G_7(t)=E\cdot g_{os}(\omega_0)\cdot e^{j(\omega_0 t-\theta_0)}\Bigg[1-(1-e^{jk})\frac{1}{2\pi}\int_{-\infty}^{\infty}\frac{2\sin(\omega-\omega_0)T_1/2}{\omega-\omega_0}\cdot e^{-\alpha(\omega-\omega_0)^2}\\ \cdot e^{-j[\theta_1(\omega-\omega_0)-\theta_2(\omega-\omega_0)^2]}\cdot e^{j(\omega-\omega_0)t}d\omega+b(1-e^{jk})\cdot\frac{1}{2\pi}\int_{-\infty}^{\infty}2\sin(\omega-\omega_0)\frac{T_1}{2}\cdot e^{-\alpha(\omega-\omega_0)^2}\\ \cdot e^{-j[\theta_1(\omega-\omega_0)-\theta_2(\omega-\omega_0)^2]}\cdot e^{j(\omega-\omega_0)t}d\omega=E\cdot g_{os}(\omega_0)\cdot e^{j(\omega_0 t-\theta_0)}\Bigg[1-(1-e^{jk})\cdot\frac{1}{2}\\ \cdot\left\{\varepsilon_{rf}\left(\frac{T_1/2+t-\theta_1}{2(\alpha^2+\theta_2^2)^{1/4}}\cdot e^{j(1/2)\tan^{-1}(\theta_2/\alpha)}\right)+\varepsilon_{rf}\left(\frac{T_1/2-(t-\theta_1)}{2(\alpha^2+\theta_2^2)^{1/4}}\cdot e^{j(1/2)\tan^{-1}(\theta_2/\alpha)}\right)\right\}\\ -j(1-e^{jk})\cdot b\cdot\frac{1}{2\sqrt{\pi}(\alpha^2+\theta_2^2)^{1/4}}e^{j(1/2)\tan^{-1}(\theta_2/\alpha)}\cdot\left\{\exp\left(-\frac{(T_1/2+t-\theta_1)^2}{4(\alpha^2+\theta_2^2)^{1/2}}e^{j\tan^{-1}(\theta_2/\alpha)}\right)\right.\\ \left.-\exp\left(-\frac{(T_1/2-(t-\theta_1))^2}{4(\alpha^2+\theta_2^2)^{1/2}}\cdot e^{j\tan^{-1}(\theta_2/\alpha)}\right)\right\}\Bigg]\end{aligned} \tag{21}$$

Now, in considering the value of θ_2/α, from $\alpha=(1.178/2\pi\Delta F_B)^2$, $\Delta F_B<0.7\text{GHz}$, $\theta_2=0.1\text{rad}/(2\pi\cdot 0.5\text{GHz})^2$, and $\theta_2/\alpha<0.14$. Consequently,

$$e^{j(1/2)\tan^{-1}(\theta_2/\alpha)}\fallingdotseq 1+j\frac{1}{2}\cdot\frac{\theta_2}{\alpha},\quad (\alpha^2+\theta_2^2)^{1/4}=\sqrt{\alpha}\left\{1+\left(\frac{\theta_2}{\alpha}\right)^2\right\}^{1/4}\fallingdotseq\sqrt{\alpha}$$

can be put into the above equation to obtain

$$\begin{aligned}G_T(t)\fallingdotseq E\cdot g_{os}(\omega_0)\cdot e^{j(\omega_0 t-\theta_0)}\Bigg[1-\frac{(1-e^{jk})}{2}\Bigg\{&\varepsilon_{rf}\left(\frac{T_1/2+t-\theta_1}{2\sqrt{\alpha}}\left(1+j\frac{1}{2}\cdot\frac{\theta_2}{\alpha}\right)\right)\\&+\varepsilon_{rf}\left(\frac{T_1/2-(t-\theta_1}{2\sqrt{\alpha}}\left(1+j\frac{1}{2}\cdot\frac{\theta_2}{\alpha}\right)\right)\Bigg\}-jb(1-e^{jk})\cdot\frac{1+j(1/2)\cdot(\theta_2/\alpha)}{2\sqrt{\pi\alpha}}\\&\cdot\left\{\exp\left(-\frac{T_1/2+t-\theta_1)^2}{4\alpha}\left(1+j\frac{\theta_2}{\alpha}\right)\right)-\exp\left(-\frac{(T_1/2-(t-\theta_1))^2}{4\alpha}\left(1+j\frac{\theta_2}{\alpha}\right)\right)\Bigg\}\Bigg]\end{aligned}\qquad (21')$$

Now since /118

$$\begin{aligned}\varepsilon_{rf}\left(\frac{T_1/2\pm(t-\theta_1)}{2\sqrt{\alpha}}\left(1+j\frac{1}{2}\frac{\theta_2}{\alpha}\right)\right)\fallingdotseq&\varepsilon_{rf}\left(\frac{T_1/2\pm(t-\theta_1)}{2\sqrt{\alpha}}\right)+j\frac{1}{\sqrt{\pi}}\cdot\frac{\theta_2}{\alpha}\cdot\frac{T_1/2\pm(t-\theta_1)}{2\sqrt{\alpha}}\\&\cdot e^{-\left(\frac{T_1/2\pm(t-\theta_1)}{2\sqrt{\alpha}}\right)^2}\cdot\exp\left(-\frac{(T_1/2\pm(t-\theta_1))^2}{4\alpha}\left(1+j\frac{\theta_2}{\alpha}\right)\right)=\exp\cdot-\left(\frac{T_1/2\pm(t-\theta_1)}{2\sqrt{\alpha}}\right)^2\\&\cdot\left\{\cos\frac{\theta_2}{\alpha}\left(\frac{T_1/2\pm(t-\theta_1)}{2\sqrt{\alpha}}\right)^2-j\sin\frac{\theta_2}{\alpha}\left(\frac{T_1/2\pm(t-\theta_1)}{2\sqrt{\alpha}}\right)^2\right\}\end{aligned}$$

Equation (21') can again be rewritten as

$$\begin{aligned}G_T(t)\fallingdotseq E\cdot g_{os}(\omega_0)\cdot e^{j(\omega_0 t-\theta_0)}[1-(1-e^{jk})A(t)+j(1-e^{jk})B(t)]&A(t)=\frac{1}{2}\left\{\varepsilon_{rf}\left(\frac{1+x_3}{d_2}\right)\right.\\&\left.+\varepsilon_{rf}\left(\frac{1-x_3}{d_2}\right)+\frac{b}{2\sqrt{\pi\alpha}}\left\{-e^{-\left(\frac{1+x_3}{d_2}\right)^2}\sin\frac{\theta_2}{\alpha}\left(\frac{1+x_3}{d_2}\right)^2+e^{-\left(\frac{1-x_3}{d_2}\right)^2}\sin\frac{\theta_2}{\alpha}\left(\frac{1-x_3}{d_2}\right)^2\right\}\right]\\B(t)=&\left\{\frac{-1}{2\sqrt{\pi}}\cdot\frac{\theta_2}{\alpha}\cdot\frac{1+x_3}{d_2}-\frac{b}{2\sqrt{\pi\alpha}}\cos\frac{\theta_2}{\alpha}\left(\frac{1+x_3}{d_2}\right)^2\right\}\cdot e^{-\left(\frac{1+x_3}{d_2}\right)^2}\\&+\left\{\frac{-1}{2\sqrt{\pi}}\cdot\frac{\theta_2}{\alpha}\cdot\frac{1-x_3}{d_2}+\frac{b}{2\sqrt{\pi\alpha}}\cos\frac{\theta_2}{\alpha}\left(\frac{1-x_3}{d_2}\right)^2\right\}\cdot e^{-\left(\frac{1-x_3}{d_2}\right)^2}\end{aligned}\qquad (22)$$

where

$$x_3=\frac{t-\theta_1}{T_1/2},\quad d_2=\frac{4\sqrt{\alpha}}{T_1}$$

For k = π,

$$G_7(t)=E\cdot g_{os}(\omega_0)\cdot e^{j(\omega_0 t-\theta_0)}[1-2A(t)+j2B(t)]$$

$$=E\cdot g_{os}(\omega_0)\cdot e^{j(\omega_0 t-\theta_0)}\cdot\{(1-2A(t))^2+4B(t)^2\}^{1/2}\cdot e^{j\tan^{-1}\frac{2B(t)}{1-2A(t)}}$$

and for k = π/2

$$G_7(t)=E\cdot g_{os}(\omega_0)\cdot e^{j(\omega_0 t-\theta_0)}[1-(1-j)A(t)+j(1-j)B(t)]$$

$$=E\cdot g_{os}(\omega_0)\cdot e^{j(\omega_0 t-\theta_0)}\cdot\{(1-A(t)+B(t))^2+(A(t)+B(t))^2\}^{1/2}\cdot e^{j\tan^{-1}\frac{A(t)+B(t)}{1-A(t)+B(t)}} \quad (22')$$

Now since

$$\frac{\Delta G_{os}}{\Delta f}=3\text{dB/GHz},$$

and

$$\theta_2=\frac{0.1\text{rad}}{(2\pi\cdot 0.5\text{GHz})^2}$$

$$d_2=\frac{4\sqrt{\alpha}}{T_1}=\frac{2.356}{\pi}\cdot\frac{1}{\alpha_2}\fallingdotseq 0.75\frac{1}{\alpha_2},\quad \alpha_2=\frac{\Delta F_B}{1/T_1}$$

$$\frac{\theta_2}{\alpha}=\frac{0.1}{(1.178)^2}\cdot\left(\frac{\Delta F_B}{0.5}\right)^2=\frac{0.1}{(1.178\times 0.5)^2}\left(\frac{\alpha_2}{T_1(\text{ns})}\right)^2\fallingdotseq 0.288\left(\frac{\alpha_2}{T_1(\text{ns})}\right)^2$$

$$\frac{b}{2\sqrt{\pi\alpha}}=\frac{3}{8.68\times 2\pi}\cdot\frac{2\pi\Delta F_B}{2\sqrt{\pi}\cdot 1.178}\fallingdotseq 0.0826\left(\frac{\alpha_2}{T_1(\text{ns})}\right)$$

Consequently, for T_1 = 3 ns and α = 1.5 or 3.0, Equation (22') can be calculated and shown as in Figures 15a and b and Figures 16a and b. In the figures, the in-phase component is shown as an absolute value. The abscissa shows x_3 where $x_3\fallingdotseq t'/(T_1/2)$. The perpendicular component for the case of α = 1.0 is 1/1.5 times of the case of α = 1.5. Hence, the in-phase component and the envelope are equivalent to the wave form of α_2 = 1.0 in Figures 7a and b. /119

From the above results, one can find the following facts. As regards the distortion of the wave forms, according to Figures 15 and 16, a large perpendicular component appears at $t/(T_1/2)$ = ±1, namely around the turning point of the phase, but no distortion shows up at the points $t/(T_1/2)$ = 0 and ±2.

Next, in the interference of signs, we have

$$\text{Interference between signs}=\left|\frac{E\cdot g_{os}(\omega_0)-|G_7(0)|}{E\cdot g_{os}(\omega_0)}\right| \quad (23)$$

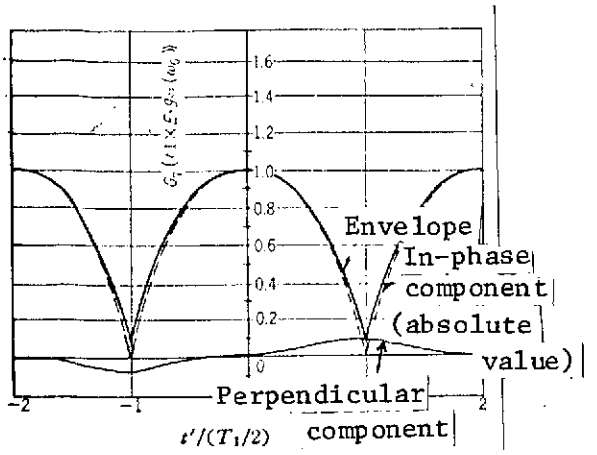

a) The input pulse $k=\pi$, $\alpha_2=1.5$

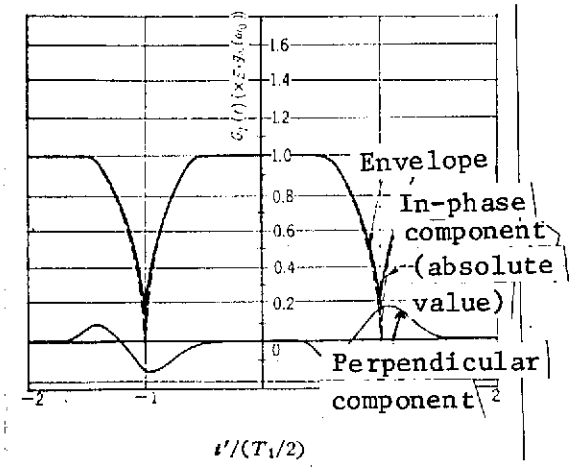

b) The input pulse $k=\pi$, $\alpha_2=3.0$

Figure 15. The output wave form of the AM component with respect to the PM pulse (Figure 7a) (in a small signal region).

Conditions: $\alpha_2=dF_B/(1/T_1)$; T_1- pulse amplitude = 3 ns; ΔF_B- 3 dB width of Gaussian filter; $\frac{dG_{os}}{df}=3\text{dB/GHz}$

$\theta_2=\frac{0.1\text{rad}}{(2\pi\cdot 0.5\text{GHz})^2}$

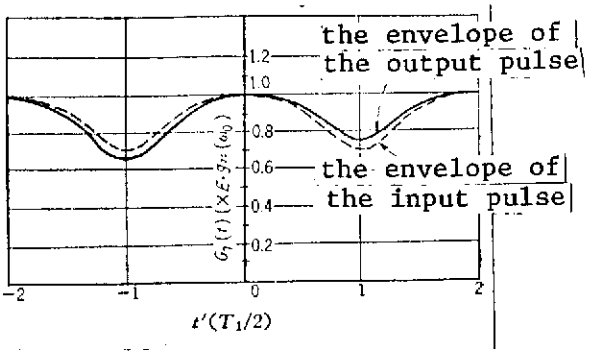

a) The input pulse $k=\frac{\pi}{2}$, $\alpha_2=1.5$

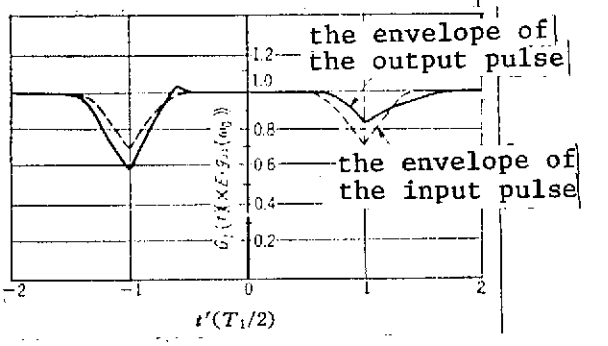

b) The input pulse $k=\frac{\pi}{2}$, $\alpha_2=3.0$

Figure 16. The output wave form of the AM component with respect to the PM pulse (Figure 7b) (in a small signal region).

where $G_7(0)$ is defined as the value of $G_7(t)$ at $k = \pi$ in Equation (22').

As mentioned above, at $t/(T_1/2) = 0$ or ± 2, there is no distortion in the wave form. Consequently, from Equation (23), the increase of the interference between signs can cease to exist.

In regards to the interference between different channels, strictly speaking, one has to consider the characteristics of the band distribution in the transmitting side, as well as the receiving side, and the distance between neighboring channels, etc. However, with an appropriate assumption made on these points, one can obtain the results of the channel interference with a simple method. The interference shows a variation of about ±0.5 dB. This degree of variation can be practically neglected.

Another evaluation method of the sign interference is by evaluating the rectified output wave form, namely finding the delay rectified wave form in Figure 15.

Now as a delay rectifier, usually this is a 1-beat delay integral rectification method, and the output electric voltage is found as follows. /120
A general PM pulse form is

$$G(t)=[G_r(t)+jG_j(t)]e^{j\omega_0 t} \tag{24}$$

then the 1-beat (τ) retarded wave form will be

$$G(t-\tau)=[G_r(t-\tau)+jG_j(t-\tau)]e^{j\omega_0(t-\tau)}$$

Now, adjusting the retardation circuit such that $\omega_0\tau=n\pi(n=1,\ 2,\ 3\cdots\cdots)$ from the sum and difference of G(t) and G(t = τ), one finds the difference square of the rectified output, namely:

$$\begin{aligned}\text{Retarded rectified output} &= K_0[|G(t)+G(t-\tau)|^2 \\ &\quad -|G(t)-G(t-\tau)|^2] \\ &= -4K_0[G_r(t)\cdot G_r(t-\tau) \\ &\quad +G_j(t)\cdot G_j(t-\tau)]\end{aligned} \tag{25}$$

where K_0 is the rectification sensitivity.

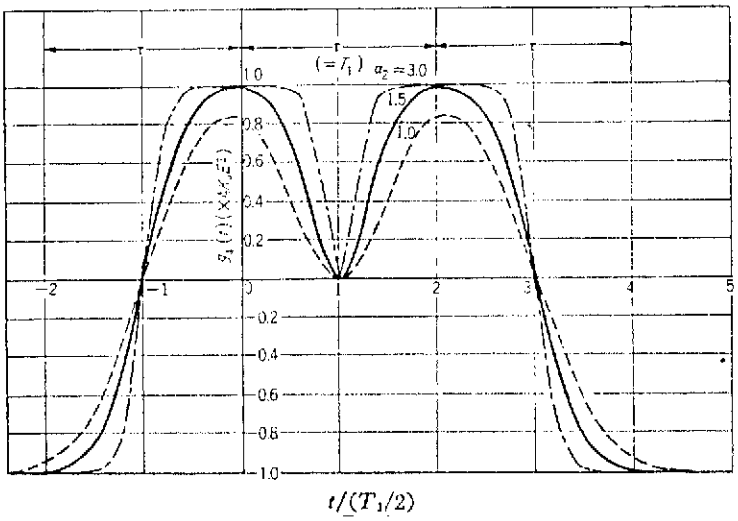

Figure 17. The retarded rectified wave form of a square PM pulse (Figure 7a) (100% duty).

Consequently, for the input wave form, namely $G_3(t)$ at $k = \pi$ of Equation (8) (Figure 7a), the retarded rectified output $g_4(t)$ can be found by use of the above formula and for $\tau = T_1$ (100% duty), it is

$$g_4(t) = -4K_0E^2\left[1-\left\{\varepsilon_{rf}\left(\frac{1+x_1}{d_2}\right)+\varepsilon_{rf}\left(\frac{1-x_1}{d_2}\right)\right\}\right.$$
$$\left.\cdot\left[1-\left\{\varepsilon_{rf}\left(\frac{-1+x_1}{d_2}\right)+\varepsilon_{rf}\left(\frac{3-x_1}{d_2}\right)\right\}\right] \qquad (26)$$

Next, for G(t) at $k = \pi$ of Formula (22') (Figures 15a and b), the retarded rectified output $G_7(t)$ can also be obtained with the same Formula (25') and $\tau = T_1$,

$$g_7(t) = -4K_0E^2g_{os}^2(\omega_0)[\{1-2A(t)\}$$
$$\cdot\{1-2A(t-T_1)\}+2B(t)\cdot 2B(t-T_1)] \qquad (27)$$

Hence, for $\alpha_2 = 1.0$, 1.5, and 3.0, for the abscissa to show and $t/(T_2/2)$ and $t'/(T_1/2)$, one can show Formulas (26) and (27) as in Figures 17 and 18.

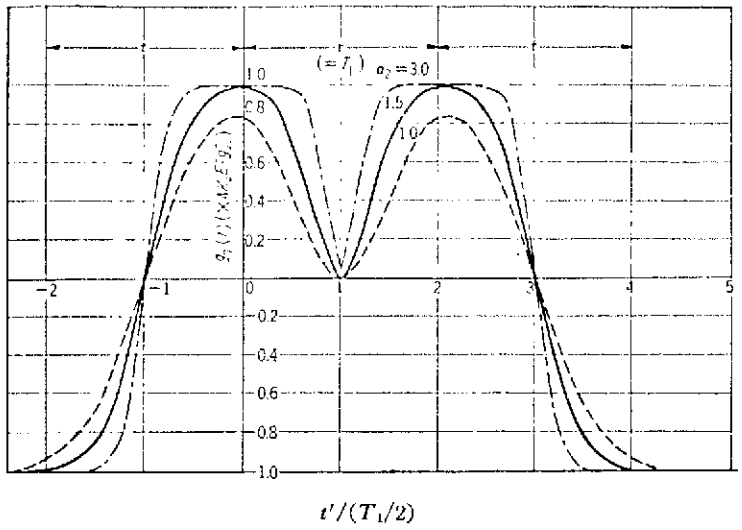

Figure 18. The retarded rectified wave form of TWT output (Figures 15a and b).

By comparing these two figures, one sees that the effects of the perpendicular component in Figure 15 is extremely small and Figure 17 is very similar to Figure 18, namely only around $t/(T_1/2) = 1$ in the case of $\alpha_2 = 3$ is there any discrepancy. However, at the sample points such as $t/(T_1/2) = 0$, ± 2, ± 4, etc., no change is observable, and from the viewpoint of observing the retarded rectified output, the increase of the sign interference ceases to exist.

ii) When the input is a Gaussian PM pulse under the restriction of a Gaussian band distribution:

For this case, the wave form and the spectrum of the input pulse are $G_6(t)$ of Formula (13) and $F_3(\omega) \cdot F_4(\omega)$ of Formulas (6) and (10). (see Figures 9, 12, and 13). Consequently,

$$G_6(t) = E \cdot e^{j\omega_0 t}\left[1 + \sum_{n=1}^{\infty} j^n \frac{k^n}{n!} \cdot \frac{1}{\sqrt{1+n(\Delta F/\Delta F_B)^2}} \cdot e^{-\frac{n(1.665\, t/T_3)^2}{1+n(\Delta F/\Delta F_B)^2}}\right] \qquad (13)$$

/121

and

$$F_3(\omega) \cdot F_4(\omega) = E\left[S_0(f - f_0) + \sum_{n=1}^{\infty} j^n \frac{k^n}{n!} \sqrt{\frac{\pi}{na}} \cdot e^{-\frac{(\omega-\omega_0)^2}{4na}}\right] \cdot e^{-\alpha(\omega-\omega_0)^2} \qquad (28)$$

However, the frequency number characteristic of a traveling wave tube $F(\omega)$ is shown by Formula (18) as

$$F(\omega)=g_{os}(\omega_0)\cdot e^{-b(\omega-\omega_0)}\cdot e^{-j[\theta_0+\theta_1\cdot(\omega-\omega_0)-\theta_2\cdot(\omega-\omega_0)^2]} \tag{18}$$

where

$$b=\frac{1}{8.68}\cdot\frac{\Delta G_{os}}{\Delta\omega}(\mathrm{dB})$$

Hence, the spectrum $F_8(\omega)$ and the wave form $G_8(t)$ of the output pulse are

$$F_8(\omega)=F_3(\omega)\cdot F_4(\omega)\cdot F(\omega) \tag{29}$$

$$G_8(t)=\frac{1}{2\pi}\int_{-\infty}^{\infty}F_8(\omega)e^{j\omega t}d\omega \tag{30}$$

To simplify the calculation, with the values of $\Delta G_{os}/\Delta f=3\mathrm{dB/GHz}$, $\theta_2=0.1\mathrm{rad}/(2\pi\cdot 0.5\mathrm{GHz})^2$, $|f-f_0|<0.7\mathrm{GHz}$ (T_2 = 3 ns), the replacement

$$e^{-b(\omega-\omega_0)}\cdot e^{j\theta_2\cdot(\omega-\omega_0)^2}\doteq 1-b(\omega-\omega_0)+j\theta_2\cdot(\omega-\omega_0)^2$$

can be made; then Formula (30) becomes

$$\begin{aligned}G_8(t)=&E_i g_{os}(\omega_0)\cdot e^{j(\omega_0 t-\theta_0)}\Bigg\{1+\frac{1}{2\pi}\int_{-\infty}^{\infty}\sum_{n=1}^{\infty}j^n\frac{k^n}{n!}\sqrt{\frac{\pi}{na}}\cdot e^{-\left\{\frac{1}{n}+\left(\frac{\Delta F}{\Delta F_B}\right)^2\right\}\frac{(\omega-\omega_0)^2}{4a}}\cdot e^{j(\omega-\omega_0)(t-\theta_1)}d\omega\\&-b\frac{1}{2\pi}\int_{-\infty}^{\infty}\sum_{n=1}^{\infty}j^n\frac{k^n}{n!}\sqrt{\frac{\pi}{na}}(\omega-\omega_0)e^{-\left\{\frac{1}{n}+\left(\frac{\Delta F}{\Delta F_B}\right)^2\right\}\frac{(\omega-\omega_0)^2}{4a}}\cdot e^{j(\omega-\omega_0)(t-\theta_1)}d\omega\\&+j\theta_2\frac{1}{2\pi}\int_{-\infty}^{\infty}\sum_{n=1}^{\infty}j^n\frac{k^n}{n!}\sqrt{\frac{\pi}{na}}(\omega-\omega_0)^2e^{-\left\{\frac{1}{n}+\left(\frac{\Delta F}{\Delta F_B}\right)^2\right\}\frac{(\omega-\omega_0)^2}{4a}}\cdot e^{j(\omega-\omega_0)(t-\theta_1)}d\omega\Bigg\}\\&=Eg_{os}(\omega_0)\cdot e^{j(\omega_0 t-\theta_0)}\cdot\Bigg\{1+\sum_{n=1}^{\infty}j^n\frac{k^n}{n!}\frac{1}{\sqrt{1+n(\Delta F/\Delta F_B)^2}}\cdot e^{-\frac{na(t-\theta_1)^2}{1+n(\Delta F/\Delta F_B)^2}}\\&-j\sum_{n=1}^{\infty}j^n\frac{k^n}{n!}\left\{b\cdot a(t-\theta_1)+\theta_2\cdot a\left(-1+\frac{2na(t-\theta_1)^2}{1+n(\Delta F/\Delta F_B)^2}\right)\right\}\cdot\frac{2n}{1+n(\Delta F/\Delta F_B)^2}\\&\cdot\frac{1}{\sqrt{1+n(\Delta F/\Delta F_B)^2}}\cdot e^{-\frac{na(t-\theta_1)^2}{1+n(\Delta F/\Delta F_B)^2}}\Bigg\}\end{aligned} \tag{31}$$

/122

In the above formula, with $x_4=\dfrac{t-\theta_1}{T_2/2}$, $\alpha_4=\dfrac{\Delta F_n}{1/T_2}$

$$\begin{cases}a(t+\theta_1)^2=\left(\dfrac{1.665}{T_2}(t+\theta_1)\right)^2=(0.833x_4)^2\\[2ex]\dfrac{\Delta F}{\Delta F_B}=\dfrac{0.624}{\Delta F_B\cdot T_2}=\dfrac{0.624}{\alpha_4}\end{cases}$$

and, therefore, if

$$\left.\begin{aligned} A_n(t) &= \frac{k^n}{n!}\cdot\frac{1}{\sqrt{1+n(\Delta F/\Delta F_B)^2}}\cdot e^{-\frac{n(0.833x_4)^2}{1+n(0.624/24)^2}} \\ B_n(t) &= \left\{b\cdot\left(\frac{1.665}{T_2}\right)(0.833x_4)+\theta_2\cdot\left(\frac{1.665}{T_2}\right)^2\left(-1+\frac{2n(0.833x_4)^2}{1+n(0.624/\alpha_4)^2}\right)\right\}\frac{2n}{1+n(0.624/\alpha_4)^2} \end{aligned}\right\} \quad (32)$$

then Formula (31) becomes the following:

$$\left.\begin{aligned} &G_8(t)=E\cdot g_{os}(\omega_0)\cdot e^{j(\omega_0 t+\theta_0)}\cdot\{\mathrm{Re}(t)^2+\mathrm{Im}(t)^2\}^{1/2}\cdot e^{j\tan^{-1}\frac{\mathrm{Im}(t)}{\mathrm{Re}(t)}} \\ &\mathrm{Re}(t)=1-A_2(t)+A_4(t)-A_6(t)\cdots\cdots+A_1(t)B_1(t)-A_3(t)B_3(t)+A_5(t)B_5(t)\cdots\cdots \\ &\mathrm{Im}(t)=A_1(t)-A_3(t)+A_5(t)\cdots\cdots+A_2(t)B_2(t)-A_4(t)B_4(t)+A_6(t)B_6(t)\cdots\cdots \\ &|G_8(t)|=E\cdot g_{os}(\omega_0)\cdot\{\mathrm{Re}(t)^2+\mathrm{Im}(t)^2\}^{1/2},\quad \varphi_8(t)=\tan^{-1}\frac{\mathrm{Im}(t)}{\mathrm{Re}(t)} \end{aligned}\right\} \quad (32')$$

Now, since

$$\left.\begin{aligned} &\frac{\Delta G_{os}}{\Delta F}=\frac{3\mathrm{dB}}{\mathrm{GHz}},\quad \theta_2=\frac{0.1\mathrm{rad}}{(2\pi\cdot 0.5\mathrm{GHz})} \\ &T_2=3\mathrm{ns},\quad \alpha_4=1.25,\ 2,\ 3 \end{aligned}\right\}$$

at k = π/2, the calculation of Formula (32') shows $|G_8(t)|$ and $\varphi_8(t)$ as are shown in Figures 19a and b and Figures 20a and b, respectively.

The abscissa x_4 represents $x_4=t'/(T_2/2)$.

From these results, one finds the following.

In regard to the wave distortion, in Figure 12, the envelope of the output wave form is symmetrical with respect to the vertical axis; but in Figure 19, it is asymmetrical. Around $t/(T_2/2)=\pm 1$, the amplitude distortion is noticeable, but around $t/(T_2/2)=0$ and ±2, the distortion is extremely small. By comparing Figure 13 with Figure 20, one sees that the phase distortion is generally very small.

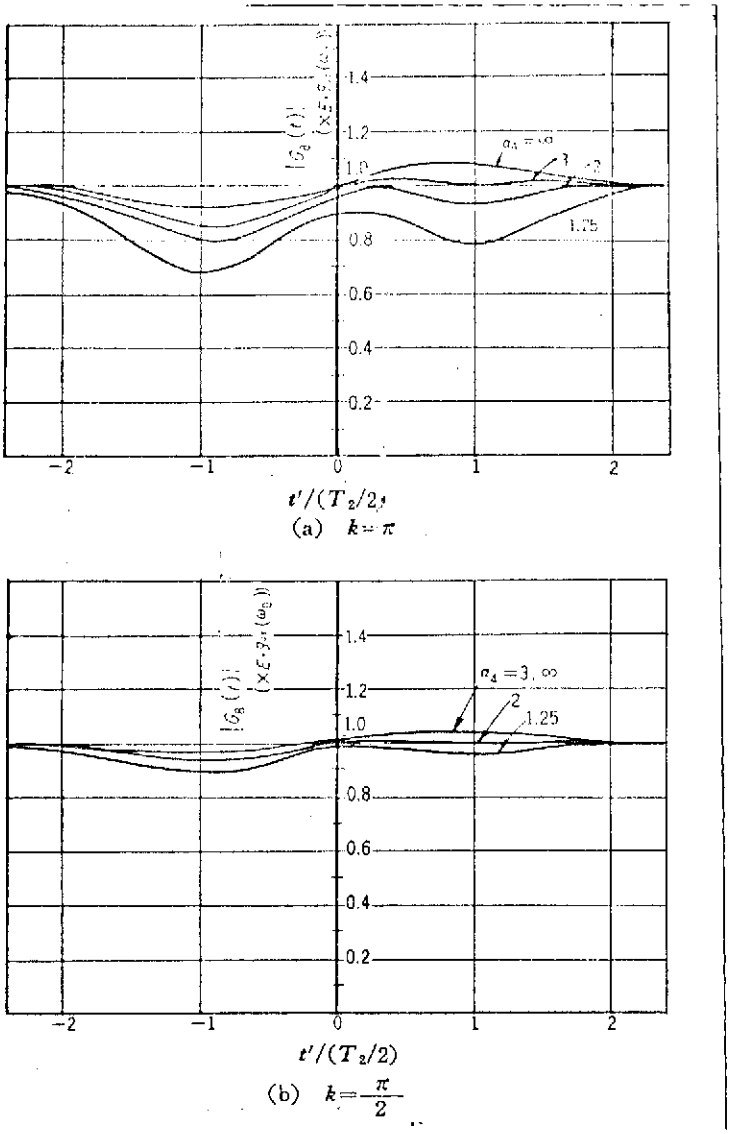

Figure 19. The output wave form of the AM component with respect to the PM pulse (Figure 12) (in a small signal region).

Conditions: $\alpha_4=\Delta F_B/(1/T_2)$; T_2 = 3 ns where T_2 is the half-width; ΔF_B = 3 dB width of the Gaussian filter; $\frac{\Delta G_{os}}{\Delta f}=3\text{dB/GHz}$ $\theta_2=\frac{0.1\text{rad}}{(2\pi\cdot 0.5\text{GHz})^2}$

From these facts, it is expected that the increase in the sign interference should be as small as shown by Formula (23). According to the rest of the calculation, $\Delta F_B/f_r=1.1\sim1.2$ (where $1/T_2 = f_r$) and an increase of about 1.5 dB appears. Now the reason of asymmetry in the wave form of Figure 19 is due to the fact that, while the characteristic of the gain

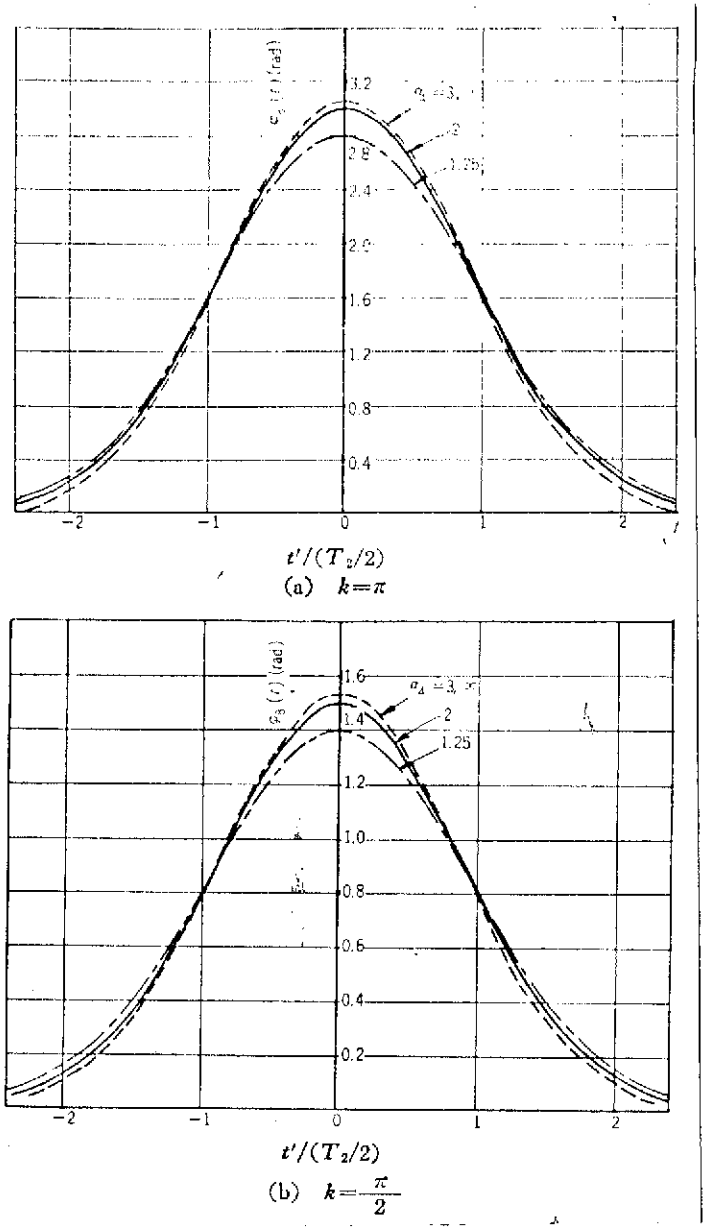

Figure 20. The output phase of the AM component with respect to the PM pulse (Figure 12) (in a small signal region).

frequency number in a traveling wave tube is a first linear slope ($\Delta G_{os}/\Delta\omega$), a Gaussian PM pulse is similar to an FM wave, and, therefore, the effect is similar to the case when an FM wave is added to a frequency selector and an FM-AM transformation occurs to generate plus and minus AM components. As

regards channel interference, if one makes a reasonable assumption on the characteristics of the band distribution of the transmitting and receiving system, and the distance between neighboring channels, the result shows almost /123 exactly as before - a change of about ±0.5 dB is observable. Consequently, the wave form of the retarded rectified output can also be studied by the equivalent Formula (25). With $\tau = T_2$ (100% duty) at the input wave form $G_6(t)$ of Formula (14) at $k = \pi$ (Figure 12a), the retarded rectified output $g_6(t)$ can be found to be

$$g_6(t) = -4K_0E^2[\mathrm{Re}(t)\cdot\mathrm{Re}(t-T_2) + \mathrm{Im}(t)\cdot\mathrm{Im}(t-T_2)] \tag{33}$$

Next, for the output wave form, namely $G_8(t)$ at $k = \pi$ of Formula (32') (Figure 19(a)) the retarded rectified output $g_8(t)$ can be found to be

$$g_8(t) = -4K_0E^2g_{0s}^2(\omega_0)[\mathrm{Re}(t)\cdot\mathrm{Re}(t-T_2) + \mathrm{Im}(t)\cdot\mathrm{Im}(t-T_2)] \tag{34}$$

If one shows Formulas (33) and (34) in figures, they are Figures 21 and 22.

In Figure 22, the asymmetry which appeared in Figure 19 shows up slightly, /124 but by comparing Figures 21 and 22, one finds that, around the point of $t/(T_1/2) = 2$ with $\alpha_4 = 3$, the difference between the two becomes extremely small. Actually, if one stays around the region of $\alpha_4 = 1.25 \text{ —— } 2$, at sample points of $i/(T_2/2) = 0, \pm 2, \pm 4$, etc., the distortion effect is really small. Consequently, from the viewpoint of the retarded rectified output, the increase of the signal interference would be extremely small.

3.2.2. The distortion due to higher order components of the gain and the phase

We will discuss the distortion due to higher orders of the gain and phase as mentioned in Figure 14 (c).

In general, the PM pulse of an AM component can be written as follows:

$$G_{1P}(t) = E\left(1 - \frac{\Delta E(t)}{E}\right)e^{j(\omega_0 t + \varphi(t))} \tag{35}$$

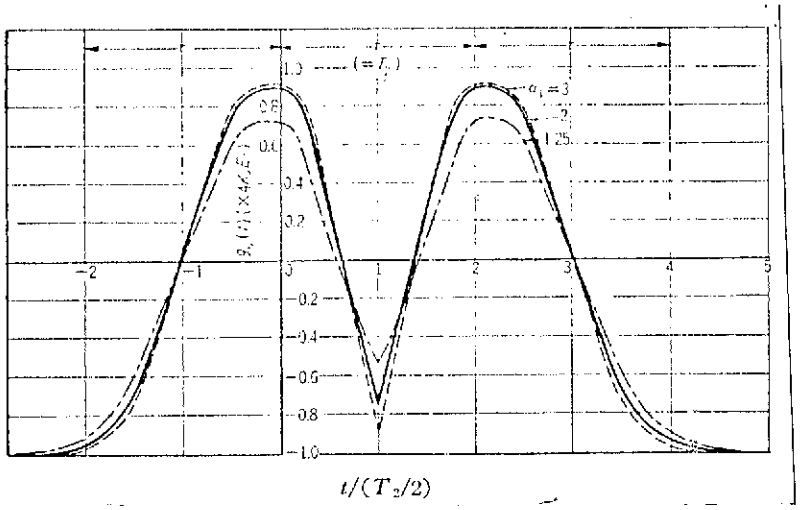

Figure 21. The retarded rectified wave form (100% duty) of a Gaussian PM pulse (Figure 12 (a)).

Now the expression of /125

$$e^{j\varphi(t)} = \sum_{n=0}^{\infty} j^n \frac{\varphi(t)^n}{n!}$$

is used to transform the above formula

$$G_{1P}(t) = Ee^{j\omega_0 t} + E\sum_{n=1}^{\infty} j^n \frac{\varphi(t)^n}{n!} e^{j\omega_0 t} - \Delta E(t)\sum_{n=1}^{\infty} j^n \frac{\varphi(t)^n}{n!} e^{j\omega_0 t} \qquad (35')$$

namely, $G_{1p}(t)$ has a continuous wave of $Ee^{j\omega_0 t}$, the frequency number of the carrier wave is always ω_0, and $E(\varphi(t)^n/n!)$ and $\Delta E(t)(\varphi(t)^n/n!)$ are understood to be the perpendicular AM pulse group. Consequently, the higher order effects with respect to the AM pulse can be obtained by utilizing the results in Formula (35') to obtain the higher order effects with respect to the PM pulse.

Now to simplify the ripple characteristics in Figure 14c, the wave is approximated by a cosine wave, as follows:

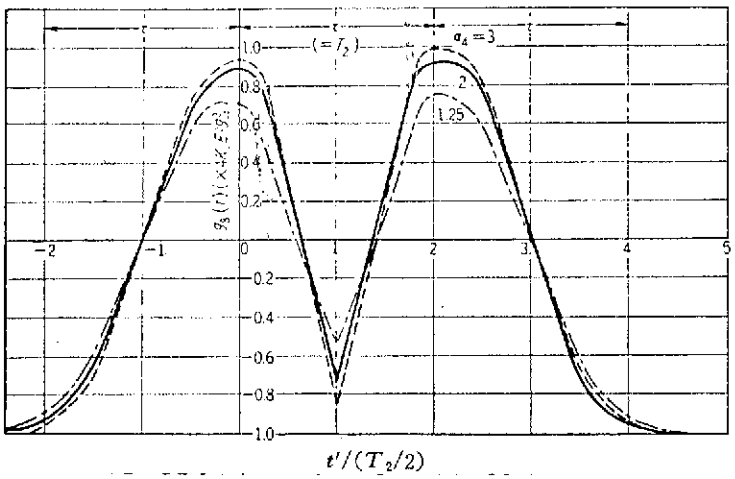

Figure 22. The retarded rectified wave form of the TWT output (Figure 19(a)).

Gain characteristics: $10\log_{10} g_{os}(\omega)^2$

$$= 10\log_{10} g_{os}(\omega_0)^2 + \Delta G \cos\frac{f-f_0}{\Delta F_1}$$

namely,

$$g_{os}(\omega) = g_{os}(\omega_0) \cdot \exp\left(\frac{\Delta G}{8.68}\cos\frac{f-f_0}{\Delta F_1}\right) \tag{36}$$

Phase characteristics:

$$\theta(\omega) = \theta_1 \cdot (\omega - \omega_0) - \Delta\theta \cdot \sin\frac{f-f_0}{\Delta F_2} \tag{37}$$

where ΔG(dB) and $\Delta\theta$(rad) are the Fourier amplitudes, while ΔF_1 and ΔF_2 are the variation pitch. The quantities $\Delta G \ll 10\log_{10} g_{os}(\omega_0)^2$, $\Delta\theta \ll \theta_1(\omega_0)$ /126

Now, for $1/\Delta F_1 \doteqdot 1/\Delta F_2 = \tau$, the output $G_{2A}(t)$ with respect to the AM pulse $G_{1A}(t)$ is shown by the following formula:

$$G_{2A}(t) \doteqdot g_{os}(\omega_0)\left[G_{1A}(t) + \left(\frac{\Delta G}{8.68} + \Delta\theta\right) \cdot G_{1A}(t+\tau) + \frac{1}{2}\left(\frac{\Delta G}{8.68} - \Delta\theta\right) \cdot G_{1A}(t-\tau)\right] \tag{38}$$

However, the output $G_{1P}(t)$ with respect to the PM pulse $G_{2p}(t)$ can be obtained with Formulas (35') and (38):

$$\begin{aligned} G_{2P}(t) = E \cdot g_{os}(\omega_0) \cdot e^{j\theta_1}\Bigg\{ & e^{j\omega_0 t} + \sum_{n=1}^{\infty} j^n \frac{\varphi(t)^n}{n!} e^{j\omega_0 t} + \frac{1}{2}\left(\frac{\Delta G}{8.68} + \Delta\theta\right) \sum_{n=1}^{\infty} j^n \frac{\varphi(t+\tau)^n}{n!} e^{j\omega_0(t+\tau)} \\ & + \frac{1}{2}\left(\frac{\Delta G}{8.68} - \Delta\theta\right) \sum_{n=1}^{\infty} j^n \frac{\varphi(t-\tau)^n}{n!} e^{j\omega_0(t-\tau)} - \left\{\frac{\Delta E(t)}{E} \sum_{n=0}^{\infty} j^n \frac{\varphi(t)^n}{n!} e^{j\omega_0 t}\right. \\ & + \frac{1}{2}\left(\frac{\Delta G}{8.68} + \Delta\theta\right) \cdot \frac{\Delta E(t+\pi)}{E} \sum_{n=0}^{\infty} j^n \frac{\varphi(t+\tau)^n}{n!} \cdot e^{j\omega_0(t+\tau)} + \frac{1}{2}\left(\frac{\Delta G}{8.68} + \Delta\theta\right) \frac{\Delta E(t-\tau)}{E} \\ & \left. \cdot \sum_{n=0}^{\infty} j^n \frac{\varphi(t-\tau)^n}{n!} \cdot e^{j\omega_0(t-\tau)}\right\} = g_{os}(\omega_0) \cdot e^{j\theta_1}\Bigg[G_{1P}(t) + \frac{1}{2}\left(\frac{\Delta G}{8.68} + \Delta\theta\right)\{G_{1P}(t+\tau) - Ee^{j\omega_0(t+\tau)}\} \\ & + \frac{1}{2}\left(\frac{\Delta G}{8.68} - \Delta\theta\right)\{G_{1P}(t-\tau) - Ee^{j\omega_0(t-\tau)}\}\Bigg] \end{aligned} \tag{39}$$

In the above formula, the first term in [ ] is the desired wave output, and the second and third terms are the echo pulses, which appear at the time τ before or after the desired wave output. Consequently, it is due to the sign interference.

To estimate the magnitude of an echo pulse, we take the following case as an example. The input pulse is a square PM pulse in the restriction of a Gaussian band distribution. This pulse $G_{1P}(t)$ can be expressed by $G_3(t)$ at $k = \pi$ with Formula (8'), namely:

$$\begin{aligned} & G_3(t) = E\left[1 - \left\{\varepsilon_{rf}\left(\frac{1+x_1}{d_2}\right) + \varepsilon_{rf}\left(\frac{1-x_1}{d_2}\right)\right\}\right] e^{j\omega_0 t} \\ & G_3(t) - Ee^{j\omega_0 t} = -E\left\{\varepsilon_{rf}\left(\frac{1+x_1}{d_2}\right) + \varepsilon_{rf}\left(\frac{1-x_1}{d_2}\right)\right\} e^{j\omega_0 t} \end{aligned}$$

Consequently,

$$|G_3(t)|_{max}=E,\ |G_1(t)-Ee^{j\omega_0 t}|_{max}=2E \tag{40}$$

Hence, for ΔG = 0.3 dB and $\Delta\theta$ = 0.06 rad, the level of an echo pulse according to Formulas (39) and (40) is given as follows, and for the worst case of $\Delta F_1 \doteqdot \Delta F_2$,

$$\frac{\left|\frac{1}{2}\left(\frac{\Delta G}{8.68}\pm\Delta\theta\right)\cdot 2E\right|}{E}=\left|\frac{\Delta G}{8.68}\pm\Delta\theta\right| \doteqdot \begin{cases}0.095\ (-20.5\text{dB})\\ 0.025\ (-32\text{dB})\end{cases} \tag{41}$$

that is, when ΔG and $\Delta\theta$ take on the above values, an echo pulse is about -20.5 dB for the worst case. However, since in actual cases, ΔF_1 and ΔF_2 are slightly different, the level of an echo pulse should be below -21 dB. Consequently, the ripple characteristic effect is extremely small.

The measurement made with a recent packaged double ladder traveling wave tube shows that the values of ΔG and $\Delta\theta$ are below the above value.

3.3. The Amplitude Characteristics of a 1-Cycle Pulse: Operation in a Large Signal Region

From the discussion in the previous chapter, the effects due to the characteristics of the gain and the phase frequency number have become clear, and, in various PM pulse cases, the increase of the sign interference and channel interference are understood to be about 1.5 dB and 0.5 dB, respectively. /127

Hence, in the present chapter, for the convenience of analysis, we will drop the above-mentioned characteristics of the frequency number, and will only consider the nonlinear effects in the large signal region, such as the output compression due to the input and output saturation characteristics, the phase modulation due to the input and output phase shift characteristics, etc., and finally, the wave distortion and the variation of various interference due to all these effects.

In the distortion due to the saturation characteristics, beside the above effects, there is another problem of the appearance of high frequency waves. However, this problem can be prevented by use of some simple phase tube as the wave generator. Besides, the effect of high frequency waves on the fundamental wave is generally very small and causes very few problems. Consequently, the effect is always omitted from the discussion.

3.3.1. A series representation of large signal characteristics

As mentioned above, in the region of large signals, a traveling wave tube amplifier is nonlinear and, therefore, we have to use a quasi-static treatment to find the output pulse in this case. In other words, the values (as a time dependent variable) of the input pulse are substituted for the input in the input-output characteristics equation of the circuit to find the output wave form. In this case, in order to make a Fourier transformation easily to find the spectra, and, therefore, with the consideration of the physical meaning of a wave distortion, it is useful to make a series representation of the input and output characteristics equation. Hence, from the beginning, the input and output characteristics equation is represented by a series expansion.

The general equation showing the amplitude and the phase of the input and output characteristics can be shown by the following formula [11]. Hence, if p_i is the input; p_o — output; $g_{os}{}^2$ — small signal gain; p_a — saturated output without loss, δ_0 — ratio of gain and loss; γ_l — excessive phase angle of a large signal; θ — phase difference of the input and the output; γ_s — phase angle of a small signal; q_i — normalized input; q_o — normalized output; then,

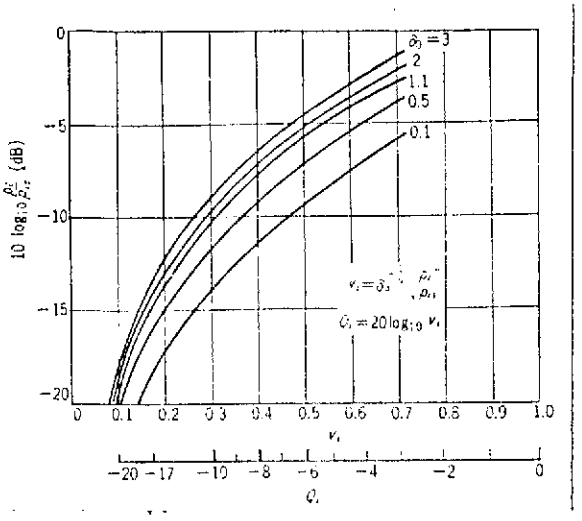

Figure 23. The relationship between v_i and p_i/p_{is}.

$$\left\{\begin{array}{ll} q_i=\dfrac{g_{os}^2 p_i}{p_a}, \quad q_o=\dfrac{p_o}{p_a} & (42) \\ q_o=\dfrac{q_i}{\sqrt{1+q_i^2(1+\delta_0 q_i)}} & (43) \\ \theta-\gamma_s=\gamma_i\cdot\log e(1+4q_i) & (44) \end{array}\right.$$

In this case, the following quantities are used as the normalized input and output electric voltage:

$$v_i\equiv\sqrt{q_i}=\frac{g_{os}\sqrt{p_i}}{\sqrt{p_a}}, \quad v_o\equiv\sqrt{q_o}=\frac{\sqrt{p_o}}{\sqrt{p_a}} \qquad (45)$$

Then, by use of the relationship $p_a=g_{os}^2\ \delta_0^{1/3}\ p_{is}$ (where p_{is} is the saturated input):

$$v_i=\delta_0^{-1/6}\sqrt{\frac{p_i}{p_{is}}}, \quad \text{and} \quad 20\log_{10}v_i=10\log_{10}\frac{p_i}{p_{is}}-3.33\log_{10}\delta_0 \qquad (46)$$

Thus, p_i/p_{is} can be used as the normalized input and, from it, the physical meaning of v_i can be understood. The relation in Equation (46) can be shown as in Figure 23.

Now, by using v_i and v_o, the input and output characteristic equation [Equations (43) and (44)] can be represented in series [1].

For $\delta_0 < 2$ and $v_i < 0.4$:

$$v_o=\left(v_i-\frac{\delta_0}{2}v_i^3\right)\cdot e^{-j(\gamma_s+\gamma_i(v_i^2-v_i^4))} \qquad (47)$$

and for $\delta_0 < 2$ and $v_i < 0.7$:

$$v_o=\left(v_i-\frac{\delta_0}{2}v_i^3+\frac{0.9\delta_0^2-1}{4}v_i^5\right)\cdot e^{-j(\gamma_s+\gamma_i(v_i^2-v_i^4+0.4v_i^6))} \qquad (48)$$

From these expressions, one can deduce that, due to the nonlinearity, higher order distortion can appear in a traveling wave tube; that is, odd order terms generate the amplitude compression distortion, while even order terms create the phase modulation distortions.

Consequently, the former case provides the cause of the wave form variation, called "AM compression" and the latter case causes the appearance of interference waves, called "AM-PM transformation." /128

Also in the above equations, one sees that, for a small v_i, $(\dot{a}_0/2)v_i^3$ can be neglected compared to v_i, so that the amplitude compression appears to be extremely small and, therefore, only the phase modulation distortion $(e^{-j\dot{a}_0 v_i^2})$ shows up. In other words, in a many cycle common amplification, before some reduction of the output caused by some amplitude compression happens, interference waves show up first caused by some AM-PM transformation.

3.3.2. Effects of the saturation characteristics and the phase shift characteristics

We use the above equations (47) — (49) as the input and output characteristics equations. We also assume a square or Gaussian PM pulse as the input wave form under a Gaussian band distribution. With this information, we will discuss the saturation characteristics and the phase shift characteristics in a large signal region.

i) When the input is a square PM pulse with a Gaussian band restriction:

In this case, the input wave form is shown by Equations (8) and (8') (see Figure 7). In other words,

$$G_3(t)=E\{1+g_3(t)^2-2g_3(t)\cos\xi\}^{1/2}\cdot e^{j\left(\omega_0 t-\tan^{-1}\frac{g_3(t)\sin\xi}{1-g_3(t)\cos\xi}\right)}$$
$$g_3(t)=\frac{\sqrt{2(1-\cos k)}}{2}\left[\varepsilon_{rf}\left(\frac{1+x_1}{d_2}\right)+\varepsilon_{rf}\left(\frac{1-x_1}{d_2}\right)\right] \qquad (8)$$

where

$$x_1=\frac{t}{T_1/2},\quad d_2=\frac{4\sqrt{\alpha}}{T_1}=\frac{2.356}{\pi}\cdot\frac{1}{\alpha_2},\quad \xi=\tan^{-1}\frac{\sin k}{1-\cos k}$$

For k = π,

$$G_3(t)=E\left[1-\left\{\varepsilon_{rf}\left(\frac{1+x_1}{d_2}\right)+\varepsilon_{rf}\left(\frac{1-x_1}{d_2}\right)\right\}\right]\cdot e^{j\omega_0 t}$$

For k = π/2,

$$G_3(t)=E\{1+g_3(t)^2-\sqrt{2}\,g_3(t)\}^{1/2}\cdot e^{j\left(\omega_0 t-\tan^{-1}\frac{g_3(t)}{\sqrt{2}-g_3(t)}\right)} \qquad (8')$$

where

$$g_3(t)=\frac{1}{\sqrt{2}}\left\{\varepsilon_{rf}\left(\frac{1+x_1}{d_2}\right)+\varepsilon_{rf}\left(\frac{1-x_1}{d_2}\right)\right\}$$

Consequently, instead of v_i of Equations (47) and (48),

$$v_i(t)=v_i\{1+g_3(t)^2-2g_3(t)\cdot\cos\xi\}^{1/2} \qquad (49)$$

is substituted to obtain the output wave form from a traveling wave tube. Now,

$$v_{i_1}(t)=v_i\left[1-\left\{\varepsilon_{rf}\left(\frac{1+x_1}{d_2}\right)+\varepsilon_{rf}\left(\frac{1-x_1}{d_2}\right)\right\}\right] \qquad (50)$$

$$v_{i_2}(t)=v_i\{1+g_3(t)^2-\sqrt{2}\,g_3(t)\}^{1/2} \qquad (51)$$

where

$$g_3(t)=\frac{1}{\sqrt{2}}\left\{\varepsilon_{rf}\left(\frac{1+x_1}{d_2}\right)+\varepsilon_{rf}\left(\frac{1-x_1}{d_2}\right)\right\}$$

Hence, for $v_i < 0.4$ and $\delta_0 < 2$, the output wave form $v_{o_1,i_1}(t)$ can be obtained by substituting Equations (50) and (51) into Equation (47), respectively. But for the sake of simplicity, $e^{-j\gamma_1}$ is dropped.

For k = π,

$$v_{o_1}(t)=\left\{v_{i_1}(t)-\frac{\delta_0}{2}v_{i_1}(t)^3\right\}\cdot e^{-j\gamma_1\{v_{i_1}(t)^2-v_{i_1}(t)^4\}}\cdot e^{j\omega_0 t}=\left\{v_{i_1}(t)-\frac{\delta_0}{2}v_{i_1}(t)^3\right\} \qquad (52)$$
$$\cdot\{\cos\gamma_1\{v_{i_1}(t)^2-v_{i_1}(t)^4\}-j\sin\gamma_1\{v_{i_1}(t)^2-v_{i_1}(t)^4\}\}\cdot e^{j\omega_0 t}$$

Now, if the component which is in phase with $e^{-j\gamma_l\{v_{i_1}(0)^2-v_{i_1}(0)^4\}}$ is called the in-phase component, while the one which is perpendicular to it is called the perpendicular component, then:

the in-phase component:

$$v_{i_1}(t)_c = \left\{v_{i_1}(t) - \frac{\delta_0}{2} v_{i_1}(t)^3\right\} \cdot \cos\gamma_l\{v_{i_1}(t)^2 - v_{i_1}(t)^4 - (v_{i_1}(0)^2 - v_{i_1}(0)^4)\}$$
$$\cdot e^{j[\omega_0 t - \gamma_l(v_{i_1}(0)^2 - v_{i_1}(0)^4)\}}$$

the perpendicular component:

$$v_{i_1}(t)_s = -\left\{v_{i_1}(t) - \frac{\delta_0}{2} v_{i_1}(t)^3\right\} \cdot \sin\gamma_l\{v_{i_1}(t)^2 - v_{i_1}(t)^4 - (v_{i_1}(0)^2 - v_{i_1}(0)^4)\} \quad (53)$$
$$\cdot e^{j[\omega_0 t - \gamma_l(v_{i_1}(0)^2 - v_{i_1}(0)^4)\}}$$

and the envelope = $\left|\left\{v_{i_1}(t) - \frac{\delta_0}{2} v_{i_1}(t)^3\right\}\right|$

For k = $\pi/2$,

$$v_{o_1}(t) = \left\{v_{i_1}(t) - \frac{\delta_0}{2} v_{i_1}(t)^3\right\} \cdot e^{-j\left\{\gamma_l(v_{i_1}(t)^2 - v_{i_1}(t)^4) + \tan^{-1}\frac{v_3(t)}{\sqrt{2} - v_3(t)}\right\}} \cdot e^{j\omega_0 t} \quad (54)$$

Consequently,

the envelope = $\left|\left\{v_{i_1}(t) - \frac{\delta_0}{2} v_{i_1}(t)^3\right\}\right|$ (55)

As an example, for v_i = 0.4, δ_0 = 2, γ_l = 1.5, and α_2 = 1, 1.5, and 3.0, one can compute Equations (53) and (55), as shown in Figures 24a and b.

From these results, one obtains the following conclusions. In Figure 30a, one sees that, as the wave distortion occurs, the output amplitude suffers a compression due to the saturation characteristics at a rate of 0.33/0.4, as compared to the linear case, namely, a compression of 2 dB, while due to the phase shift characteristics, about 6% of the perpendicular component appears. Consequently, by comparing this fact with the above-mentioned Figures 7a and 15a and b, one sees that the distortion has become smaller for an in-phase component, and the perpendicular component is much smaller than that caused by the frequency number characteristics. Hence, for the sign interference, one can further improve the situation in Figure 24a,

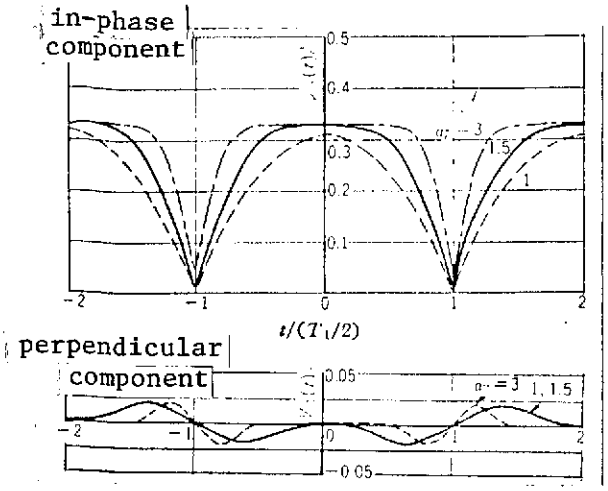

a) input pulse: k = π (Figure 7a).

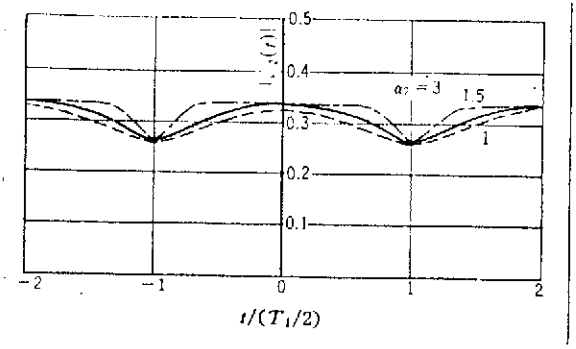

b) output pulse: k = π/2 (Figure 7b).

Figure 24. The output wave form of the AM component with respect to a PM pulse (Figure 7) (in a large signal region).

Conditions:

$$\begin{cases} \alpha_2 = 2 f_B/(1/T_1) \\ \delta_0 = 2 \\ \gamma_t = 1.5 \\ v_t = 0.4 \\ \left(10 \log_{10} \frac{p_t}{p_{ts}} \fallingdotseq -7\text{dB}\right) \end{cases}$$

as we did before, to limit the sign interference to 4 dB for the case of $\Delta F_B/f = 1.05$. However, in the channel interference, not much change can be expected.

From Equations (25) and (53), one can find the retarded rectified output $g_{o1}(t)$ of Figure 24a as follows:

$$\left.\begin{aligned} g_{o_1}(t) = -4K_o(v_{o_1}(t)_c \cdot v_{o_1}(t-\tau)_c \\ + v_{o_1}(t)_s \cdot v_{o_1}(t-\tau)_s] \end{aligned}\right| \quad (56)$$

where τ = T (100% duty).

For α_2 = 1, 1.5, and 3, Equation (56) can be computed as shown in Figure 25. /130

If one takes the input wave form in Figure 25 as the direct retarded rectified wave and compares Figure 25 with Figure 17, one sees that the branches in Figure 25 at both sides of the time axis are smaller than those in Figure 17. The sign interference also clearly appears to be smaller, and, therefore, it is a very hopeful wave form.

We observed that a traveling wave tube in a large signal region was nonlinear, when we tried to derive the amount of the sign interference and the retarded rectified output. Consequently, the model derived in Figure 2 is not applicable, as we mentioned in Chapter 2, and we ought to retain the design of Figure 1 to maintain

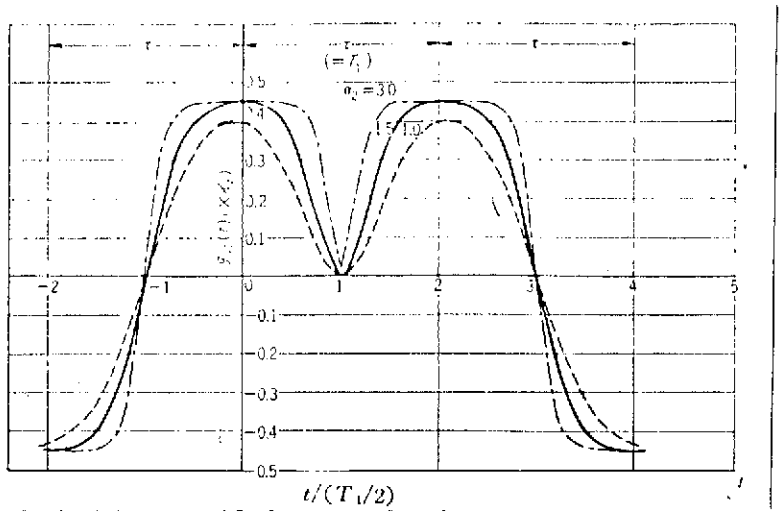

Figure 25. The retarded rectified wave form of TWT output (Figure 24a).

some accuracy in our discussion. Nevertheless, for the sake of simplicity and with the following justification, we will continue to use Figure 2 in our discussion. We can see by comparing Figure 7 with Figure 24a that the in-phase components look alike, and the perpendicular component not only has a very small amplitude, but it is also in a wave form with a very small half width. When we consider the receiver filter after amplification by a traveling wave tube of Figure 1, the effect of its band distribution in compressing the peak values affects the perpendicular component much more strongly than the in-phase component. In other words, after the wave has passed through the receiving filter, the perpendicular component becomes negligible. Consequently, the effect of the wave distortion is more exaggerated in Figure 2 than in Figure 1. Thus, it is a safer way to deal with the problem.

ii) When the input is a Gaussian PM pulse in a Gaussian band distribution.

In this case, the input wave form is given by Equation 14 (see Figure 12), namely

$$G_0(t)=|G_0(t)|e^{j(\omega_0 t+\varphi_0(t))}=E\{\mathrm{Re}(t)^2+\mathrm{Im}(t)^2\}^{1/2}\cdot e^{j\left(\omega_0 t+\tan^{-1}\frac{\mathrm{Im}(t)}{\mathrm{Re}(t)}\right)}$$

$$\mathrm{Re}(t)=1-\frac{k^2}{2!}\cdot\frac{1}{\sqrt{1+2\alpha_5^2}}\cdot e^{-\frac{2(0.833x_2)^2}{1+2\alpha_5^2}}+\frac{k^4}{4!}\cdot\frac{1}{\sqrt{1+4\alpha_5^2}}\cdot e^{-\frac{4(0.833x_2)^2}{1+4\alpha_5^2}}-\cdots\cdots$$

$$\mathrm{Im}(t)=k\frac{e^{\prime}}{\sqrt{1+\alpha_5^2}}\cdot e^{-\frac{(0.833x_2)^2}{1+\alpha_5^2}}-\frac{k^3}{3!}\frac{1}{\sqrt{1+3\alpha_5^2}}\cdot e^{-\frac{3(0.833x_2)^2}{1+3\alpha_5^2}}+\cdots\cdots \tag{14}$$

but $x_2=\dfrac{t}{T_2/2}$, $\alpha_5=\dfrac{\Delta F}{\Delta F_B}=\dfrac{0.624}{\alpha_4}$, $\alpha_4=\dfrac{\Delta F_B}{1/T_2}$

Consequently, the output wave form of a traveling wave tube can be obtained by substituting

$$v_i(t)=v_i\{\mathrm{Re}(t)^2+\mathrm{Im}(t)^2\}^{1/2} \tag{57}$$

instead of v_i of Equations (47) and (48).

Now for $v_i<0.4$ and $\theta_0<2$, the output wave form $v_o(t)$ can be obtained by substituting Equation (57) into Equation (47) as follows. However, for the sake of simplicity, we drop e^{-jr_4} /131

$$v_o(t)=\left\{v_i(t)\cdot\{\mathrm{Re}(t)^2+\mathrm{Im}(t)^2\}^{1/2}-\frac{\theta_0}{2}v_i(t)^3\cdot\{\mathrm{Re}(t)^2+\mathrm{Im}(t)^2\}^{3/2}\right\}\cdot e^{j\omega_0 t}$$
$$\cdot\exp\cdot j\left\{-\gamma_i\{v_i(t)^2\cdot(\mathrm{Re}(t)^2+\mathrm{Im}(t)^2)-v_i(t)^4\cdot(\mathrm{Re}(t)^2+\mathrm{Im}(t)^2)^2\}+\tan^{-1}\frac{\mathrm{Im}(t)}{\mathrm{Re}(t)}\right\} \tag{58}$$

where the in-phase component:

$$v_o(t)_c=\left\{v_i(t)\{\mathrm{Re}(t)^2+\mathrm{Im}(t)^2\}^{1/2}-\frac{\theta_0}{2}v_i(t)^3\cdot\{\mathrm{Re}(t)^2+\mathrm{Im}(t)^2\}^{3/2}\right\}$$
$$\cdot\cos\left\{-\gamma_i\{v_i(t)^2\cdot(\mathrm{Re}(t)^2+\mathrm{Im}(t)^2)-v_i(t)^4\cdot(\mathrm{Re}(t)^2+\mathrm{Im}(t)^2)^2\}+\tan^{-1}\frac{\mathrm{Im}(t)}{\mathrm{Re}(t)}\right\} \tag{59}$$
$$\cdot e^{j\omega_0 t}$$

the perpendicular component:

$$v_o(t)_s = \left[v_i(t) \{\mathrm{Re}(t)^2 + \mathrm{Im}(t)^2\}^{1/2} - \frac{\delta_0}{2} v_i(t)^3 \cdot \{\mathrm{Re}(t)^2 + \mathrm{Im}(t)^2\}^{3/2} \right] \cdot \sin\left[-\gamma_i \{v_i(t)^2 \cdot (\mathrm{Re}(t)^2 + \mathrm{Im}(t)^2) - v_i(t)^4 \cdot (\mathrm{Re}(t)^2 + \mathrm{Im}(t)^2)^2\} + \tan^{-1}\frac{\mathrm{Im}(t)}{\mathrm{Re}(t)} \right] \cdot e^{j\omega_0 t} \tag{60}$$

the phase angle:

$$\varphi_0(t) = \tan^{-1}\frac{v_o(t)_s}{v_o(t)_c} + \gamma_i (v_i(\infty)^2 - v_i(\infty)^4) \tag{61}$$

and the envelope = $$\left[v_i(t) \{\mathrm{Re}(t)^2 + \mathrm{Im}(t)^2\}^{1/2} - \frac{\delta_0}{2} v_i(t)^3 \cdot \{\mathrm{Re}(t)^2 + \mathrm{Im}(t)^2\}^{3/2} \right] \tag{62}$$

Hence, the retarded rectified output $g_o(t)$ from Equations (25), (59), and (60) is

$$g_o(t) = -4K_0 [v_o(t)_c \cdot v_o(t - T_2)_c + v_o(t)_s \cdot v_o(t - T_2)_s] \tag{63}$$

where $\tau_j = T_2$ (100% duty).

As an example, for $\bar{v} = 0.4$, $\delta_0 = 2$, $\gamma_i = 1.5$, and α_4 = 1.25, 2, and 3, Equations (61), (62), and (63) can be computed to show Figures 26a and b, Figures 27a and b, and Figure 28.

From these results, one reaches the following conclusion. Comparing Figure 12 with Figure 26, one sees that, in the latter case, due to the saturation characteristics of a traveling wave tube, the AM component is noticeably compressed. However, the AM-PM transformation, due to the phase shift characteristics, is also much smaller than in Figure 24. In any event, the phase distortion is generally very small in Figure 27, as compared with that in Figure 13. For instance, around $(t/T_2)/2 = \pm 1$ and at α_4 = 2, it is about 0.05 rad. Thus, one may say that nonlinearity has a very small effect in all these cases. In Figure 26a, as in the above cases, the sign interference reduces the intensity by about 2.5 dB for the case of $\Delta F_B/f_r = 1.1 \sim 1.2$

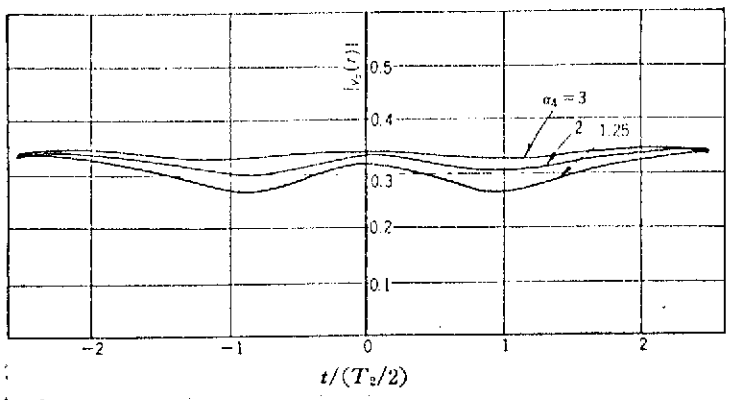

a) the input pulse: k = π (Figure 12b)

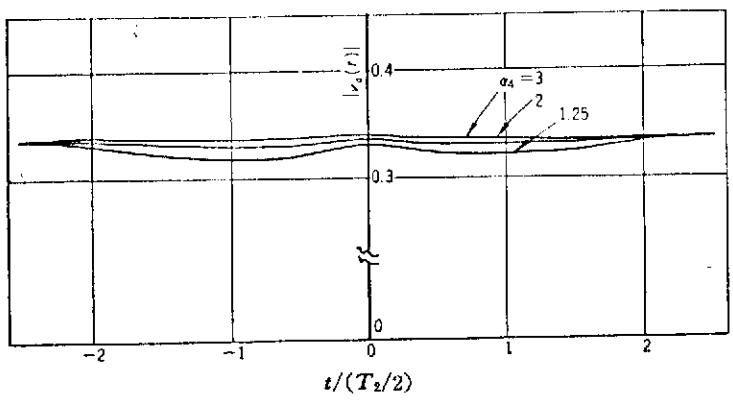

b) the input pulse: k = π/2 (Figure 12b).

Figure 26. The output wave form of the AM component with respect to the PM pulse (Figure 12) (in the large signal region).

Conditions:

$$\begin{cases} \alpha_4 = dF_B/(1/T_2) \\ \delta_0 = 2 \qquad \gamma_1 = 1.5 \\ v_i = 0.4 \\ \quad \left(10 \log_{10} \dfrac{p_i}{p_{is}} \fallingdotseq -7\text{dB}\right) \end{cases}$$

Next, in regard to the channel interference, it is difficult to find out the spectrum of the output pulse from Equation (58), and it is also not very easy to estimate the effect by looking at the wave form of the output pulse. However, from the above few facts, the wave distortion is extremely small. Nevertheless, it has the tendency of reducing the AM component. Consequently, it looks as though the output pulse is not affected by the band restriction.

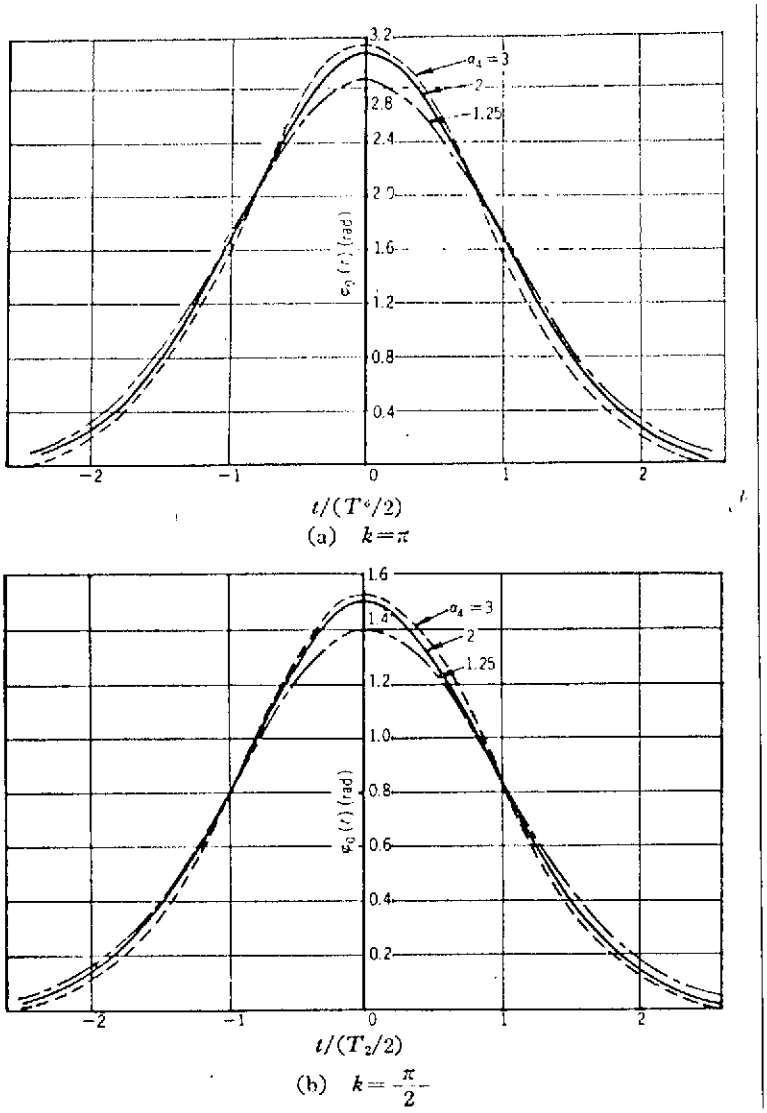

Figure 27. The output phase of the AM component with respect to the PM pulse (Figure 12a) (in the large signal region).

Hence, the output spectrum seems to be small, but the lower part seems to increase somewhat. Thus, it is estimated that the increase of channel interference may be less than 0.5 dB.

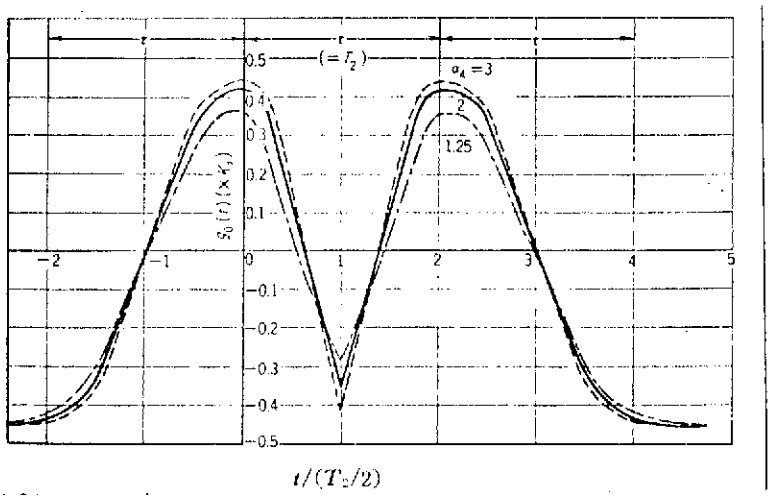

Figure 28. The retarded rectified wave form of the TWT output (Figure 26a).

Therefore, by comparing Figure 21 with Figure 28, one sees that, in the retarded rectified output, as expected from the above, the sign interference clearly gets smaller. Nevertheless, as a whole, both cases seem to be very similar, and Figure 28 presents a very hopeful wave form.

In this case, too, as mentioned before, the discussion ought to be made /132
with the design shown in Figure 1, in order to maintain some degree of accuracy. However, for the sake of simplicity, again the model of Figure 2 is used. Because the wave distortion is very small, the discussion with Figure 2 would result in only a minor error.

3.3.3. The output compression coefficient and the AM-PM transformation coefficient

The indices of the nonlinearity of a traveling wave tube are conventionally defined by the following two coefficients, namely:

The output compression coefficient: $C=1-\frac{\Delta P_{out}(\mathrm{dB})}{\Delta P_{in}(\mathrm{dB})}$ (64)

The AM-PM transformation coefficient: $K=0.152K'$ (65)

where

$$K' = \frac{\Delta\theta(\text{deg})}{\Delta P_{in}(\text{dB})} \tag{66}$$

Now with Equations (43) and (44), which represent the input and output saturation characteristics and the input and output phase shift characteristics, one can find C and K' from the above definitions; namely:

$$C = 1 - \frac{1-\delta_0 q_l^3}{(1+q_l^3)(1+\delta_0 q_l)} \left(\text{if } \frac{\Delta P_{out}}{P_{out}} \ll 1 \right) \tag{67}$$

$$K' \doteq 57.3\gamma_1 \cdot \frac{1}{4}\{\log_e(1+1.26\times 4q_l) - \log_e(1+4q_l)\} \tag{68}$$

These quantities are shown in Figure 29.

By use of Figure 29, one can easily and accurately find the AM compression and the AM-PM transformation when a PM pulse, which contains some element of the AM components, is amplified. As an example, for the case of Figure 26, if $v_i = 0.4$, $\delta_o = 2$, and $\gamma_1 = 1.5$, the compression coefficient and the AM-PM transformation coefficient, according to Figure 29, are 0.27 and 2 degrees/dB, respectively. However, for $\alpha_4 = 2$, the AM element in the input is about 1.3 dB, according to Figure 12a, and that in the output is /134 /135

$$1.3\times(1-0.27) \doteq 0.95\,\text{dB}$$

The phase distortion around $t(T_2/2) = \pm 1$ is expected to be

$$1.3\times 2(\text{deg}) \doteq 0.045(\text{rad})$$

This claim can be made by comparing Figures 12 and 13 with Figures 26 and 27.

It is convenient to be able to evaluate the distortion caused by nonlinearity simply with Figure 29.

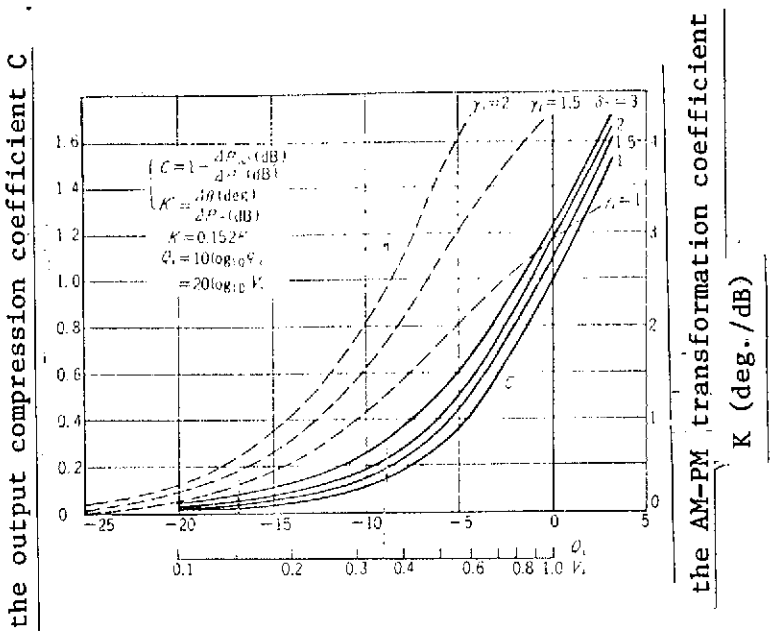

Figure 29. The output compression coefficient and the AM-PM transformation coefficient.

From the values in Figure 29, $Q_i < -2$ (namely, $v_i < 0.8$) with respect to C, while $Q_i < -5$ (namely, $v_i < 0.6$) with respect to K'; this agrees very well with the experimental values.

3.3.4. Summary on large signal amplification

Actually, in a large signal region, the effects, caused both by the frequency number characteristics discussed in Chapter 3.2 and by the nonlinearity discussed in the present chapter, appear simultaneously. Hence, a summary on what we have so far discussed are given in Tables 4 and 5 to show what the characteristics in an actual case would be.

3.4. The Characteristics of 2-Cycle Pulse Common Amplification: Operation in a Large Signal Region

A 2-cycle PM pulse common amplification in a small signal region can be evaluated with what we have discussed in the previous chapter; that is, a traveling wave tube amplifier is a linear amplifier, the interference output

TABLE 4

THE WAVE DISTORTION WHEN THE INPUT IS A SQUARE PM PULSE* UNDER A GAUSSIAN BAND RESTRICTION

			Wave form distortions			Change in sign interference	Change in channel interference	Conditions
			Envelope	Perpendicular components**	Phase distortion			
Small signal region	Effects due to frequency number characteristics	First linear slope of the gain	Small distortion	Even symmetry $\alpha b \cdot \Delta F_B$	Small	0 dB	± 0.5 dB	$\frac{dG_{os}}{df} = 3$ dB/GHz $\theta_2 = \frac{0.1\text{rad}}{(2\pi 0.5\text{GHz})^2}$ $T_t = \frac{1}{f_r} = 3$ ns $\Delta F_B = 1.5 f_r$ $f_s = 2.5 f_r$
		Second order component of phase	"	Odd symmetry $\alpha\theta_2 \cdot \Delta F_B$***				
Large signal region	Effects due to nonlinearity	Higher order of gain and phase	Internal echo pulses			below −21 dB	0 dB	Gain filter: ± 0.3 dB Phase filter: ± 0.06 rad
Large signal region	General characteristics	Saturation characteristics	Output compression of 2 dB	0	0		below + 0.5 dB	$v_t = 0.4$ $p_t - p_{ts} \fallingdotseq -7$ dB $\delta_0 = 2$ $\gamma_t = 1.5$
		Phase shift characteristics	Small distortion	Odd symmetry due to AM-PM transformation	Small			
		Combination of frequency number characteristics and nonlinearity	Output compression of 2 dB	Asymmetry	Small	− 4 dB	Tendency of $f_{adj} < f_0 + 1$dB Tendency of $f_{adj} < f_0$ 0dB	Same as above

*The case of a 2-phase PM with a 0-π modulation.

**Appears at the turning points of the phase.

***The phase distortion around the center of the pulse.

TABLE 5

THE WAVE FORM DISTORTION WHEN THE INPUT IS A GAUSSIAN PM PULSE* IN A GAUSSIAN BAND RESTRICTION

			Wave form distortions		Change in sign interference	Change in channel interference	Conditions
			Envelope	Phase** distortion			
Small signal region	Effects due to the frequency number characteristics	First linear slope of the gain	Odd symmetry due to AM-PM transformation	Small	+1.5 dB	± 0.4 dB	$\frac{\Delta G_{ns}}{\Delta f}=3\,\mathrm{dB/GHz}$ $\theta_2=\frac{0.1\,\mathrm{rad}}{(2\pi 0.5\,\mathrm{GHz})^2}$ $T_2=\frac{1}{f_r}=3\,\mathrm{ns}$ $\Delta F_D=1.5 f_r$ $f_s=2.3 f_r$
		Second order of phase	Even s, symmetry	Small			
		Higher order of components of gain and phase	Internal	echo pulses	Below −21 dB	0 dB	Gain filter: ± 0.3 dB Phase filter: ± 0.06 rad
Large signal region	Effects due to nonlinearity	Saturation characteristics	Output compression of 2 dB AM compression of 0.4 dB	0	−2.5 dB	± 0.5 dB Below	$v_t=0.4$ $p_t-p_{ts}=-7\,\mathrm{dB}$ $\delta_0=2$ $\gamma_t=1.5$
		Phase shift characteristics	Distortion small	0.05 rad*** due to AM-PM transformation			
Large signal region	General characteristics	Combination of frequency number characteristics and nonlinearity	Asymmetry due to AM-PM transformation; Output compression of 2 dB; AM compression of 0.4 dB	0.05 rad*** due to AM-PM transformation	−1 dB	Tendency of $f_{adj}<f_0$, 0.9 dB Tendency of $f_{adj}<f_0$, 0.1 dB	Same as above

*The case of a 2-phase PM with a 0-π modulation; **Phase distortion appears at the center of the pulse; ***Phase distortion appears at the points where the pulse has one half its magnitude ($\alpha_4 = 2$).

is also very small and, therefore, it is reasonable just to consider the characteristics of frequency number. In short, we may as well use the results discussed in Section 3.2. Thus, in the present chapter, we will only consider the operation of a 2-cycle PM pulse common amplification in a large signal region. However, in this case, in a general discussion, consideration of the frequency number characteristics must also accompany with what we have discussed in the previous chapter in Equations (74) — (77) to obtain the output wave. This takes a very complex calculation. In order to simplify analysis somewhat, the 2-cycle PM pulse is assumed to be of an equal strength, and the cases are divided into two types, namely the equal time slot case (f_1 : ……00100……, f_2 : ……00100……; case) and the different time slot case (f_1 : ……00100……, f_2 : ……00001……; case). As in the previous cases, we discuss the problem without considering the frequency number characteristics, and the result will be compared with those of Section 3.2 to make a general evaluation of actual behaviors. /136

3.4.1. The series representation of a 2-cycle common amplification characteristic

We define the following quantities: ω_1 and ω_2 are the angular frequencies of the two cycles, respectively; the inputs are p_{i1} and p_{i2}; the saturation inputs are p_{is1} and p_{is2}; the ratios between losses and gains are δ_{01} and δ_{02}; the large signal excessive phase angles are γ_{l1}* and γ_{l2}. Then the normalized input voltages v_{i1} and v_{i2} can be obtained from Equation (46) as

$$v_{i_1}=\delta_{01}^{-1/6}\cdot\sqrt{\frac{p_{i_1}}{p_{is_1}}},\quad v_{i_2}=\delta_{02}^{-1/6}\sqrt{\frac{p_{i_2}}{p_{is_2}}} \tag{69}$$

Consequently, if both cycles are applied simultaneously, the normalized input voltage $v_i(t)$ is

$$v_i(t)=v_{i_1}\cdot e^{j(\omega_1 t+\theta_1)}+v_{i_2}\cdot e^{j(\omega_2 t+\theta_2)} \tag{70}$$

where θ_1 and θ_2 are their phase angles, respectively.

*Translator's Note: This was mistakenly printed as λ in the foreign text.

Hence, if the normalized input voltage is used as the input, then as the output, the normalized output voltage shown by Equation (45) is used (for each output frequency, the output is normalized by the no-loss saturation output). Then it is possible to take into account all the characteristic values of the frequency number characteristics of a traveling wave tube, and it is a very convenient way to make a general analysis. In other words, especially for the case of a millimeter wave double ladder tube, as will be described later, these general characteristics values of the frequency number characteristics are very substantial and they cannot be totally neglected. The frequency number characteristics of a small signal gain and the phase characteristics are shown in Figure 14.

Equation (70) can be written as

$$\begin{aligned} v_i(t) = {} & \{v_{i_1}^2 + v_{i_2}^2 + 2v_{i_1} \cdot v_{i_2} \cos \\ & \cdot \{(\omega_1 - \omega_2)t + \theta_1 - \theta_2\}\}^{1/2} \cdot \exp j \\ & \cdot \left[\frac{\omega_1 + \omega_2}{2} t + \tan^{-1}\left\{\frac{v_{i_1} - v_{i_2}}{v_{i_1} + v_{i_2}} \right.\right. \\ & \left.\left. \cdot \tan \frac{1}{2}(\omega_1 - \omega_2)t + \theta_1 - \theta_2)\right\}\right] \end{aligned} \tag{70'}$$

Now if the conditions

$$\begin{aligned} & (v_{i_1} + v_{i_2}) < 0.7 \\ & \delta_0 = \frac{1}{2}(\delta_{01} + \delta_{02}), \quad \frac{1}{2}(\delta_{01} - \delta_{02}) \ll \delta_0 \\ & \gamma_i = \frac{1}{2}(\gamma_{i_1} + \gamma_{i_2}), \quad \frac{1}{2}(\gamma_{i_1} - \gamma_{i_2}) \ll \gamma_i \end{aligned} \tag{71}$$

are true, then the normalized output $v_o(t)$ is shown by the large signal characteristics Equation (48), namely,

$$\begin{aligned} v_o = {} & \left(v_i - \frac{\delta_0}{2} v_i^3 + \frac{0.9\delta_0^2 - 1}{4} v_i^5\right) \\ & \cdot e^{-j\{\gamma_i + \gamma_i(v_i^2 - v_i^4 + 0.6v_i^6)\}} \end{aligned} \tag{72}$$

Instead of v_i of the above formula,

$$v_i(t)=\{v_{i_1}^2+v_{i_2}^2+2v_{i_1}\cdot v_{i_2}\cdot\cos\{(\omega_1-\omega_2)t+\theta_1-\theta_2\}\}^{1/2} \tag{73}$$

is substituted to obtain the result. Since the conditions of Equation (71) are actually in the range of 45 — 47 GHz, namely about $\omega_1-\omega_2\fallingdotseq 2\pi\times 600$ MHz, it generally satisfies the requirement.

By substituting Equation (73) into Equation (72) and $\gamma_I = 1.5$, one can simplify the formula and find an approximate formula [1] for $v_o(t)$ as follows:

$$\begin{aligned}v_o(t)=&\{v_{oa}e^{j(\omega_1t+\theta_1)}+v_{ob}e^{j(\omega_2t+\theta_2)}\}\cdot e^{-j(\gamma_t+\sigma_0)}\cdot\{J_0(\sigma_1)-jJ_1(\sigma_1)e^{j(\Delta\omega t+\theta_1-\theta_2)}\\&+jJ_{-1}(\sigma_1)e^{-j(\Delta\omega t+\theta_1-\theta_2)}-\{J_2(\sigma_1)-jJ_0(\sigma_1)\cdot J_2(\sigma_2)\}\cdot e^{j2(\Delta\omega t+\theta_1-\theta_2)}\\&-\{J_{-2}(\sigma_1)+jJ_0(\sigma_1)\cdot J_{-1}(\sigma_2)\}\cdot e^{-j2(\Delta\omega t+\theta_1-\theta_2)}\}\end{aligned} \tag{74}$$

where /137

$$\begin{aligned}&v_{ia}\equiv v_{i_1}-\frac{\delta_0}{2}(v_{i_1}^3+3v_{i_1}v_{i_2}^2)+\frac{0.9\delta_0^2-1}{4}(v_{i_1}^5+5v_{i_1}v_{i_2}^4+10v_{i_1}^3v_{i_2}^2)\\&v_{ib}\equiv v_{i_2}-\frac{\delta_0}{2}(v_{i_2}^3+3v_{i_1}^2v_{i_2})+\frac{0.9\delta_0^2-1}{4}(v_{i_2}^5+5v_{i_1}^4v_{i_2}+10v_{i_1}^2v_{i_2}^3)\\&\sigma_0\equiv\gamma_i\{v_{i_1}^2+v_{i_2}^2-v_{i_1}^4-v_{i_2}^4-4v_{i_1}^2\cdot v_{i_2}^2+0.4(v_{i_1}^2+v_{i_2}^2)(v_{i_1}^4+5v_{i_1}^2\cdot v_{i_2}^2+v_{i_2}^4)\}\\&\sigma_1\equiv 2\cdot\gamma_i\cdot v_{i_1}\cdot v_{i_2}\{1-2v_{i_1}^2-2v_{i_2}^2+1.2(v_{i_1}^4+3v_{i_1}^2\cdot v_{i_2}^2+v_{i_2}^4)\}\\&\sigma_2\equiv 2\cdot\gamma_i\cdot v_{i_1}^2\cdot v_{i_2}^2\{1-0.6(v_{i_1}^2+v_{i_2}^2)\}\\&\Delta\omega=\omega_1-\omega_2,\ J_n(\ )\text{ は第 1 種ベッセル関数}\\&J_0(x)\fallingdotseq 1-\frac{x^2}{4}+\frac{x^4}{64},\ J_1(x)\fallingdotseq\frac{x}{2}-\frac{x^3}{16},\ J_2(x)\fallingdotseq\frac{x^2}{8}-\frac{x^4}{96}\\&J_{-n}(x)=(-1)^nJ_n(x),\ J_0(-x)=J_0(x),\ J_1(-x)=-J_1(x),\ J_2(-x)=J_2(x)\end{aligned}$$

From these relations, one sees that the output contains not only the hoped output components of ω_1 and ω_2, but it also contains a number of interference components such as $\omega_1+\Delta\omega$, $\omega_2-\Delta\omega$, $\omega_1+2\Delta\omega$, and $\omega_2 - 2\Delta\omega$, etc. (see Figure 30). For the interference waves, they are called, in the above order, beginning with the one closest to the desired component, the first interference wave, the second interference wave, etc. These waves can then be found in the above expression.

The desired wave output

$$\begin{aligned}v_o(t)(\omega_1)&=\{J_0(\sigma_1)v_{oa}-jJ_1(\sigma_1)v_{ob}\}\cdot e^{j(\omega_1t+\theta_1-\gamma_t-\sigma_0)}\\v_o(t)(\omega_2)&=\{jJ_{-1}(\sigma_1)v_{oa}+J_0(\sigma_1)v_{ob}\}\cdot e^{j(\omega_2t+\theta_2-\gamma_t-\sigma_0)}\end{aligned} \tag{75}$$

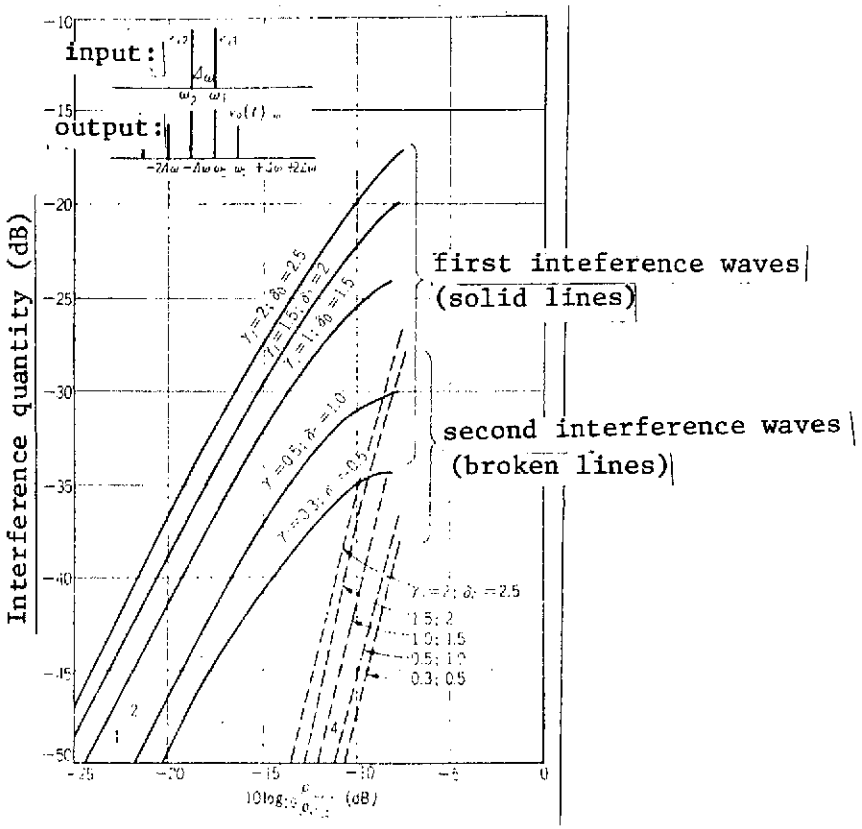

Figure 30. The interference quantity curves for the case of a 2-cycle normalized input.

The first interference wave output:

$$\left.\begin{aligned} v_o(t)_{(\omega_1+\Delta\omega)} &= \{-j\{J_1(\sigma_1)v_{oa}-J_0(\sigma_1)\cdot J_1(\sigma_2)v_{ob}\}-J_2(\sigma_1)v_{ob}\}\cdot e^{j[(\omega_1+\Delta\omega)t+2\theta_1-\theta_2-\gamma_s-\sigma_0]} \\ v_o(t)_{(\omega_2-\Delta\omega)} &= \{-j\{J_{-1}(\sigma_1)v_{ob}+J_0(\sigma_1)\cdot J_{-1}(\sigma_2)v_{oa}\}-J_{-2}(\sigma_1)v_{oa}\}\cdot e^{j[(\omega_2-\Delta\omega)t-\theta_1+2\theta_2-\gamma_s-\sigma_0]} \end{aligned}\right\} \quad (76)$$

The second interference wave output:

$$\left.\begin{aligned} v_o(t)_{(\omega_1+2\Delta\omega)} &= -\{-jJ_0(\sigma_1)\cdot J_1(\sigma_2)+J_1(\sigma_2)\}v_{oa}\cdot e^{j[(\omega_1+2\Delta\omega)t+3\theta_1-2\theta_2-\gamma_s-\sigma_0]} \\ v_o(t)_{(\omega_2-2\Delta\omega)} &= \{-jJ_0(\sigma_1)\cdot J_{-1}(\sigma_2)-J_{-2}(\sigma_1)\}v_{ob}\cdot e^{j[(\omega_2-2\Delta\omega)t-2\theta_1+3\theta_2-\gamma_s-\sigma_0]} \end{aligned}\right\} \quad (77)$$

Consequently, when the values of the above expression v_{oa}, v_{ob}, σ_0 are substituted into the above-mentioned series representation, one finds a general expression of the series representation for all these output components, but it is a very complex expression. Hence, as a somewhat simpler example, the series representation for the case of a 2-cycle normalized input will be obtained.

The case of a 2-cycle normalized input:

$$v_{i_1}=v_{i_2}\equiv v_i(v_i<0.35)$$

then in Equation (74),

$$\begin{cases} v_{oa}=v_{ob}=v_i-2\delta_0 v_i^3+4(0.9\delta_0^2-1)v_i^5\equiv v_o \\ \sigma_0=2\gamma_i(v_i^2-3v_i^4+6.4v_i^6) \\ \sigma_1=2\gamma_i(v_i^2-4v_i^4+6v_i^6) \\ \delta_2=2\gamma_i(v_i^4-1.2v_i^6) \end{cases}$$

Now if the series representation of $J_n(x)$ is used, one can find the corresponding expressions for Equations (75) — (77).

The hoped wave output:

$$\begin{aligned} v_o(t)_{(\omega_1)}&=v_o\sqrt{J_0(\sigma_1)^2+J_1(\sigma_1)^2}\cdot e^{j\left\{\omega_1 t+\theta_1-\gamma_3-\sigma_0-\tan^{-1}\frac{J_1(\sigma_1)}{J_0(\sigma_1)}\right\}} \\ &\fallingdotseq\{v_i-2\delta_0 v_i^3+4(0.9\delta_0^2-1)v_i^5\}\cdot\left(1-\frac{1}{2}\gamma_i^2 v_i^4\right)\cdot e^{j(\omega_1 t+\theta_1-\gamma_3-\gamma_i(3v_i^2-10v_i^4))} \\ v_o(t)_{(\omega_2)}&=v_o\sqrt{J_0(\sigma_1)^2+J_1(\sigma_1)^2}\cdot e^{j\left\{\omega_2 t+\theta_2-\gamma_4-\sigma_0-\tan^{-1}\frac{J_1(\sigma_1)}{J_0(\sigma_1)}\right\}} \\ &\fallingdotseq\{v_i-2\delta_0 v_i^3+4(0.9\delta_0^2-1)v_i^5\}\cdot\left(1-\frac{1}{2}\gamma_i^2\cdot v_i^4\right)\cdot e^{j(\omega_2 t+\theta_2-\gamma_4-\gamma_i(3v_i^2-10v_i^4))} \end{aligned} \quad (78)$$

The first interference wave output: /138

$$\begin{aligned} v_o(t)_{(\omega_1+\Delta\omega)}&=-jv_o\sqrt{A_1^2+J_2(\sigma_1)^2}\cdot e^{j\left\{(\omega_1+\Delta\omega)t+2\theta_1-\theta_2-\gamma_3-\sigma_0-\tan^{-1}\frac{J_2(\sigma_1)}{A_1}\right\}} \\ &\fallingdotseq-j\{v_i-2\delta_0 v_i^3+4(0.9\delta_0^2-1)v_i^5\}\cdot\gamma_i\cdot\{v_i^2-5v_i^4+7.2v_i^6\} \\ &\cdot e^{j(\omega_1+\Delta\omega)t+2\theta_1-\theta_2-\gamma_3-2\gamma_i(v_i^2-3v_i^4)} \\ v_o(t)_{(\omega_2-\Delta\omega)}&=-jv_o\sqrt{A_1^2+J_2(\sigma_1)^2}\cdot e^{j\left\{(\omega_2-\Delta\omega)t-\theta_1+2\theta_2-\gamma_3-\sigma_0-\tan^{-1}\frac{J_2(\sigma_1)}{A_1}\right\}} \\ &\fallingdotseq-j\{v_i-2\delta_0 v_i^3+4(0.9\delta_0^2-1)v_i^5\}\cdot\gamma_i\cdot\{v_i^2-5v_i^4+7.2v_i^6\} \\ &\cdot e^{j\{(\omega_2-\Delta\omega)t-\theta_1+2\theta_2-\gamma_3-2\gamma_i(v_i^2-3v_i^4)\}} \end{aligned} \quad (79)$$

where $$A_1\equiv J_1(\sigma_1)-J_0(\sigma_1)\cdot J_1(\sigma_2)$$

The second interference wave output:

$$
\left.
\begin{aligned}
v_-(t)_{(\omega_1+2\Delta\omega)} &= jv_0\sqrt{J_0(\sigma_1)^2\cdot J_1(\sigma_2)^2+J_2(\sigma_1)^2}\cdot e^{j\left\{(\omega_1+2\Delta\omega)t+3\theta_1-2\theta_2-\gamma_s-\sigma_0+\tan^{-1}\frac{J_2(\sigma_1)}{J_0(\sigma_1)\cdot J_1(\sigma_2)}\right\}} \\
&\fallingdotseq j\{v_i-2\delta_0 v_i^3+4(0.9\delta_0^2-1)v_i^5\}\cdot\gamma_i\cdot\sqrt{1+\frac{1}{4}\gamma_i^2}\cdot v_i^4 \\
&\quad\cdot e^{j[(\omega_1+2\Delta\omega)t+3\theta_1-2\theta_2-\gamma_s+\gamma_i(1/2-6v_i^2+14v_i^4)]} \\
v_-(t)_{(\omega_2-2\Delta\omega)} &= jv_0\sqrt{J_0(\sigma_1)^2\cdot J_1(\sigma_2)^2+J_2(\sigma_1)^2}\cdot e^{j\left\{(\omega_2-2\Delta\omega)t-2\theta_1+3\theta_2-\gamma_s-\sigma_0+\tan^{-1}\frac{J_2(\sigma_1)}{J_0(\sigma_1)\cdot J_1(\sigma_2)}\right\}} \\
&\fallingdotseq j\{v_i-2\delta_0 v_i^3+4(0.9\delta_0^2-1)v_i^5\}\cdot\gamma_i\cdot\sqrt{1+\frac{1}{4}\gamma_i^2}\cdot v_i^4 \\
&\quad\cdot e^{j[(\omega_2-2\Delta\omega)t+2\theta_1+3\theta_2-\gamma_s+\gamma_i(1/2-6v_i^2+14v_i^4)]}
\end{aligned}
\right\} \quad (80)
$$

Consequently, if the ratios of the interference wave outputs with respect to the hoped wave output are called the first and second interference quantity, etc., then they can be obtained from Equations (78) — (80).

$$
\left.
\begin{aligned}
&\text{The first interference quantity } \fallingdotseq \gamma_i\left\{v_i^2-5v_i^4+\left(7.2+\frac{1}{2}\gamma_i^2\right)v_i^6\right\} \\
&\text{The second interference quantity: } \fallingdotseq \gamma_i\cdot\sqrt{1+\frac{1}{4}\gamma_i^2}\cdot v_i^4
\end{aligned}
\right\} \quad (81)
$$

Now, if one finds the quantities p_{i1}/p_{is1} and p_{i2}/p_{is2} from Equation (69) as the abscissa, and the interference quantity is taken as the coordinate, the relationship of (81) can be found as in Figure 30.

For the case of a millimeter double ladder tube, as shown in Figure 14, the frequency number characteristics appear in G_{os} and in the characteristic quantities of p_{is}, δ_0, γ_i, etc.; quite a large amount of other frequency number characteristics also appear. Hence, it is a problem whether Equation (81) will hold true for this case. However, as shown in [1], under certain conditions, this expression can be established, and thus they can be established for a double ladder type tube. Thus, Figure 30 also is applicable for a double ladder type tube.

3.4.2. The 2-cycle pulse normalized input — equal time slot case /139

In this case, all the expressions for a 2-cycle normalized input, namely Equations (78) — (81), can be simply used for the calculation. Now we again consider these expressions.

In an idealized PM pulse, v_{i1} and v_{i2} are constant, but θ_1 and θ_2 alone are time dependent. From Equation (78) for the desired wave output, one sees that an output compression appears only due to δ_0, but none appears due to γ_l. Also, no modulation shows up because of θ_1 and θ_2; that is, one of the noticeable properties of this case is that the phase does not contribute to amplification. However, in the interference wave output, there are the mixed modulations of $-\theta_2$ and $-\theta_1$ to $-2\theta_2$ and $-2\theta_1$, respectively. So far, 2-cycle common amplification by an idealized PM pulse is a very simple case, but in an actual case, v_{i1} and v_{i2} do vary; that is, in a common amplification of a PM pulse with some element of AM components, there is an added effect, namely, a phase distortion related to γ_l and the input amplitude (the AM-PM transformation), which causes some added complexity. For a PM input pulse, as we did in the previous chapter, we will study a square and Gaussian PM pulse under a Gaussian band restriction for their output properties.

i) When the input is a square PM pulse with a Gaussian band restriction:

The input pulse form is expressed in Equations (8) and (8'). If the 2-cycle input pulse is shown by $v_{i1}(t)$ and $v_{i2}(t)$, then for $k = \pi$

$$\left.\begin{aligned} v_{i_1}(t) &= v_i\left[1-\left\{\varepsilon_{rf}\left(\frac{1+x_1}{d_2}\right)+\varepsilon_{rf}\left(\frac{1-x_1}{d_2}\right)\right\}\right] \\ &\quad \cdot e^{j(\omega_1 t+\theta_1)} \\ v_{i_2}(t) &= v_i\left[1-\left\{\varepsilon_{rf}\left(\frac{1+x_1}{d_2}\right)+\varepsilon_{rf}\left(\frac{1-x_1}{d_2}\right)\right\}\right] \\ &\quad \cdot e^{j(\omega_2 t+\theta_2)} \end{aligned}\right\} \qquad (82)$$

$$x_1=\frac{t}{T_1/2},\quad d_2=\frac{4\sqrt{\alpha}}{T_1}=\frac{2.356}{\pi}\cdot\frac{1}{\alpha_2}$$

Consequently, for $v_i < 0.35$ and $\delta_0 < 2$, instead of the quasistatic formulas (78) — (80),

$$v_i\left[1-\left\{\varepsilon_{rf}\left(\frac{1+x_1}{d_2}\right)+\varepsilon_{rf}\left(\frac{1-x_1}{d_2}\right)\right\}\right]$$

is used to obtain the result.

Since the second interference output is very small, we only consider the desired wave and the first interference output.

For the desired output pulse, one can use Equation (78) to obtain it, but for the sake of simplicity, we will omit $(1/2)\gamma_i^2 v_i^4$ and $(\theta_1-\gamma_s)$

$$\left.\begin{aligned}
v_o(t)_{(\omega_1)}&=\{v_i(t)-2\delta_0 v_i(t)^3+4(0.9\delta_0^2-1)\cdot v_i(t)^5\}\cdot e^{j(\omega_1 t-\gamma_i(3v_i(t)^2-10v_i(t)^4)}\\
v_o(t)_{(\omega_2)}&=\{v_i(t)-2\delta_0 v_i(t)^3+4(0.9\delta_0^2-1)\cdot v_i(t)^5\}\cdot e^{j(\omega_2 t-\gamma_i(3v_i(t)^2-10v_i(t)^4)}\\
v_i(t)&=v_i\left[1-\left\{\varepsilon_{rf}\left(\frac{1+x_1}{d_2}\right)+\varepsilon_{rf}\left(\frac{1-x_1}{d_2}\right)\right\}\right]
\end{aligned}\right\}\quad(83)$$

Now, if the component which is in phase with $e^{-j\gamma_i(3v_i(0)^2-10v_i(0)^4)}$ is called the in-phase component, and that which is perpendicular to it is called the perpendicular component, they are as follows:

the in-phase component:

$$\left.\begin{aligned}
\left.\begin{matrix}v_o(t)_{(\omega_1)c}\\ v_o(t)_{(\omega_2)c}\end{matrix}\right\}&=\{v_i(t)-2\delta_0 v_i(t)^3+4(0.9\delta_0^2-1)v_i(t)^5\}\cdot\cos\gamma_i[3v_i(t)^2-10v_i(t)^4\\
&\quad-(3v_i(0)^2-10v_i(0)^4)\}\cdot e^{j\left\{\frac{\omega_1}{\omega_2}t-\gamma_i(3v_i(0)^2-10v_i(0)^4)\right\}}
\end{aligned}\right\}\quad(84)$$

the perpendicular component:

$$\left.\begin{matrix} v_o(t)_{(\omega_1)s} \\ v_o(t)_{(\omega_3)s} \end{matrix}\right\} = -\{v_i(t)-2\delta_0 v_i(t)^3+4(0.9\delta_0^2-1)v_i(t)^5\}\cdot\sin\gamma_i\{3v_i(t)^2-10v_i(t)^4 - (3v_i(0)^2-10v_i(0)^4)\}\cdot e^{j\left\{\begin{matrix}\omega_1\\ \omega_3\end{matrix}\right.t-\gamma_i(3v_i(0)^2-10v_i(0)^4)\}} \quad (85)$$

the envelope = $\{v_i(t)-2\delta_0 v_i(t)^3+4(0.9\delta_0^2-1)v_i(5)^5\}$ (86) /140

Consequently, the retarded scientific output $g_o(t)$ for ω_1 and ω_3, according to Equation (25) and the above formula, are

$$g_o(t) = -4K_0[v_o(t)_{(\omega_1)c}\cdot v_o(t-T_1)_{(\omega_1)c} + v_o(t)_{(\omega_1)s}\cdot v_o(t-T_1)_{(\omega_1)s}] \quad (87)$$

where $\tau = T_1$ (100% duty).

Next, the first order interference output pulse can be obtained from Equation (79), but for the sake of simplicity, we drop 7.2 v 16 $(2\theta_1-\theta_2-\gamma_s)$, $(-\theta_1+2\theta_2-\gamma_s)$

$$\left.\begin{matrix} v_o(t)_{(\omega_1+\Delta\omega)} = -jv_o(t)\cdot\gamma_i\cdot\{v_i(t)^2-5v_i(t)^4\}\cdot e^{j\{(\omega_1+\Delta\omega)t-2\gamma_i(v_i(t)^2-3v_i(t)^4)\}} \\ v_o(t)_{(\omega_3-\Delta\omega)} = -jv_o(t)\cdot\gamma_i\cdot\{v_i(t)^2-5v_i(t)^4\}\cdot e^{j\{(\omega_3-\Delta\omega)t-2\gamma_i(v_i(t)^2-3v_i(t)^4)\}} \\ v_o(t) = v_i(t)-2\delta_0 v_i(t)^2+4(0.9\delta_0^2-1)v_i(t)^4 \end{matrix}\right\} \quad (88)$$

Now the components which are in phase with $e^{-j\gamma_i(v_i(0)^2-3v_i(0)^4)}$ are called the in-phase components, while those which are perpendicular to it are called the perpendicular components.

The in-phase components:

$$\left.\begin{matrix} v_o(t)_{(\omega_1+\Delta\omega)c} \\ v_o(t)_{(\omega_3-\Delta\omega)c} \end{matrix}\right\} = -v_o(t)\cdot\gamma_i\cdot\{v_i(t)^2-5v_i(t)^4\}\cdot\cos2\gamma_i\{v_i(t)^2-v_i(t)^4 - (v_i(0)^2-v_i(0)^4)\}\cdot e^{j\left\{\begin{matrix}(\omega_1+\Delta\omega)\\ (\omega_3-\Delta\omega)\end{matrix}\right.t-2\gamma_i(v_i(0)^2-v_i(0)^4)\}} \quad (89)$$

The perpendicular components:

$$\left.\begin{matrix} v_o(t)_{(\omega_1+\Delta\omega)s} \\ v_o(t)_{(\omega_3-\Delta\omega)s} \end{matrix}\right\} = -v_o(t)\cdot\gamma_i\cdot\{v_i(t)^2-5v_i(t)^4\}\cdot\sin2\gamma_i\{v_i(t)^2-v_i(t)^4 - (v_i(0)^2-v_i(0)^4)\}\cdot e^{j\left\{\begin{matrix}(\omega_1+\Delta\omega)\\ (\omega_3-\Delta\omega)\end{matrix}\right.t-2\gamma_i(v_i(0)^2-v_i(0)^4)\}} \quad (90)$$

The envelope = $v_i(t)\cdot\gamma_1\cdot\{v_i(t)^2-5v_i(t)^4\}$ | (91)

As an example, for $v_i=0.35$, $\delta_0=2$, $\gamma_1=1.5$ and for α_2 = 1, 1.5, and 3.0, the calculation of Equations (84) — (87) and Equation (91) is shown in Figures 31a and b and Figure 32.

When one compares this wave form with the case of the 1-cycle pulse amplification in a large signal region which is described in Chapter 3.3, namely Figure 24a and Figure 25, one sees that the in-phase component of the desired wave output is compressed by about 20 $\log_{10}$ (0.33/0.4) = 1.7 dB in the case of Figure 24a, while that in Figure 31a is 20 $\log_{10}$ (0.23/ /0.35) = -3.5 dB, but beside this difference in intensities, the wave forms in general look quite similar to each other. Also, in the perpendicular component, it is somewhat larger in Figure 31, but the wave forms are also alike for both cases. From these facts, one could expect that the sign interference and channel interference in Figure 31 should be about the same as those in Figure 24a. However, in the present case, Figure 31b shows the appearance of the first order interference wave, and because of it, a "cross docking among the interference waves" may appear. The level of an interference wave, as is shown in Figure 30, varies, depending on the input level, γ_1 and δ_0, but in the present case, it is about 20 $\log_{10}$ (0.02/0.23) = -21 dB; this value is a quite practical value, and because of it, v_i is about 0.35.

ii) When the input is a Gaussian PM pulse with a Gaussian band restriction:

In this case, the input wave form is described by Equation (14); namely, if the 2-cycle input pulse is shown by $v_{i1}(t)$ and $v_{i2}(t)$, for $k = \pi$,

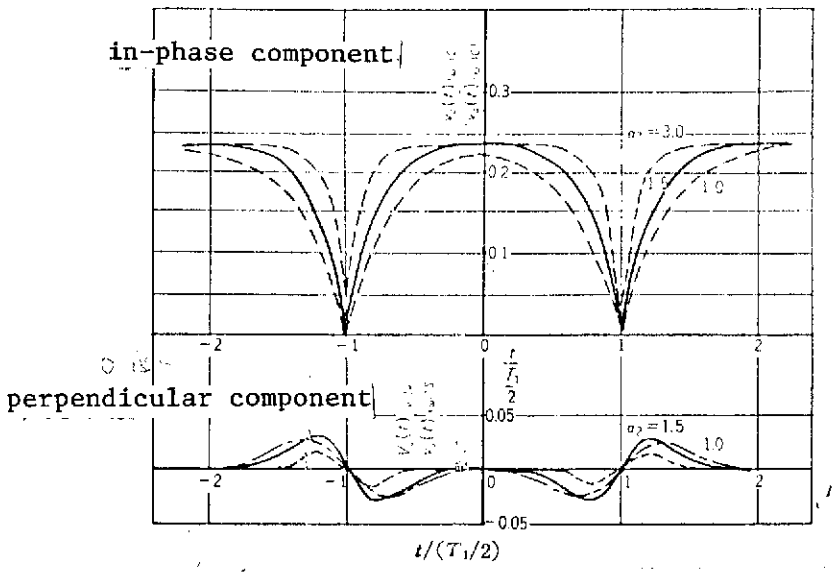

a) the desired output pulse

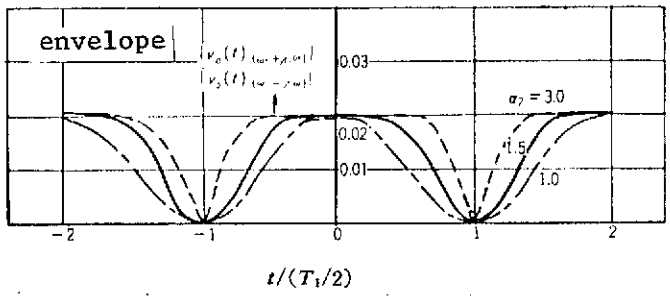

b) the first order interference output pulse

Conditions: $v_i = 0.35$ $\delta_0 = 2$ $\gamma_i = 1.5$

Figure 31. The wave forms of the desired wave and the interference pulse (a 2-cycle equally normalized input. The case of equal time slot).

/142

$$\left.\begin{matrix} v_{i_1}(t) \\ v_{i_2}(t) \end{matrix}\right\} = v_i \{\mathrm{Re}(t)^2 + \mathrm{Im}(t)^2\}^{1/2} \cdot e^{j\left\{\begin{matrix}\omega_1 t + \theta_1 \\ \omega_2 t + \theta_2\end{matrix} + \tan^{-1}\frac{\mathrm{Im}(t)}{\mathrm{Re}(t)}\right\}}$$

$$\mathrm{Re}(t) = 1 - \frac{\pi^2}{2!} \cdot \frac{1}{\sqrt{1+2\alpha_5^2}} \cdot e^{-\frac{2(0.833x_2)^2}{1+2\alpha_5^2}} + \frac{\pi^4}{4!} \cdot \frac{1}{\sqrt{1+4\alpha_5^2}} \cdot e^{-\frac{4(0.833x_2)^2}{1+4\alpha_5^2}} - \cdots\cdots$$

$$\mathrm{Im}(t) = \pi \cdot \frac{1}{\sqrt{1+\alpha_5^2}} \cdot e^{-\frac{(0.833x_2)^2}{1+\alpha_5^2}} - \frac{\pi^3}{3!} \cdot \frac{1}{\sqrt{1+3\alpha_5^2}} \cdot e^{-\frac{3(0.833x_2)^2}{1+3\alpha_5^2}} + \cdots\cdots \qquad (92)$$

$$x_2 = \frac{t}{T_2/2}, \quad \alpha_5 = \frac{\Delta F}{\Delta F_B} = \frac{0.624}{\alpha_4}, \quad \alpha_4 = \frac{\Delta F_B}{1/T_2}$$

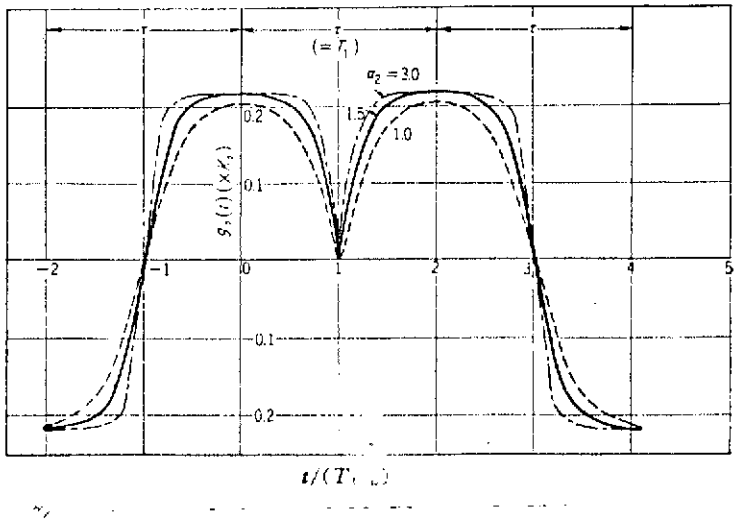

Figure 32. The retarded rectified wave form of the desired wave output pulse (Figure 31a).

Consequently, for $v_i < 0.35$ and $\delta_0 < 2$, instead of v_i of the quasi-static expression of (78) — (80),

$$v_i\{\mathrm{Re}(t)^2+\mathrm{Im}(t)^2\}^{1/2}$$

is substituted to obtain the result.

Now we neglect the second order interference output in finding the desired wave and the first order interference wave output.

For the desired wave output pulse, it can be obtained from Equation (78). For the sake of simplicity, $(1/2)\gamma_i^2 v_i^4$ and $(\theta_{1,2}-\gamma_s)$ are omitted

$$\begin{aligned} v_o(t)_{(\omega_1)} &= \{v_i(t)-2\delta_0 v_i(t)^3+4(0.9\delta_0^2-1)v_i(t)^5\}\cdot e^{j\left\{\omega_1 t-\gamma_i(3v_i(t)^2-10v_i(t)^5)+\tan^{-1}\frac{\mathrm{Im}(t)}{\mathrm{Re}(t)}\right\}} \\ v_o(t)_{(\omega_2)} &= \{v_i(t)-2\delta_0 v_i(t)^3+4(0.9\delta_0^2-1)v_i(t)^5\}\cdot e^{j\left\{\omega_2 t-\gamma_i(3v_i(t)^2-10v_i(t)^5)+\tan^{-1}\frac{\mathrm{Im}(t)}{\mathrm{Re}(t)}\right\}} \\ v_i(t) &= v_i\cdot\{\mathrm{Re}(t)^2+\mathrm{Im}(t)^2\}^{1/2} \end{aligned} \qquad (93)$$

Consequently, the in-phase and perpendicular components are:

The in-phase component:

$$\left.\begin{matrix} v_o(t)_{(\omega_1)c} \\ v_o(t)_{(\omega_2)c} \end{matrix}\right\} = \{v_i(t) - 2\delta_0 v_i(t)^3 + 4(0.9\delta_0^2 - 1)v_i(t)^5\} \cdot \cos\left\{-\gamma_i(3v_i(t)^2 - 10v_i(t)^4) + \tan^{-1}\frac{\mathrm{Im}(t)}{\mathrm{Re}(t)}\right\} \cdot e^{j\omega_1 t} \quad (94)$$

The perpendicular component:

$$\left.\begin{matrix} v_o(t)_{(\omega_1)s} \\ v_o(t)_{(\omega_2)s} \end{matrix}\right\} = \{v_i(t) - 2\delta_0 v_i(t)^3 + 4(0.9\delta_0^2 - 1)v_i(t)^5\} \cdot \sin\left\{-\gamma_i(3v_i(t)^2 - 10v_i(t)^4) + \tan^{-1}\frac{\mathrm{Im}(t)}{\mathrm{Re}(t)}\right\} \cdot e^{j\omega_2 t} \quad (95)$$

The envelope = $\{v_i(t) - 2\delta_0 v_i(t)^3 + 4(0.9\delta_0^2 - 1)v_i(t)^5\}$ (96)

The phase angle: $\varphi_0(t)_{(\omega_1,\omega_2)} = \tan^{-1}\dfrac{v_o(t)_{(\omega_1,\omega_2)s}}{v_o(t)_{(\omega_1,\omega_2)c}} + \gamma_i(3v_i(\infty)^2 - 10v_i(\infty)^4)$ (97)

Hence, the retarded rectified wave output $g_o(t)$ can be obtained with Equation (25) and the above expression for ω_1 and ω_2 as follows:

$$g_o(t) = -4K_o[v_o(t)_{(\omega_1)c} \cdot v_o(t-T_2)_{(\omega_1)c} + v_o(t)_{(\omega_1)s} \cdot v_o(t-T_2)_{(\omega_1)s}] \quad (98)$$

where $\tau = T_2$ (100% duty).

Next, for the first order interference wave output, it can be obtained from Equation (79). For the sake of simplicity, $7.2v_i^6$, $(2\theta_1 - \theta_2 - \gamma_s)$, $(-\theta_1 + 2\theta_2 - \gamma_s)$ are omitted

/143

$$\begin{aligned} v_o(t)_{(\omega_1+j\omega)} &= -jv_o(t) \cdot \gamma_i \cdot \{v_i(t)^2 - 5v_i(t)^4\} \cdot e^{j\left\{(\omega_1+j\omega)t - 2\gamma_i(v_i(t)^2 - 3v_i(t)^4) + \tan^{-1}\frac{\mathrm{Im}(t)}{\mathrm{Re}(t)}\right\}} \\ v_o(t)_{(\omega_2-j\omega)} &= -jv_o(t) \cdot \gamma_i \cdot \{v_i(t)^2 - 5v_i(t)^4\} \cdot e^{j\left\{(\omega_2-j\omega)t - 2\gamma_i(v_i(t)^2 - 3v_i(t)^4) + \tan^{-1}\frac{\mathrm{Im}(t)}{\mathrm{Re}(t)}\right\}} \\ v_o(t) &= v_i(t) - 2\delta_0 v_i(t)^2 + 4(0.9\delta_0^2 - 1)v_i(t)^4 \end{aligned} \quad (99)$$

The in-phase component:

$$\left.\begin{matrix} v_o(t)_{(\omega_1+j\omega)c} \\ v_o(t)_{(\omega_2-j\omega)c} \end{matrix}\right\} = -v_o(t) \cdot \gamma_i \cdot \{v_i(t)^2 - 5v_i(t)^4\} \cdot \cos\left\{-2\gamma_i(v_i(t)^2 - 3v_i(t)^4) + \tan^{-1}\frac{\mathrm{Im}(t)}{\mathrm{Re}(t)}\right\} \cdot e^{j\binom{\omega_1+j\omega}{\omega_2-j\omega}t} \quad (100)$$

The perpendicular component:

$$\left.\begin{matrix} v_o(t)_{(\omega_1+\Delta\omega)s} \\ v_o(t)_{(\omega_2-\Delta\omega)s} \end{matrix}\right\} = v_o(t)\cdot\gamma_l\cdot\{v_i(t)^2-5v_i(t)^4\}\cdot\sin\left\{-2\gamma_l(v_i(t)^2-3v_i(t)^4) + \tan^{-1}\frac{\mathrm{Im}(t)}{\mathrm{Re}(t)}\right\}\cdot e^{j\binom{\omega_1+\Delta\omega}{\omega_2-\Delta\omega}t} \Bigg| \tag{101}$$

The envelope = $v_o(t)\cdot\gamma_l\cdot\{v_i(t)^2-5v_i(t)^4\}$ | (102)

The phase angle: $\varphi_o(t)_{(\omega_1+\Delta\omega,\,\omega_2-\Delta\omega)} = -2\gamma_l(v_i(t)^2-3v_i(t)^4)+\tan^{-1}\frac{\mathrm{Im}(t)}{\mathrm{Re}(t)}$ | (103)

As an example, for v_i = 0.35, δ_0 = 2, γ_l = 1.5, and for α_4 = 1.25, 2, and 3, the calculation of Equations (94) — (98) and Equation (102) are shown in Figures 33a and b and Figure 34.

If one compares this wave form with that in the case of the 1-cycle pulse amplification in a large signal region of Section 3.3, namely that of Figure 26a, Figure 27a, and Figure 28, then in the desired wave output pulse, as in the previous section, one finds the output compression of about -3.5 dB, but the AM component surprisingly is found to be smaller in Figure 33, and the phase variation is found to be about the same in both cases. For the retarded rectified wave form too, they also look very much alike in Figures 34 and 28. Hence, from these facts, one could expect that the sign interference or the channel interference in the Figure 33 should be about the same as in Figure 26a, and may be even smaller.

However, in this case too, as in the previous case, the first order interference wave pulse shows up in Figure 33b, and because of it, "interference wave cross docking" can appear. The level of the interference wave, as in the previous case, is about -21 dB.

(a) the hoped wave output pulse

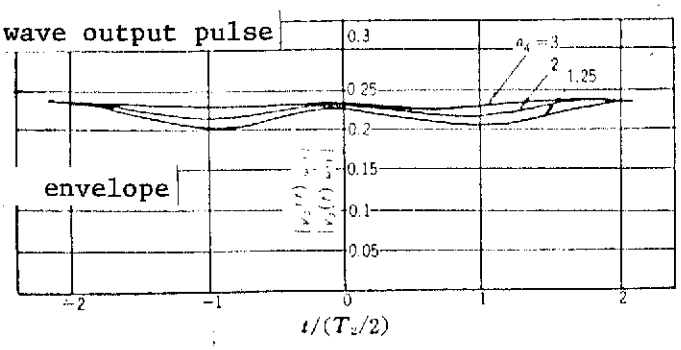

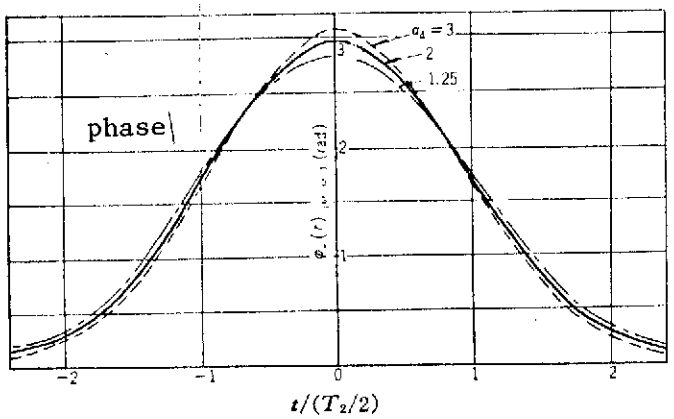

(b) the first order interference wave pulse

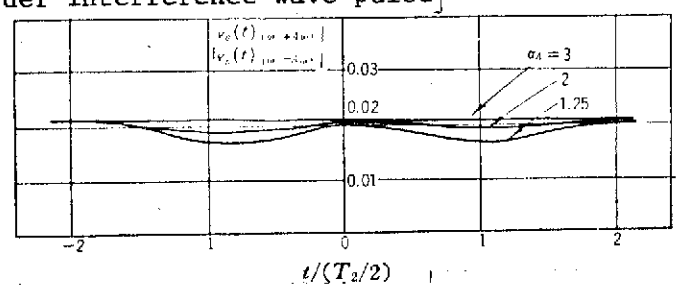

Figure 33. The output wave pulse wave form of the desired wave and the interference wave (2-cycle of equal input and equal time slot).

Conditions: $v_i = 0.35$ $\delta_0 = 2$ $\gamma_i = 1.5$

3.4.2. Two-cycle wave pulse with equally normalized input but of different time slot

It is the case of $(f_1 : \cdots\cdots 00100 \cdots\cdots,\ f_2 : 00001 \cdots\cdots)$ in which there is a continuous wave at one side, while at the other side, there is a PM pulse common amplification. In this case, Equations (74) — (77) are used with

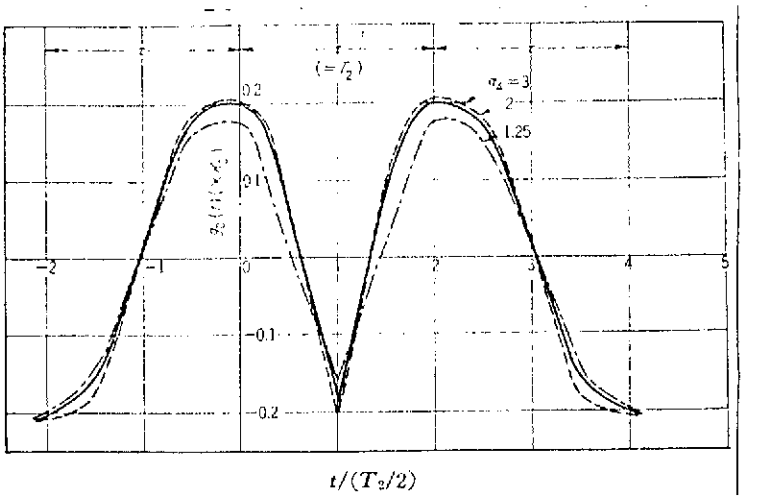

Figure 34. The retarded rectified wave form of the desired wave output pulse (Figure 33a).

v_{i1} = constant and θ_1 = constant. The quantities v_{i2} and θ_2 are obtained by using $v_{i2}(t)$ of Equations (82) and (92) in finding the output wave.

i) When the input is a square PM pulse in a Gaussian band restriction:

In this case, the 2-cycle wave input power $v_{i1}(t)$ and $v_{i2}(t)$ can be obtained by the above Equation (82) as follows:

$$\left.\begin{aligned} v_{i_1}(t) &= v_i \cdot e^{j(\omega_1 t+\theta_1)} \\ v_{i_2}(t) &= v_i\left[1-\left\{\varepsilon_{rf}\left(\frac{1+x_1}{d_2}\right)\right.\right. \\ &\quad \left.\left.+\varepsilon_{rf}\left(\frac{1-x_1}{d_2}\right)\right\}\right]\cdot e^{j(\omega_2 t+\theta_2)} \\ x_1 &= \frac{t}{T_1/2},\quad d_2=\frac{4\sqrt{\alpha}}{T_1}=\frac{2.356}{\pi}\cdot\frac{1}{\alpha_2} \end{aligned}\right\} \tag{104}$$

Consequently, for v_{i1} and v_{i2} in Equation (74),

$$\left.\begin{aligned} v_{i_1} &= v_i \\ v_{i_2} &= v_i\left[1-\left\{\varepsilon_{rf}\left(\frac{1+x_1}{d_2}\right)+\varepsilon_{rf}\left(\frac{1-x_1}{d_2}\right)\right\}\right] \end{aligned}\right\} \tag{105}$$

a) the desired wave output (envelope)

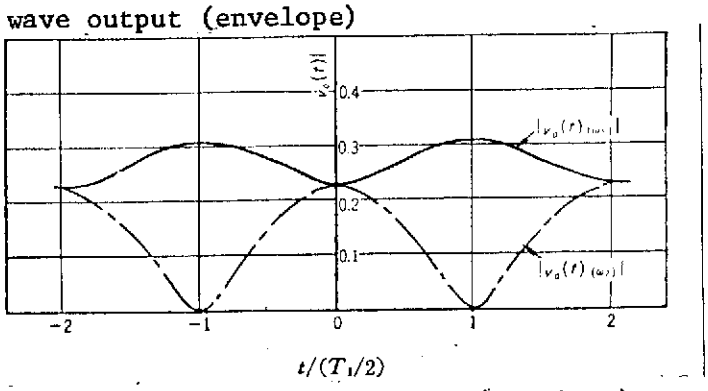

b) the first order interference wave output (envelope)

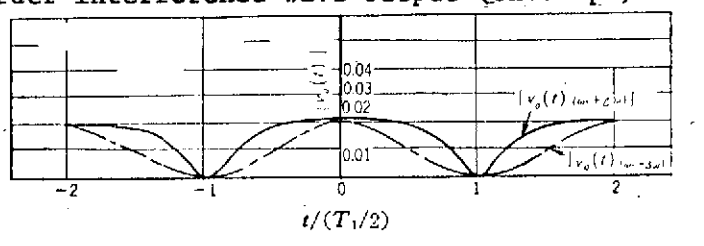

c) the retarded rectified output wave form $[v_0(t)(\omega_2)]$

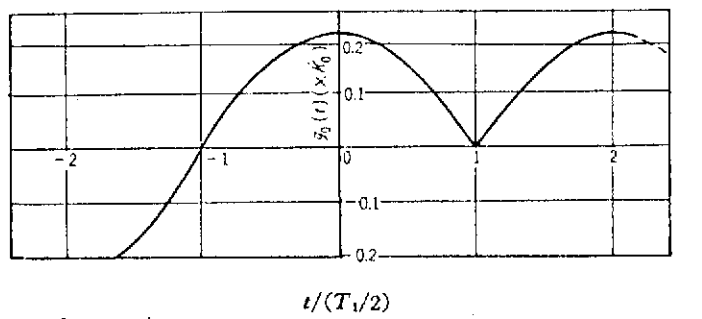

Figure 35. Various output wave forms (2-cycle equal input but of different time slot).

Conditions: $v_i=0.35$ $\delta_0=2$ $\gamma_1=1.5$ $\alpha^2=1.5$

are substituted, and then from Equations (75) — (78), one finds $v_o(t)(\omega_1,\omega_2)$ and $v_o(t)(\omega_1+\Delta\omega)$, etc.

Now as an example, for $v_i = 0.35$, $\delta_0 = 2$, $\gamma_1 = 1.5$, and $\alpha_2 = 1.5$, from Equations (75) and (76), one finds the desired wave output power and the envelope of the first order interference wave output, as shown in Figures 35a and b. From $v_o(t)(\omega_2)$, one finds the retarded rectified wave form, as shown in Figure 35c. /144

From these results, we determine the following. In the desired wave output, $v_o(t)(\omega_1)$ does not contain any AM element in the case of a 1-cycle wave amplitude, but due to the button effect, in a 2-cycle amplitude, some AM element of about $20\log_{10}(0.31/0.27)\fallingdotseq 1.1\,\mathrm{dB}$ appears, as shown in the figure.

Next, in $v_o(t)(\omega_2)$, as described before, there is an output compression of about 1.7 dB, and the general wave form looks smoother compared to Figure 31. Comparing the large signal with the small signal region, the small signal region shows more compression ("AM compression"). At $t/(T_1/2)=\pm 0.5$ and ±1.5, the phase change appears to be very small, to be less than 0.13 rad; that is, the perpendicular component is very small. Consequently, the retarded rectified wave form of $|v_o(t)(\omega_2)|$, as shown in Figure 35c, and the absolute values at the sample points of $t/(T_1/2)=0$ and ±2 are the same. In other words, in this case, the change in the sign interference is zero. In regard to the channel interference, the wave form of $|v_o(t)(\omega_2)|$ in Figure 35a looks smoother than that of Figure 31 and, therefore, it is estimated to be smaller for this case. /146

The first order interference wave output is equivalent to the peak level of Figure 31 (about -21 dB) and the envelopes also look alike.

ii) When the input is a Gaussian PM pulse in a Gaussian band restriction:

If the 2-cycle wave output is designated by $v_{i1}(t)$ and $v_{i2}(t)$, they can be obtained from Equations (84) and (92) as follows:

$$\left.\begin{aligned}
&v_{i_1}(t)=v_i\cdot e^{j(\omega_1 t+\theta_1)}\\
&v_{i_2}(t)=v_i\{\mathrm{Re}(t)^2+\mathrm{Im}(t)^2\}^{1/2}\\
&\qquad\cdot e^{j\left(\omega_2 t+\theta_2+\tan^{-1}\frac{\mathrm{Im}(t)}{\mathrm{Re}(t)}\right)}\\
&\mathrm{Re}(t)=1-\frac{\pi^2}{2!}\cdot\frac{1}{\sqrt{1+2\alpha_0^2}}e^{-\frac{2(0.833x_2)^2}{1+2\alpha_0^2}}\\
&\qquad+\frac{\pi^4}{4!}\cdot\frac{1}{\sqrt{1+2\alpha_0^2}}\cdot e^{-\frac{4(0.833x_2)^2}{1+4\alpha_0^2}}-\cdots\cdots\\
&\mathrm{Im}(t)=\pi\cdot\frac{1}{\sqrt{1+\alpha_0^2}}\cdot e^{-\frac{(0.833x_2)^2}{1+\alpha_0^2}}\\
&\qquad-\frac{\pi^3}{3!}\cdot\frac{1}{\sqrt{1+3\alpha_0^2}}\cdot e^{-\frac{3(0.833x_2)^2}{1+3\alpha_0^2}}+\cdots\cdots
\end{aligned}\right\}\qquad(106)$$

where /147

$$x_2=\frac{t}{T_2/2},\ \alpha_3=\frac{\Delta F}{\Delta F_n}=\frac{0.624}{\alpha_4},\ \alpha_4=\frac{\Delta F_n}{1/T_2}$$

Consequently, v_{i1}, v_{i2}, and θ_2 of Equations (74) — (77),

$$\left.\begin{aligned} v_{i_1}&=v_i\\ v_{i_2}&=v_i\{\mathrm{Re}(t)^2+\mathrm{Im}(t)^2\}^{1/2}\\ \theta_2&=\theta_2+\tan^{-1}\frac{\mathrm{Im}(t)}{\mathrm{Re}(t)}\end{aligned}\right\} \qquad (107)$$

are substituted to find $v_o(t)(\omega_1,\omega_2)$, $v_o(t)(\omega_1+j\omega_2)$, etc.

Now as an example, for $v_i = 0.35$, $\delta_0 = 2$, $\gamma_2 = 1.5$, and for $\alpha_4 = 1.5$, Equations (75) and (76) can be computed for the desired wave output (outputs for both ω_1 and ω_2), and the envelope of the first order wave output, as shown in Figures 36a and b. For $v_o(t)(\omega_2)$, the retarded rectified wave form can be obtained as shown in Figure 36c.

From these results, one sees the following. In the desired wave output, as in the previous section, because of the button effect, the 2-cycle amplitude shows some AM elements of about $20\log_{10}(0.27/0.22)\fallingdotseq 1.8$ dB in $v_o(t)(\omega_1)$, and the AM element of about $20\log_{10}(0.22/0.17)=2.3$ dB in $v_o(t)(\omega_2)$, and they are much larger than the case of Figure 33. At $t/(T_2/2) = \pm 1$, the phase change is about 0.13 rad and the distortion is very small. The retarded rectified wave form of $v_o(t)(\omega_2)$ is shown in Figure 36c, and at $t/(T_1/2) = 0$ and ± 2, the output value is about the same as that in Figure 34. Consequently, this case has almost no sign interference. The wave form of $|v_o(t)(\omega_2)|$ in Figure 36a contains a large amount of AM elements, as compared to the case of Figure 33a, and the width of the spectrum becomes smaller. Consequently, the channel interference is expected to be small.

The first interference wave output is about the same as in Figure 33, and the wave form looks quite similar.

a) the desired wave output (envelope)

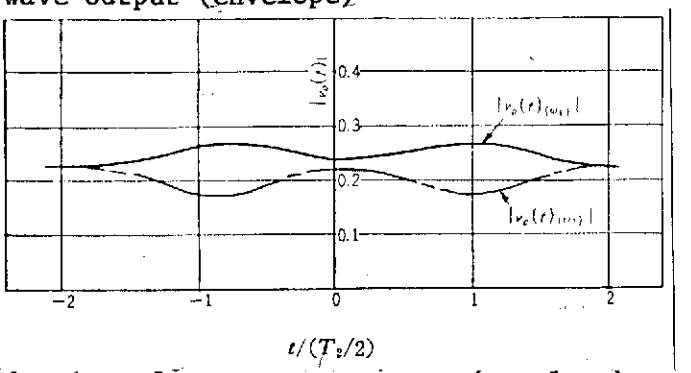

b) the first order interference wave output (envelope)

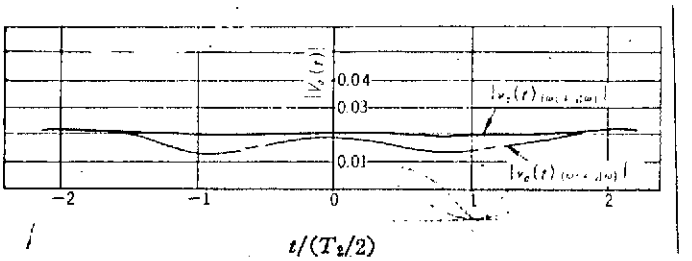

c) the retarded rectified wave output wave form*

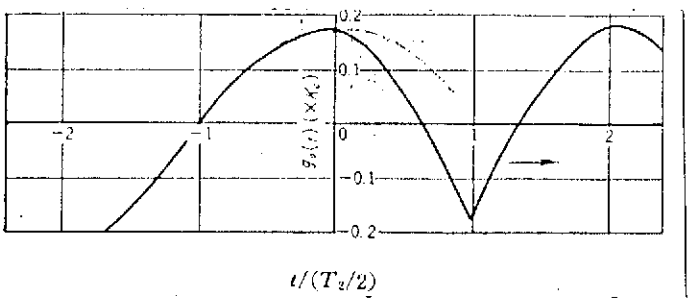

Figure 36. Various output wave forms (2-cycle equal input but of different time slot).

Conditions: $\nu_t=0.35$ $\delta_0=2$ $\gamma_t=1.5$ $\alpha_t=1.25$

3.4.4. Summary of 2-cycle common amplification

In Sections 3.4.2 and 3.4.3, we have discussed two special cases of the 2-cycle pulse, namely the equal time slot case and the completely different time slot case. However, in the general case, with two different periods, a 2-cycle pulse lies somewhere between these two special situations, and the

*Translator's note: Illegible in foreign text.

output pulse wave form is extremely variable. Therefore, if one wants to obtain the output wave form for such general cases, as we did in Section 3.2, to find the pulse distortion due to the traveling wave tube f characteristics, the calculation is very complex and it is very difficult to find an exact solution for these cases. Consequently, the best we can do is to utilize the results of Sections 3.4.2 and 3.4.3 and that of Section 3.2 to estimate the general cases and to evaluate the maximum wave distortion and the amount of interference. We will make an evaluation of this with the input pulse either for a square wave shape PM pulse or for a Gaussian shape pulse.

i) When a 2-cycle input is a square PM pulse with a Gaussian band restriction:

We study this problem by summarizing Figures 15a, 21, 31, 32, and, therefore, Figure 35.

In other words, the case is with

$$v_{t_1}=v_{t_2}=0.35,\ \delta_0=2,\ \gamma_t=1.5,$$
$$\alpha_2=\frac{\Delta F_B}{1/T_1}=1.5$$

Effects of the f characteristics: at the turning points of the phase, about 10% of the peak value appears to be the perpendicular component, but the change in the retarded rectified wave form and the sign interference due to the presence of the perpendicular component is very small.

Compression of the peak value: 3.5 dB.

Change of the peak value due to the responding pulse: 1.4 dB.

Phase change: below 0.13 rad.

Peak value level of the first order interference wave: -21 dB.

Increase of the sign interference: almost 0 dB.

Increase of the frequency interference: almost 0 dB.

ii) When a 2-cycle wave input pulse is a Gaussian PM pulse in a Gaussian band restriction:

The problem can be understood by summarizing Figures 22a, 28, 33, 34, and, therefore, Figure 36. The case also has $v_{i1} = v_{i2} = 0.35$, $\delta_0 = 2$, but $\gamma_\zeta = 1.5$ and $\alpha_4 = \Delta F_B/(1/T_2) = 1.25$.

Effects of the f characteristics: about 4% of assymmetry appears in the envelope wave form, due to the "PM-AM" transformation, but the change in the retarded rectified wave form and the sign interference is small.

Compression of the peak value: 3.5 dB.

Change in the peak value due to the responding pulse: 1.8 dB. /148

Phase change: below 0.13 rad.

Peak value level of the first order interference: -21 dB.

Increase in the sign interference: almost 0 dB.

Increase in the frequency interference: almost 0 dB.

iii) Consequently, in regard to the system number of a common amplification, for any wave form, the compression of the peak value in a 2-cycle pulse amplitude is about 3.5 dB; the envelope of PM waves vanishes only for a very short period of time. If we want a large output, whether it is an equal period amplitude of a non-equal period amplitude, a 2-cycle pulse amplitude is about the best we can get.

4. An Experiment with PM Pulse Amplification Characteristics in a Millimeter Double Ladder Traveling Wave Tube [3]

4.1. Measurement of Static Characteristics of a Traveling Wave Tube

The traveling wave tube used in the experiment is designed in a package (a permanent magnet shape), namely, in a tube of a double ladder shape, with a central frequency number of 46.5 GHz. For the intermediate frequency number, the small signal gain is about 14 dB and the saturated output is about 22 dBm. These values are lower than our target values, namely 20 dB and 30 dBm, respectively; but this is due to our intention to use less electrical power, and also due to a shorter circuit in the package shape circuit design. On the other hand, due to the package shape, the stability has much increased, phenomena can be easily duplicated and repeated, and the setup can be used continuously for more than 300 hours, without creating any change in the electric current, voltage, and gain, etc. The design also shows good input-output characteristics, and it can be well used for a high speed pulse amplification.

The characteristics of this traveling wave tube (TC50DA#109, manufactured by Okidenki Co., Ltd.), such as the input-out saturation characteristics, phase characteristics, and the frequency number characteristics of various characteristic values, have been reported in [1] and thus are omitted here.

4.2. Generation of a PM Pulse

There are two methods to generate a PM pulse in the millimeter band region, namely:

i) first to generate a PM pulse in the microwave region, then by use of a frequency transformation to bring it to a PM pulse in the millimeter range.

ii) To generate a PM pulse directly in the millimeter range.

These two methods both have strong points, as well as shortcomings. For the simplicity of the apparatus, method (ii) can be recommended and, in this method, the carrier frequency number can also easily be varied. However, there are again two methods in the latter method, as shown in Figure 37. In Figure 37a, the case is similar to the conventional method for generating AM pulses, by using crystal reflectors and circulators. These AM pulses can be combined with a continuous wave which has a phase difference of π, to obtain a 2-phase PM pulse of 0-π modulation. Hence, this method has a shortcoming that the modulation loss is large (more than 9 dB) and, therefore, a large output is hard to obtain. Contrary to this method, the method as shown in Figure 37b also employs crystal reflectors and circulators, but the difference is in that, in this case, there is an E-H tuner and thus, the continuous wave (with a phase difference of π) can be obtained from it. As compared to the method of Figure 37a, this method does not need the branching off nor two hybrid circuits. Consequently, the circuit structure looks more elegant and the modulation loss is also far smaller. In Figures 38a and b, an example of the PM pulse, generated by the method of Figure 37b, is given. It shows the envelope shape (heterodyne rectified wave), the in-phase and the perpendicular component. In Figure 38a, the perpendicular component appears to be in odd symmetry, but in Figure 38b, it looks more like in even symmetry. In these experiments, the crystal reflector is made of diode 1N26.

From the experimental wave forms, one can see that, in the PM pulse so obtained, there is a strong perpendicular component. Thus, it is really not very suitable for our purpose, because we want to observe the appearance of perpendicular components and to measure phase distortion, but we can't help the situation. We believe that the appearance of the perpendicular component is due to the fundamental nature of Figure 38, as long as we use such a crystal reflector to obtain an AM pulse. Thus, we have to proceed the experiment with the PM pulse which is close to the PM wave we want, and

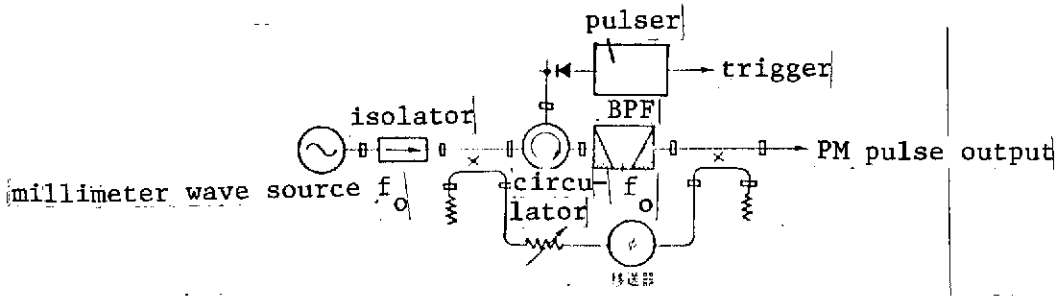

(a) Generation of a PM pulse by combining a AM pulse with CW

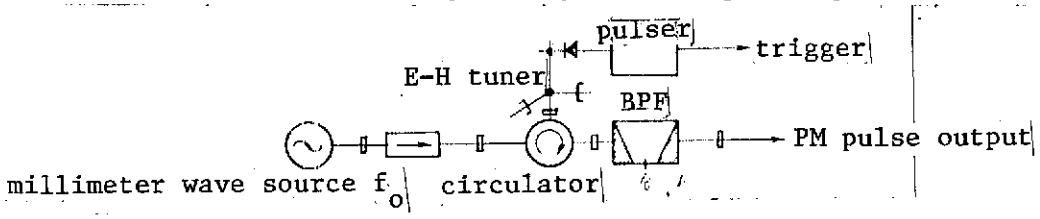

(b) Generation of a PM pulse with a single modulator

Figure 37. PM pulse generator.

measure the relationship between the magnitude of the perpendicular component and the envelope wave form. The theoretical discussion of wave distortion due to the effect of the band restriction is made, according to [3]. As an example, the wave distortion due to a band restriction is measured and shown /149 in Figures 39a, b, and c. They show the envelope wave form, the in-phase component, and the perpendicular component, respectively. The top part shows the output wave form from the pulser (f_o = 48.2 GHz, 0-π 2-phase PM pulse), the middle part shows the wave form of the 380 MHz filter output of 3 dB in width, and the bottom part shows the wave form of the 280 MHz filter output of 3 dB in width.

4.3. The Amplification Characteristics of a 1-Cycle Pulse

The PM pulse (an independent pulse) is generated by the method mentioned in the previous section, and by use of a double ladder tube (TC50DA#109), the wave form is measured with respect to the 1-cycle amplification characteristics in the small as well as in the large signal region.

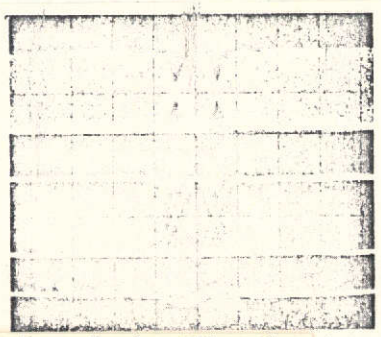

→ wave form of the envelope

→ wave form of the in-phase component

→ wave form of the perpendicular component

(a) An example of the PM pulse (f_0=48.0GHz, H : 2.5ns/div)

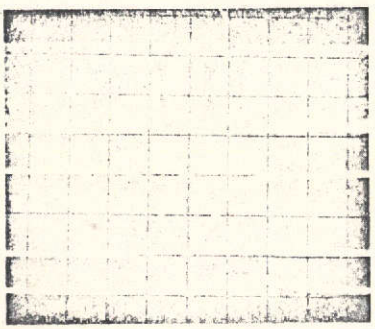

← wave form of the envelope

← wave form of the in-phase component

← wave form of the perpendicular component

(b) An example of the PM pulse (f_0=48.0GHz, H : 2.5ns/Div)

Figure 38. The wave form of a PM pulse.

4.3.1. Operation in the small signal region

To investigate the effect of frequency number characteristics and the appearance of internal echo pulse, a 0-π modulated phase of 46.8 GHz frequency is generated by the method indicated in the Figure 37 (a), and this output is amplified by a traveling wave tube with -9.3 dBm at its input terminal. The saturation input p_i is 15 dBm at this frequency, and

$$p_{is} - p_i \fallingdotseq -24\text{dB}$$

and it is in the small signal region.

The measurements made for this case, such as the wave form of the output envelope, the in-phase component, and the perpendicular component, are shown in Figures 40a and b. From the results, one sees that the increase in the perpendicular component and the wave distortion in the in-phase component in

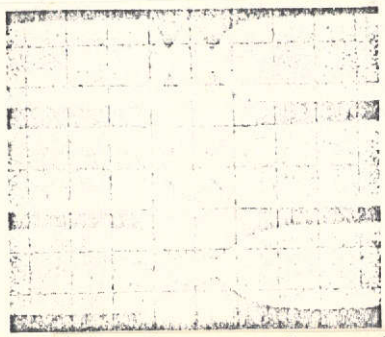

← wave form of the input PM wave

← wave form from 380 MHz wave generator (3 dB width)

← wave form from 280 MHz wave generator

(a) The wave form of an envelope wave

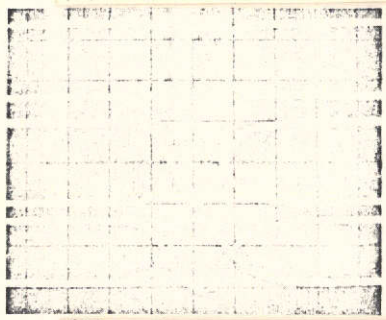

(b) The wave form of an in-phase component

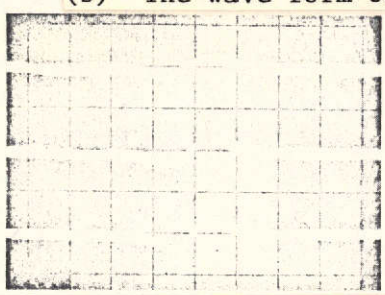

(c) The wave form of a perpendicular component

Figure 39. The change in the PM pulse due to the band restriction.

(f_0=48.2 GHz, H . 2.5ns/div)

this amplification is extremely small. This agrees with the prediction made in i) of Section 3.2. However, since the input PM pulse contains quite a sizeable perpendicular component, the perpendicular component generated by /150
the traveling wave tube should be observed as in Figure 15a. The gain is observed to be 12.5 dB and this value is about the range of the measurement error of 12.4 dB in the small signal case. In short, the effect of the frequency number characteristics is very small and it can be practically neglected.

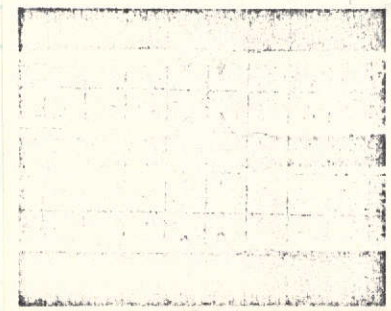

(a) The wave form of the envelope

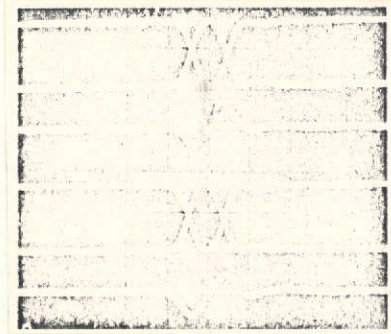

(b) Wave forms of the in-phase and perpendicular component

(In the small signal region : $p_i = p_{is} - 24$dB)
(f_0=46.8GHz, p_i=−9.3dBm, H : 2.5ns/div)

Figure 40. Amplification characteristics of a 1-cycle pulse.

4.3.2. Operation in the large signal region

The frequency number is 46.8 GHz, as in the above case, but this time, the PM pulse is generated as in Figure 37b, and it is amplified with the traveling wave tube (#603). The peak electric power reaches 7.4 dBm and it was sent into the traveling wave tube (#109) on which the study was being made. Hence, in this case, $p_{is} - p_i = -7.6$ dB and it is considered to be in a large signal region. The observation made on the envelope wave form of the input and output wave, the in-phase component, and the perpendicular component are shown as in Figures 41a — c. From these results, the following can be stated:

In Figures 41a and b, it is clearly recognized that the peak is compressed due to the saturation characteristics. The amount of compression is about 0.4 dB, which agrees with the predicted value (about 0.5 dB) due to the static

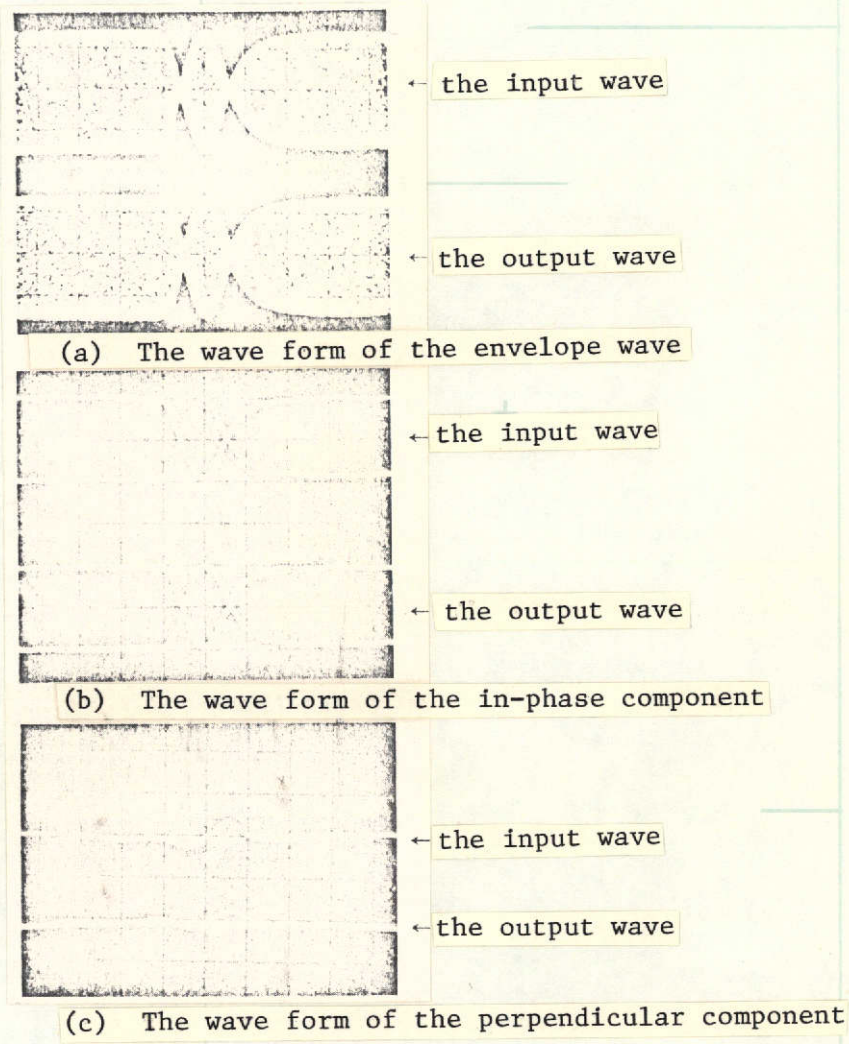
← the input wave
← the output wave
(a) The wave form of the envelope wave
←the input wave
← the output wave
(b) The wave form of the in-phase component
←the input wave
←the output wave
(c) The wave form of the perpendicular component

Figure 41. The amplification characteristics of a 1-cycle pulse (in a large signal region: $p_i = p_{is} - 7.6$ dB) (f_0=46.8 GHz, p_i=7.4 dBm, H : 2.5 ns/div)

characteristics. From Figure 41c, the increase in the perpendicular component due to amplification appears to be extremely small, as before. This is due to the phase shift characteristics of a traveling wave tube, and the appearance of the perpendicular component due to this property, as shown in Figure 24, is extremely small and, thus, it agrees with the experiment.

Consequently, in the large signal region, the peak compression due to the saturation characteristics is even larger, but other kinds of distortions are extremely small and are practically negligible.

4.4. The Common Amplification Characteristics of a 2-Cycle Pulse

In this case, the situation is similar to the 1-cycle pulse amplification as far as the small signal region is concerned. Hence, we measure only activities in the large signal region. The modulation sign of the 2-cycle wave are both (...00100...) when they belong to the same time slot and both /151
undergo a 0-π modulation. However, when one is (...00100...) and the other is (...00001...), these two are considered to be the two representative cases of the different time slot problem. With these, a lot of experiments can be handled quasi-statically. In the former case, the output wave can be estimated by the common amplification characteristics of a 2-cycle continuous wave.

In the latter case, only the common amplification of an independent PM pulse and a continuous wave have been understood, and, therefore, the experiment is made on this case. Figure 42 shows the circuit for this experiment. For the 2-cycle wave, the frequency numbers are 46.68 GHz and 47.36 GHz. For the former frequency, the method shown in Figure 37b is used to modulate the PM pulse. As before, it was amplified by the preliminary amplifier so that 6.8 dBm can reach the input terminal of the principal amplifier. For the 47.36 GHz frequency, the process is the same so that 7.6 dBm is adjusted to the input terminal of the principal amplifier. Thus, a set of the 2-cycle equally normalized input is obtained. In the output wave of the traveling wave tube, beside the desired output (46.68 and 47.36 GHz), the above mentioned first order interference output (46.0 GHz and 48.04 GHz) also shows up. As shown in Figure 42, these are analyzed by the analyzer at the output side and are observed separately with the heterodyne method for their envelope wave forms. The results are shown in Figures 43a — c.

In other words, Figure 43a shows the input wave, Figure 43b shows the desired output wave form, and Figure 43c shows the first order output wave form and their envelopes.

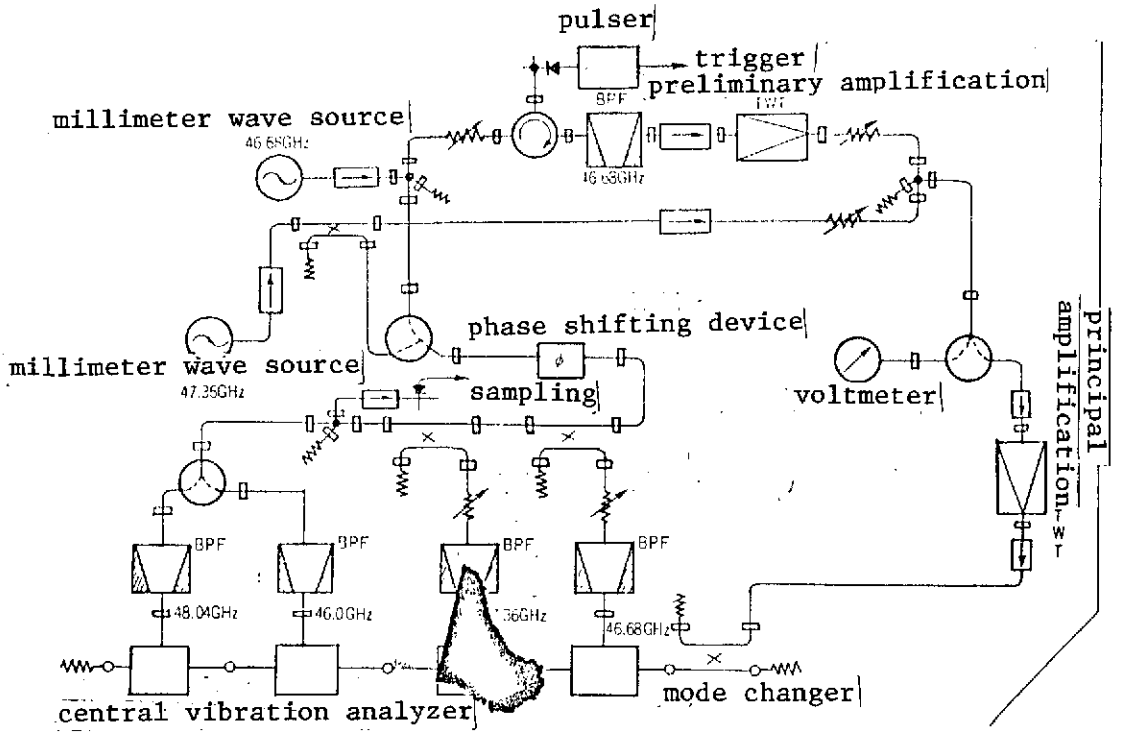

Figure 42. The circuit to measure the common amplification of a 2-cycle PM pulse.

The wave forms of Figures 43a and b and the 48.04 GHz wave form of Figure 43c agree well with the expected wave form of Figure 35. However, the 46.0 GHz wave form of Figure 43c is very different from the expected wave form. The reason is conjectured as due to the imperfection of the analyzer characteristics which causes some cross docking effects, but we do not yet understand this discrepancy to our satisfaction.

Next, we will discuss the experimental results for the level of the output wave and the gains. The input level is 6.8 dBm for the 46.68 GHz PM pulse, and it is 7.6 dBm for the 47.36 GHz continuous wave. First, we measured the gain in the 1-cycle wave amplification, and the values 11.9 dB and 9.9 dB, respectively, are obtained. The compression degrees are 0.7 dB and 0.9 dB with respect to the linear amplification.

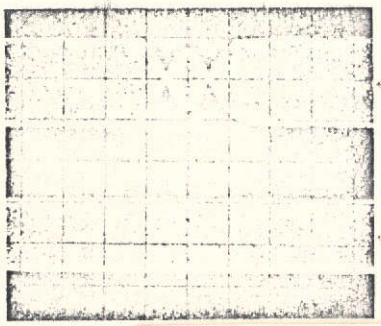

(a) The input wave form

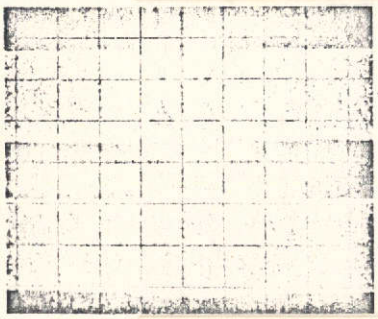

(b) The desired output wave form

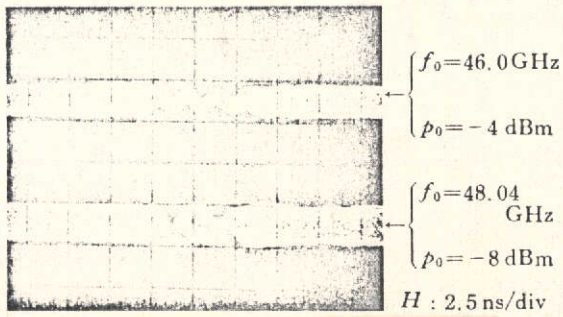

(c) The wave form of the first order interference wave

Figure 43. The common amplification characteristics of a 2-cycle wave pulse (in the large signal region: $P_i = P_{is} = -8$ dB).

Next, the gain is measured for the 2-cycle common amplification. The results are 10.68 dB and 8.55 dB, respectively. In this case, the compression degrees are 1.25 dB and 1.35 dB with respect to the 1-cycle amplification. At this moment, the desired output level is 17.45 dBm for the 46.68 GHz frequency, and it is 16.15 dBm for the 47.36 GHz frequency.

Now the measurement on the first order interference output shows that it is -4 dBm for the 46.0 GHz interference wave, while it is -8 dBm for the 48.04 GHz wave. Consequently, the amounts of the first order interference are

$$-4-17.45=-21.45\ \text{dB},$$
$$-8-16.15=-24.15\ \text{dB}$$

These values agree with the expected values of Figure 30 (γ_l = 1 — 1.5, δ_0 = 1.5 — 2).

From the above test, we see that, in the 2-cycle common amplification /152
case, the peak compression due to the saturation characteristic and the appearance of interference waves due to the phase shift characteristics pose a great problem. However, they can be estimated correctly by static characteristics.

5. Summary

We have made a theoretical and experimental study on the 1-cycle and 2-cycle wave common amplification of high speed PM pulses by use of millimeter wave double ladder type tubes. The results can be summarized as follows:

i) In the frequency number characteristics, there are the first order slope of the gain and the second order component of the phase, but the effect of the former is larger. In a square PM pulse, the perpendicular component /153
appears, while in a Gaussian PM pulse, the envelope wave becomes asymmetrical, but these are due to comparatively weak effect of the delay rectified wave form. Consequently, these effects can be practically neglected. The Fourier components of the gain and the phase must be kept low and it is important to keep the input and output VSWR below 1.2 in the necessary band region.

ii) Next, in regard to the nonlinear effect, for a 1-cycle amplification, it is better to keep the AM component of the PM pulse smaller by a peak compression with the saturation characteristics and to reduce the sign interference. In this case, some perpendicular component may appear due to the phase shift characteristics, but they are comparatively small, and in general, the effects due to a delay rectified wave form are small enough to be practically neglected.

iii) In the 2-cycle pulse common amplification case, besides what happened in ii), a large number of interference waves appear due to the phase shift characteristics. However, when the peak electric power of the input is -8 dB less than the saturated input power, the level of the first order interference wave is below -25 dB and it is very small.

C-8

iv) The system number which is capable of carrying out the common amplification in a PCM-PM method must yield a strong output intensity, but such cases can only be expected in 2-cycle cases.

From the above summary, when millimeter wave double ladder type tubes are used for the communication amplification, 2-cycle common amplification of high speed PCM-PM pulse with frequency number of 400 — 500 MHz is most practical.

However, we have to make some further study in the areas, such as on the various reasons which cause the appearance of the perpendicular components, and more theoretical study is needed on what effects the appearance of the perpendicular component may have both on the 2-phase and the 4-phase PM method. Consequently, some experimental confirmations are also needed with respect to the wave forms of delay rectified wave and they are needed in developing some theoretical understanding of the problem.

Acknowledgement

We acknowledge the guidance given to us by the director of Yoshida Millimeter Wave Research Laboratory and cooperation given to us by our colleague of the laboratory. We are also grateful to Director Ikeda, and Chief of Research Miyawuchi of Electronic Tube Research Lab, for their assistance in preparing traveling wave tubes.

REFERENCES

1. Tuchiya and Ishio: A Study on the AM Pulse Amplification Characteristics with Millimeter Wave Double Ladder Type Traveling Wave Tubes. Bulletin of Communication Research, Vol. 18, No. 4, 1969, p. 963.

2. Nakamura and Wueno. A Phase Modulator for the 2 Gc Band Pulses by Use of Circulators and Diode Switches. Technical Reports of Communication Research, No. 2639, 1965.

3. Yamamoto, Miyakawa, and Miyawuchi. Analysis and Experiments with Microwave PCM Delay Rectifier. Technical Reports, No. 2749, 1966.

4. Okuho, Yamamoto, and Kyokawa. Experiments on 2-phase and 4-phase Delay Rectification. Technical Reports, No. 3122, 1967.

5. Ishida and Ishihara. Discussions on AM and PM Pulses in the 4 Gc Band. Technical Reports, No. 2358, 1967.

6. Waters, W. D. A Phase Modulated PCM Repeater for Millimeter Wave or Other RF Carrier Systems. NEREM Record, No. 200, 1966.

7. Hubbard, W. M. The Effect of Intersymbol Interference on Error Rate in Binary Differentially Coherent Phase Shift Keyed Systems. B.S.T.J., vol. 46, No. 6, 1967, p. 1149.

8. Hubbard, W. M., and G. D. Mandeville. Experimented Verification of the Error Rate Performance of Two Types of Regenerative Repeaters for DCPSK Signals. B.S.T.J., Vol. 46, No. 6, 1967, p. 1173.

9. Nakamua, Yamomoto, Wueno, and Yoshida. Wave Distortion, Sign Interference, and Channel Interference in the Wireless PCM. Technical Reports, No. 3129, 1967.

10. Campbell, G. A. The Practical Application of the Fourier Integral. B.S.T.J., Vol. 7, 1928, p. 639.

11. Zuda. A Study on Traveling Wave Tube Amplifiers. Technical Reports, No. 1700, 1962.

12. Hoshiko. Pulse Sign Communication. Maruzen Publishes, 1965.

13. Sunde, E. D. Pulse Transmission by AM, FM, and PM in the Presence of Phase Distortion. B.S.T.J., Vol. 40, No. 2, 1961, p. 353.

14. Tanaka, Kuwaoki, and Zuda. Generation of Modulated Waves of Millimeter Wave Pulse. 1967 General Conference of the Electrical Communication Society. No. 490, 1967.

Translated for National Aeronautics and Space Administration under Contract No. NASw-2483 by SCITRAN, P. O. Box 5456, Santa Barbara, California 93108.